フライアッシュおよび高炉スラグ微粉末を用いたコンクリートの凍害との複合劣化に関する研究

STUDY ON COMBINED DERGRADATION ON FROST DAMAGE OF CONCRETE CONTAINING FLY ASH AND BLAST FURNACE SLAG

フライアッシュおよび高炉スラグ微粉末を用いたコンクリートの凍害との複合劣化に関する研究

DING ZHENZHAO

Doctor of Philosophy

Division of Engineering, Course of Advanced Sustainable and Environmental Engineering
MURORAN INSTITUTE OF TECHNOLOGY

ABSTRACT

The atmospheric CO_2 concentration has been increased and lead to the greenhouse effect that global temperatures increase, and a global “climate and environmental emergency” had been declared in 2019 to rise the challenge of climate change. It has become a global trend to limit and reduce carbon dioxide emissions. The study shows that the CO2 emissions due to cement manufactured accounts for 8% of all in the world, approximately. Therefore, in recent years, in the trend of CO_2 emission reduction, blast furnace slag (BFS) and fly ash (FA) are used more widely to reduce the cement consumption in the field of building materials, and the use of BFS and FA can result in a concrete with better durability.

On the other hand, for concrete structures in cold regions, concrete is subject to frost damage in winter, the effect of frost damage of concrete suffered the other three types of deterioration, which progress throughout the year, has been focused on. The combined deterioration between frost damage and salt damage has been expensively sturdily in the world. However, for most of concrete structures, carbonation is in presses to reduce the pH of concrete with intrusion of CO_2 into concrete due to a long-term exposure to air. Besides, ASR expansion is caused due to ASR aggregate to serious endanger the safety of concrete, which has been attracting new wild attention. The study on the combined deterioration between carbonation and frost damage, and ASR and frost damage. In addition, the additive of BFS and FA can decrease the carbonation resistance and restrain the ASR, which lead to change the mechanisms of combined deterioration. There is little study on this in the world.

Therefore, this study will investigate the combined deterioration between carbonation and frost damage, and ASR and frost damage of concrete containing BFS and FA, the effect on the combined deterioration would be also made clear.

In chapter 3, the change in frost resistance and pore structure of concrete containing blast furnace slag with various replacement ratio due to carbonation were investigated. As a result, there is a close relationship between the carbonation speed and 28-day compressive strength in blast furnace slag concrete. The frost

resistance, carbonation resistance and scaling resistance of blast furnace slag cement concrete decrease as blast furnace slag replacement ratio increases. Furthermore, due to carbonation, the frost durability of ordinary Portland cement concrete and the concrete with a low replacement ratio of blast furnace slag tends to decrease. However, the concrete with a high replacement ratio of blast furnace slag tends to increase. Under the carbonation conditions, the pore volume decreases due to carbonation of calcium hydroxide, and the pore structure will be coarsened due to carbonation of C-S-H. In addition, it is expected that permeability of concrete is raised and scaling is inhibited due to carbonation, and the surface area with a certain thickness in the carbonated concrete will be scaled due to freeze-thaw.

In chapter 4, the frost and scaling resistance of concrete with various fly ash (FA) replacement ratios exposure to air and accelerated carbonation conditions were investigated. The changes in water absorption were measured by RILEM / CIF test and in pore structure were measured by the Archimedes method and the mercury intrusion porosimetry method due to carbonation.

Results show that the influence of FA and carbonation on the frost and scaling resistance of concrete can be ignored due to air bubbles by air entraining (AE) admixture in case of AE FA concrete. For Non-AE FA concrete, carbonation of FA concrete does not change the gel porosity/capillary porosity ratio, which is the reason for the frost resistance is not influenced by carbonation of FA concrete. Additionally, it is noteworthy to note that the scaling resistance is strongly connected to the pore volume above 75 nm, and that when exposed to carbonation, the scaling resistance tends to rise as a result of the increase in pore volume above 75 nm that occurs as a result of carbonation. Because of the addition of FA and carbonation, the frost and scaling resistance are far more reliant on the changes in pore structure than they are on the water absorption.

In chapter 5, ASR expansion is caused due to ASR aggregate to serious endanger the safety of concrete, which has been attracting new wild attention. In clod region, concrete is always subject to frost damage in winter. In this chapter, the combined deterioration between frost damage and alkali-silica reaction was investigated.

As a result, for OPC concrete, the expansion due to alkali-silica reaction could be restrained when subjected to freeze-thaw. While, for BFS and FA concrete, it is kept a low level whether subject to freeze-thaw or not.

For OPC and FA concrete, the frost resistance can be reduced when subjected to alkali-silica reaction, and for BFS concrete, there is little change in frost resistance whether subjected to alkali-silica reaction or not. There is a close relationship between reduction of MSE and expansion rate due to ASR. the ASR deterioration can be evaluated by the reduction of MSE. Although 3-month ASR increase expansion rate, the deterioration degree is small, which little affect relationship between expansion rate and RDM. While, the 12-month ASR costly change the relationship between expansion rate and RDM, which is because that the long time ASR vastly increases expansion, but slightly decrease the RDM of concrete for OPC concrete. However, for BFS and FA concrete, the additive of BFS and FA can restrain ASR, which keeps the relationship between expansion rate and RDM.

From previous studies, it can be well known that, for AE concrete, the use BFS and FA don't reduce the frost resistance of concrete subjected to salt damage. And for Non-AE concrete, the use of BFS and FA can result in a better frost resistance due to long-term age.

From chapter 3 and chapter 4, it can be well known that, for AE concrete, the frost resistance of concrete subjected to carbonation is kept at a high level when using BFS and FA. While, for Non-AE concrete, the frost and scaling resistance subjected to carbonation tends to decrease with the additive of BFS and FA.

From chapter 5, it can be well known that, for AE concrete, the use of BFS and FA can restrain the cracks due to ASR, which can improve the frost resistance of concrete subject to ASR.

In real environment, AE concrete is used wildly for concrete construction. In various specification, AE admixture is required to add, which can ensure the good frost resistance of concrete. Therefore, in the study, it can be obtained that the use of BFS and FA don't reduce of frost resistance of concrete subjected to salt damage and carbonation, and increase the frost resistance of concrete subjected to ASR. overall evaluation, the use of BFS and FA are beneficial to the safety of concrete.

Keywords: blast furnace slag, fly ash, pore structure, carbonation; alkali-Silica Reaction; freeze-thaw; frost resistance; scaling resistance; Water absorption; Porosity; relative dynamic modulus of elasticity; expansion; combined degradation

TABLE OF CONTENTS

CHAPTER 1

INTRODUCTION

1.1 Background

In recent years, in order to establish a sustainable society with low carbon, it is expected that mineral admixtures, such as blast furnace slag (BFS) or fly ash, are increasingly used as concrete material from the viewpoint of reducing environmental load, in which the reduction of CO2 emission and effective utilization of industrial byproducts were carried out. Generally, the concrete using these materials has better durability and long-term mechanical properties than ordinary Portland cement (OPC) concrete [1,2]. BFS cement is classified into three categories according to the Japan Industrial Standards (JIS) R 5211 in Japan, i.e. type A, B and C, which contain BFS from 5 to 30%, 30 to 60% and 60 to 70% by weight, respectively. Compared to OPC, there are some advantages such as low heat generation and high long-term strength, but disadvantages such as a delay in early-age strength discovery and low carbonation resistance using BFS cement [3,4]. Similarly, fly ash cement is also classified into Type A, Type B, and Type C, which contain fly ash from 5 to 10%, 10 to 20% and 20 to 30% by weight respectively, according to the JIS R 5213. Compared to OPC, there are the same characteristics as BFS cement, such as low heat generation, high long-term strength, a delay in early-strength discovery, and low carbonation resistance, to use fly ash cement. Besides, it is used to improve water tightness and to reduce air entraining for fly ash concrete [3,5].

On the other hand, in cold regions, the weather changes greatly, so there are many types of deterioration for concrete structures, and a wide variety of deterioration occurs.

As a countermeasure against snow accumulation and freezing, the amount of antifreeze has increased in recent years, which leads to very peculiar deterioration can be seen everywhere. Antifreeze can cause salt damage and reduce frost scaling resistance in cold regions. In addition, when ASR aggregates are used in concrete, NaCl may accelerate deterioration due to ASR. Concrete is carbonation throughout the year due to the erosion of CO_2 in the air.

for the actual concrete structures, it is not possible to suffer a single deterioration only. In general, for the cause of deterioration in a concrete structure, a deterioration phenomenon called combined deterioration is often seen, in which the deterioration characteristics generated by the interaction of different deterioration phenomenon cannot be evaluated by adding two and more single deterioration model.

For concrete structures in cold regions, concrete is subject to frost damage in winter, the effect of frost damage of concrete suffered the other three types of deterioration, which progress throughout the year, has been focused on. The combined deterioration between frost damage and salt damage has been expensively sturdily in the world. However, for most of concrete structures, carbonation is in presses to reduce the pH of concrete with intrusion of CO2 into concrete due to a long-term exposure to air. Besides, ASR expansion is caused due to ASR aggregate to serious endanger the safety of concrete, which has been attracting new wild attention. The study on the combined deterioration between carbonation and frost damage, and ASR and frost damage. In addition, the additive of BFS and FA can decrease the carbonation resistance and restrain the ASR, which lead to change the mechanisms of combined deterioration. There is little study on this in the world.

Therefore, this study will investigate the combined deterioration between carbonation and frost damage, and ASR and frost damage of concrete containing BFS and FA, the effect on the combined deterioration would be also made clear.

1.2 Combined deterioration

1.2.1 Outline of concrete deterioration

More than 30 years have passed since the construction of many civil engineering structures in Japan, and the number of structures requiring some kind of countermeasure is increasing. In taking countermeasures, it is important to grasp the deterioration of structures as accurately as possible, clarify the deterioration mechanism, and select an appropriate countermeasure method to each deterioration mechanism.

A phenomenon that causes deterioration of a concrete structure is called a deterioration mechanism, and representative deterioration mechanisms include carbonation, salt damage, frost damage, and ASR.

1.2.1.1 frost damage

Frost damage of concrete is a deterioration phenomenon that occurs in cold regions, and is one of the serious deterioration phenomena accompanied by a decrease in strength and deterioration of aesthetics. The frost damage is a phenomenon in which repeated freeze-thaw of water in pores of concrete causes repeated

expansion pressure, which destroys the inside and surface of the concrete. Appears in the form of delamination, scaling, and pop-outs.

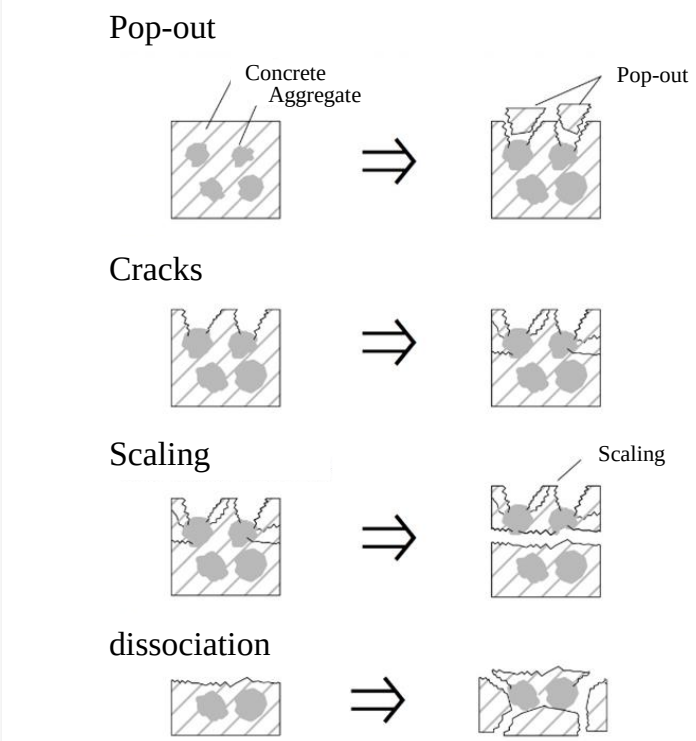

Fig. 1-1 Deterioration mechanism of frost damage

1.2.1.2 Salt damage

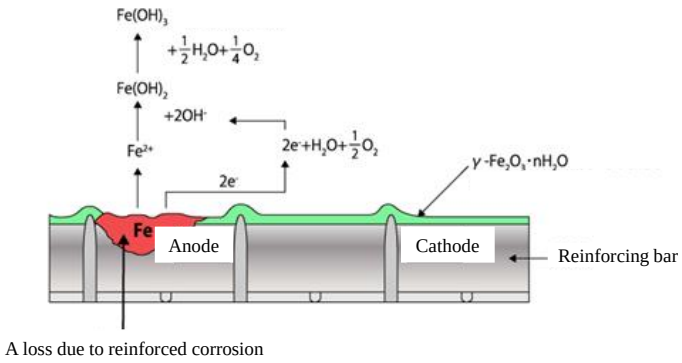

Fig. 1-2 Deterioration mechanism of salt damage

Salt damage is a phenomenon in which cracks occur in concrete due to corrosive expansion of reinforcing bars, impairing structural safety. The salt that comes from the coast penetrates into the concrete and corrodes the reinforcing bars. In mountainous areas in cold regions, salt damage is also affected when anti-freezing agents are sprayed on roads. The passive film that protects steel from corrosion is destroyed when chloride ions reach a certain concentration. By forming a corrosion battery between the part covered with the passive

film, steel material corrosion progresses violently. Fig. 1-2 shows the concept of reinforcing bar corrosion progression in concrete.

1.2.1.3 Carbonation

Steel corrosion due to carbonation is caused by the carbonation of highly alkaline concrete. Carbonation is a phenomenon in which CO_2 in the air penetrates into $Ca(OH)_2$ in hardened cement and changes to $CaCO_3$. In other words, carbonation can reduce the pH of concrete, and make the steel bars be corroded easily. Fig. 1-3 shows the concept of neutralization.

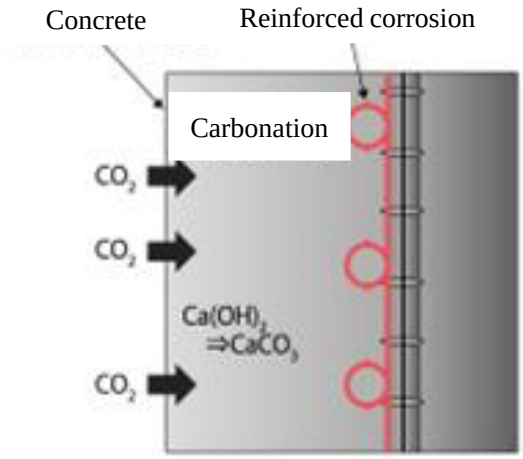

Fig. 1-3 Deterioration mechanism of carbonation

1.2.1.4 Alkali Silica Reaction

Degradation due to ASR (Alkali Silica Reaction) is a phenomenon in which alkali in cement reacts with a certain type of silica in aggregate, which causes cracks in concrete due to water absorption and expansion to lead to result in a decrease in performance. Fig. 1-4 shows the concept of deterioration due to ASR. Water-swelled aggregate causes relatively wide cracks in concrete. Then the aggregate loses its strength and the concrete structure weakens.

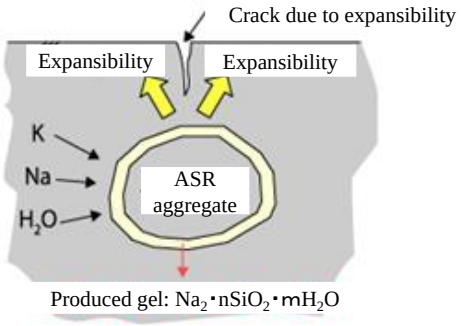

Fig. 1-4 Deterioration mechanism of ASR

1.2.3 Combined deterioration of concrete

So far, most of the studies related to the durability of concrete have focused on a single deterioration mechanism. However, as it can be well known that the cases of deterioration of actual structures cannot be evaluated by a single deterioration mechanism, interest in combined deterioration has been increasing.

Combined deterioration refers to a deterioration phenomenon in which more than one of the deterioration mechanisms described above occurs simultaneously. Since this phenomenon is complicated from an engineering point of view, and there are various combinations of deterioration, and due to the interaction of each deterioration phenomenon, it may show a different form of deterioration than when it occurs alone. The deterioration characteristics generated by the interaction of different deterioration phenomenon cannot be evaluated by adding two and more single deterioration model.

Depending on the combination, there are combinations that make each other's deterioration progress faster and more violently, so it is necessary to firmly judge whether multiple deterioration factors are acting.

1.2.4 Type of combined deterioration

Frost damage is a representative deterioration phenomenon of concrete in cold regions. Therefore, it is important to understand the change in frost damge of concrete suffered salt damage, carbonation and ASR. The combined deterioration of frost damage can be divided into three categories, combined deterioration beteeen salt damage and frost damage(S&F), combined deterioration beteeen carbonation and frost damage (C&F), combined deterioration beteeen ASR and frost damage(A&F).

1.3 Outline of fly ash (FA) cement and blast furnace slag (BFS) cement

In recent years, in order to establish a sustainable society with low carbon, it is expected that mineral

admixtures, such as blast furnace slag (BFS) or fly ash, are increasingly used as concrete material from the viewpoint of reducing environmental load, in which the reduction of CO_2 emission and effective utilization of industrial byproducts were carried out. Generally, the concrete using these materials has better durability and long-term mechanical properties than ordinary Portland cement (OPC) concrete.

1.3.1 Fly ash cement

1.3.1.1 Manufacture of fly ash cement

Fly ash is fine-grained coal ash that is generated as a by-product when coal is burned in the boiler of a coal-fired power plant. It floats in high-temperature combustion gas, becomes fine spherical particles as the temperature drops at the boiler outlet, is collected by an electrostatic precipitator, and is dried and stored in a silo. Fly ash cement is produced by mixing this fly ash with ordinary Portland cement. Fig. 1-5 shows the production flow of fly ash.

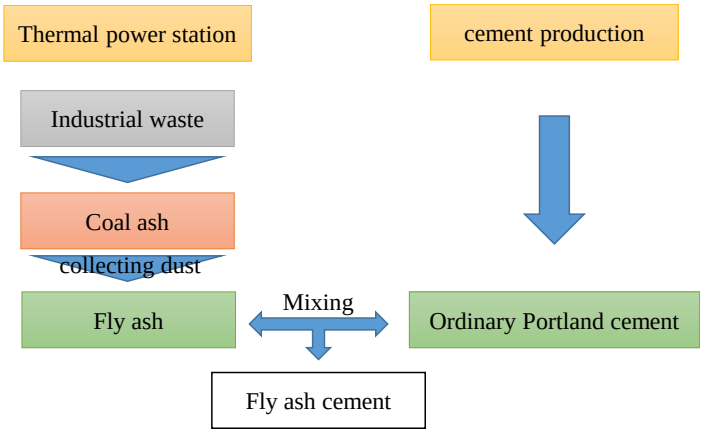

Fig. 1-5 Manufacture of fly ash cement

1.3.1.2 Environmental impact reduction effect of fly ash cement

Fly ash is an industrial by-product generated from coal-fired power plants, etc. The amount generated in Japan in 2017 was 12.8 million tons, in which 99% was effectively utilized. However, only 1.3% is used as a cement admixture [6]. Fly ash cement uses less ordinary cement, which can reduce the consumption of limestone that is the main raw material of ordinary cement, and by-products can be effectively used, which saves resources. It can be said that by expanding the replacement of fly ash cement with ordinary cement in this way, it is possible to reduce a large amount of CO_2 emissions. Table. 1-1 shows the reduction of CO2 due to fly ash replacement ratio.

Table. 1-1 Reduction of CO2 due to fly ash replacement ratio

Fly ash replacement ratio	0%	10%	20%
CO2 emissions (kg/m^3)	240.87	213.04	189.95
Reduction of CO_2	0%	11.6%	21.1%

1.3.1.3 Type of Fly ash cement

Fly ash cement is classified into types A, B, and C according to the amount of fly ash mixed. Most of the fly ash cement currently in use is type B, and data on types A and C are scarce.

Type of fly ash cement（JIS R 5213）

Type	FA replacement ratio (%)
Fly ash cement type A	5%~10%
Fly ash cement type B	10%~20%
Fly ash cement type C	20%~30%

1.3.1.4 Properties of fly ash concrete

Compared to ordinary concrete, fly ash concrete has the following properties,

- High long-term strength
- Low heat generation rate
- Improved watertightness
- Suppression of alkali-silica reaction

On the other hand, fly ash concrete has the following properties, so appropriate considerations are required when using it.

- Low initial strength.
- Decreased frost resistance due to decreased air entrainment [7]
- Low carbonation resistance

1.3.1.5 Frost resistance of concrete using fly ash

In Fig. 1-6, Ando et al. [8] reported for indoor test, fly ash concrete equivalent to fly ash cement types B and C showed lower resistance to frost damage than other levels, but the relative dynamic modulus of elasticity was

kept above 80%. In the outdoor exposure test, the fly ash concrete showed high frost damage resistance because the deterioration in winter was self-repaired in summer by the slow pozzolanic reaction for a long period of time.

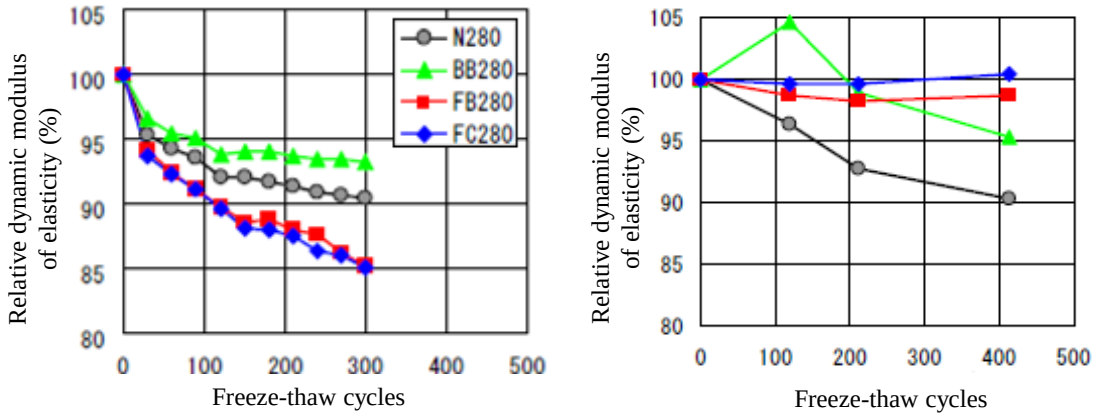

Freeze-thaw test indoor　　Freeze-thaw test outdoor

Fig. 1-6 contrast of frost resistance for indoor and outdoor test

1.3.2 BFS cement

1.3.2.1 Manufacture of BFS cement

Blast furnace slag is a by-product produced during the production of pig iron in a blast furnace. Blast furnace cement is produced by mixing ground granulated blast furnace slag, which is obtained by pulverizing granulated slag obtained by quenching this blast furnace slag with water, and ordinary cement. Figure 1-7 shows the production flow of blast furnace cement.

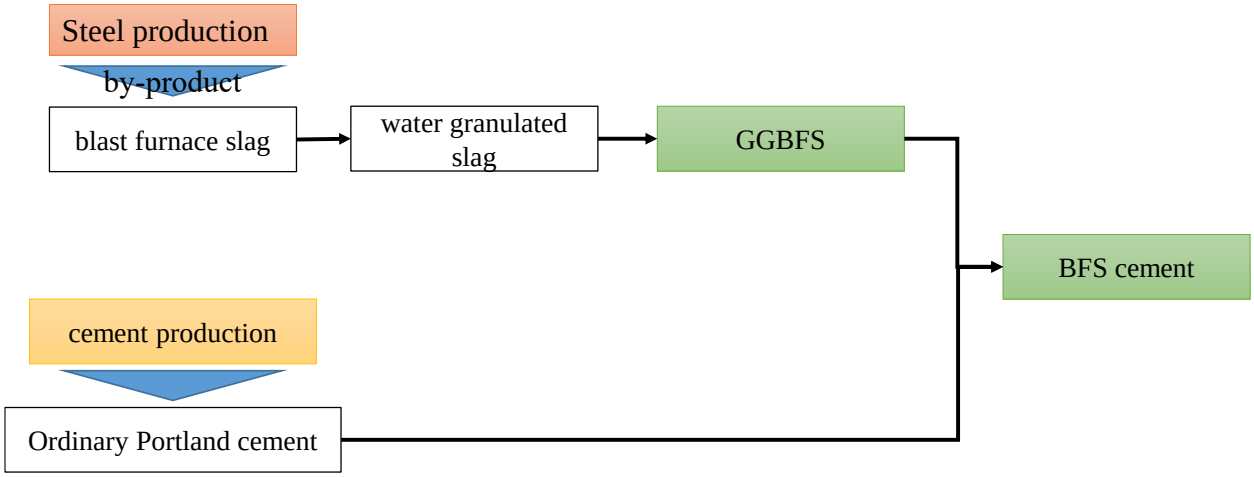

Fig. 1-7 Manufacture of BFS cement

1.3.2.2 Environmental impact reduction effect of BFS cement

When producing OPC cement, it is necessary to calcine and grind limestone, but for BFS cement, it has latent hydraulicity by mix BFS and OPC cement, which can reduce CO2 emissions. In addition, since the use of BFS can reduce the consumption of limestone, which saves resources. It can be said that a large amount of CO_2 emissions can be reduced by expanding the replacement of BFS to OPC cement. Table. 1-2 shows the amount of CO_2 reduction due to BFS replacement ratio.

Table. 1-2 Reduction of CO_2 due to BFS replacement ratio

BFS replacement ratio		0%	20%	30%	40%	50%
CO_2 emissions (kg/m³)	Caused by cement	266	213	186	160	133
	Caused by BFS	0	2	3	4	4
	Total	266	215	189	164	137
	Reduction of CO_2 (%)	0	19	29	38	48

1.3.2.3 Type of Fly ash cement

Blast-furnace cement is classified into types A, B, and C. Most of the BFS cement currently in use is type B, and other types are scarce.

Type of fly ash cement（JIS R 5213）

Type	FA replacement ratio (%)
BFS cement type A	5%~30%
BFS cement type B	30%~60%
BFS cement type C	60%~70%

1.3.2.4 Properties of BFS concrete

compared to OPC concrete Concrete using BFS has the following properties:

- High resistance to sea water and chemical attack, and low diffusion coefficient of chloride ions
- Suppression of the alkali-silica reaction.
- High watertight
- High long-term strength

On the other hand, since BFS concrete has the following properties, appropriate considerations are required when using it.

- Low initial strength
- Low carbonation resistance

1.3.1.5 Frost resistance of concrete using BFS

Chikamatsu et al. [9] prepared AE concrete using BFS cement type B and conducted freeze-thaw tests. As a result, BFS concrete has a same or better frost resistance with OPC concrete.

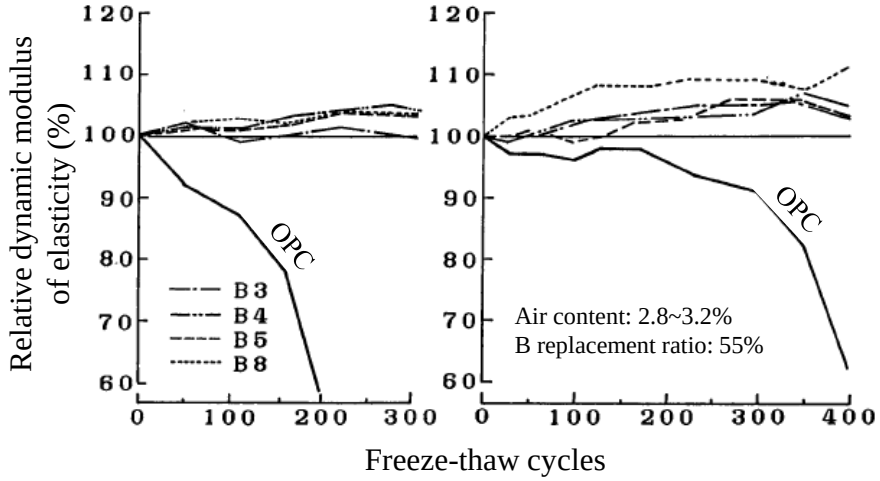

Fig. 1-7 Change in relative dynamic modulus of elasticity due to freeze-thaw cycles

1.4 Problem definition

From the previous studies in recent years, some of the main problems of investigation could be described as follows:

(1) In cold regions, the combined deterioration on frost damage of concrete has been attracting new wild attention in the world. Among them, although the combined deterioration between frost damage and salt damage has been expensively sturdied, there are few studies on the the combined deterioration between frost damage and carbonation, and between frost damage and ASR.

(2) BFS and FA are used more widely to reduce the cement consumption in the field of building materials, due to additive of BFS and FA, the carbonation resistance of concrete is reduced, and ASR resistance is improved. Based on that, it is necessary to investigate the change in frost damage of concrete subjected to carbonation and ASR.

(3) The effect of BFS and FA on the combined deterioration is little studied, it is important to grasp the deterioration mechanism of the combined deterioration. In addition, we will evaluate the use of BFS and FA on the durability of concrete.

(4) Comparing with OPC concrete, the additive of BFS and FA can change the pore structure, which is related closely to frost resistance. In addition, carbonation and ASR of concrete is also change the pore structure. Therefore, it is important to clarify their relationship.

1.5 Research aims and thesis organization

This thesis is organized into six chapters as follows:

Chapter 1 covers the research background of combined deterioration of concrete, outline of BFS and FA.

Chapter 2 discusses the previous studies of combined deterioration in recent years. It is well known that the study on S&F has extensively investigated, while C&F and A&F has attracted the wildly attention in the world. The effect of BFS and FA on S&F is also investigated. However, the effects of BFS and FA on C&F and A&F have little researched in the world.

Chapter 3 investigates the change in frost resistance and pore structure of concrete containing BFS with various replacement ratio due to carbonation. The changes in water absorption were measured by RILEM / CIF test and in pore structure were measured by the mercury intrusion porosimetry method due to carbonation.

Chapter 4 investigates the frost and scaling resistance of concrete with various fly ash (FA) replacement ratios exposure to air and accelerated carbonation conditions. The changes in water absorption were measured by RILEM / CIF test and in pore structure were measured by the Archimedes method and the mercury intrusion porosimetry method due to carbonation.

Chapter 5 investigates the effect of BFS and FA on the combined deterioration of concrete. ASR expansion is caused due to ASR aggregate to serious endanger the safety of concrete, which has been attracting new wild attention. In clod region, concrete is always subject to frost damage in winter. And the change in combined deterioration between the ASR and frost damage is researched.

Chapter 6 shows the thesis conclusion.

The following is this thesis structure:

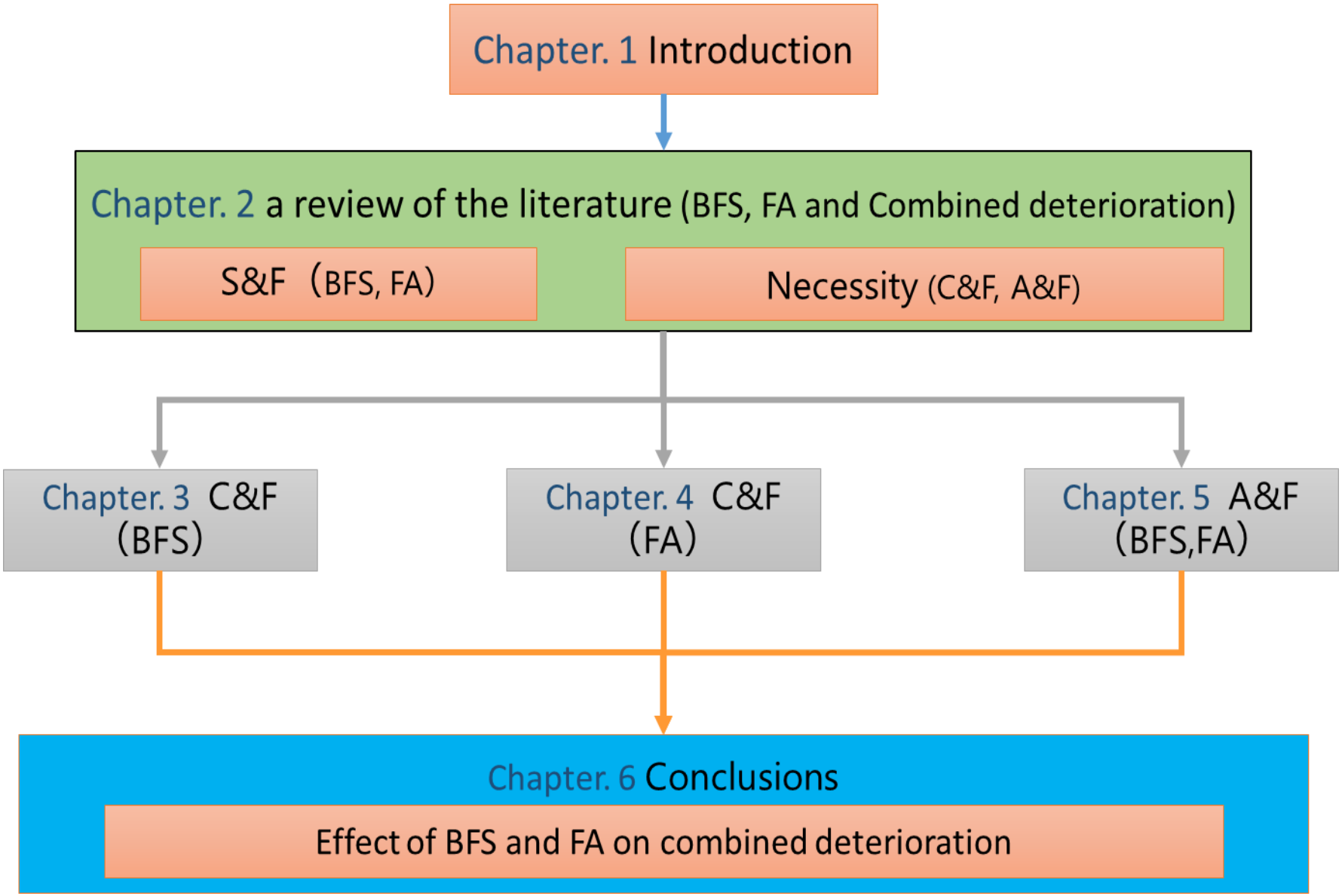
Chapter. 1 Introduction
Chapter. 2 a review of the literature (BFS, FA and Combined deterioration)
S&F （BFS, FA)
Necessity (C&F, A&F)
Chapter. 3 C&F (BFS)
Chapter. 4 C&F (FA)
Chapter. 5 A&F (BFS,FA)
Chapter. 6 Conclusions
Effect of BFS and FA on combined deterioration

References:

1. Wenyan Z., Yukio H. and Seung H.N., "Drying shrinkage and microstructure characteristics of mortar incorporating ground granulated blast furnace slag and shrinkage reducing admixture", Construction and Building Materials, Vol. 93, 2015, pp. 267–277.

2. Seung H.N., Yukio H., Madoka T., Osamu K., Takahiro S. and Mohamed Z., "Experimental investigation on reaction rate and self-healing ability in fly ash blended cement mixtures", Journal of Advanced Concrete Technology, Vol. 10, 2012, pp. 240–253.

3. Takeki M, Yasunori S, Takashi S and Kazuto F, "Low-carbon concrete using ground granulated blast-furnace slag and fly ash ", Cement Science and Concrete Technology, No. 64, 2010, pp. 295-302.

4. Ryuichi C, Yasuhiko Y and Yuzo N, "Frost resistance on the concete including Blast Furnace Slag", Proceedings of the Japan Concrete Institute, Vol. 11, 1989, pp. 355-360.

5. Masahiko K, Yasutomi A, Toshikatsu I and Yachi Y: "Research on Performance of concrete including fly ash", Proceedings of the Japan Concrete Institute, Vol. 23, No.1, 2001, pp. 301-306.

6. Coal Energy Center: Coal Ash Nationwide Survey Report (2017)

7. Osamu Chipo, Yukio Hama: Air Entrainment, Cellular Structure and Frost Damage Resistance of Fly Ash Concrete, Journal of Structural Engineering, Architectural Institute of Japan, No.558, 1-6, 2002.8

8. Mutsumi Ando, Toshiki Saito, Kazuhiro Imai: Frost Damage Resistance of Fly Ash Concrete by Exposure Test, The 66th Annual Conference of the Japan Society of Civil Engineers, V-066 (131-132)

9. Ryuichi Chikamatsu et al.: Frost damage resistance of concrete using ground granulated blast furnace slag, Proceedings of the Japan Concrete Institute, 11-1, 1989

Chapter 2

PREVIOUS STUDIED ON COMBINED DETERIORATION OF CONCRETE

2.1 Overview

In order to evaluate the durability of structures with a higher degree of accuracy, the combined deterioration problem becomes a big problem that cannot be avoided. In addition, from the viewpoint of maintenance planning for existing structures, the combined deterioration problem is an important issue that should be addressed as soon as possible. In order to take reliable measures against structures that have deteriorated, it is most important to accurately grasp the deterioration phenomenon, conduct more accurate deterioration evaluation.

Combined deterioration is mainly classified into three types: 1) independent combined deterioration, 2) synergistic combined deterioration, and 3) causal combined deterioration.

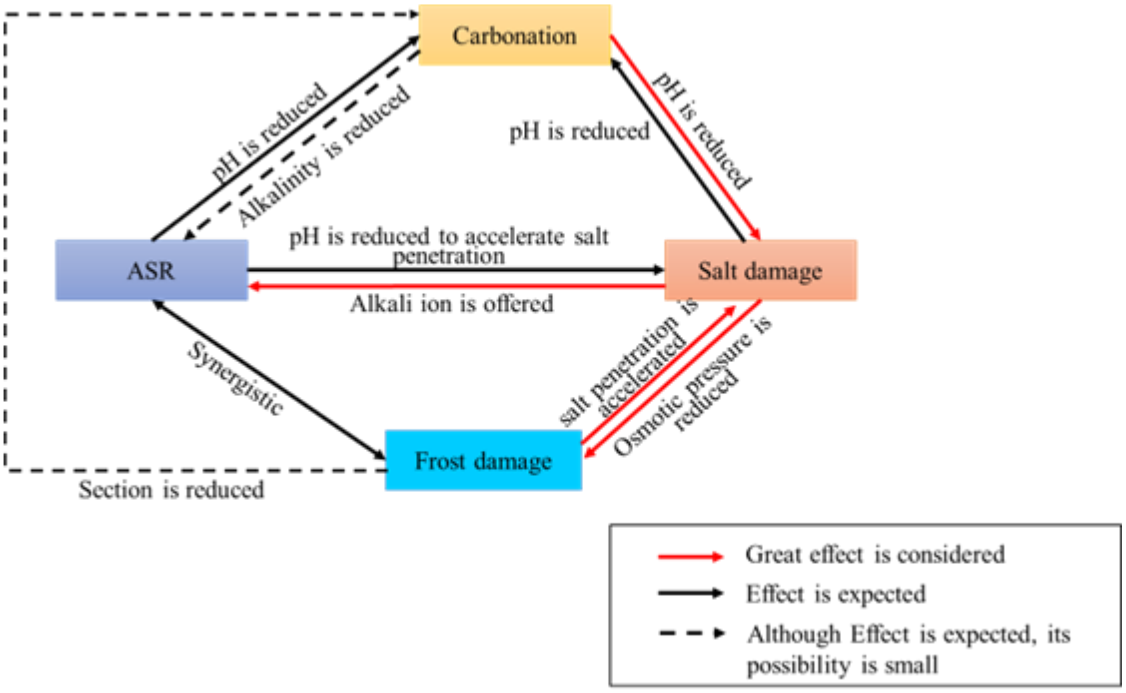

Fig. 2-1 Correlation of combined deterioration [1]

Independent combined deterioration means that the deterioration actions occur simultaneously, but no synergistic effect occurs between the deterioration actions, and the rate of deterioration progression is the same as in the case of single deterioration. Synergistic compound deterioration is combined deterioration in which the speed of deterioration progression or deterioration symptoms is accelerated more than single deterioration due to a synergistic effect at the same time of the deterioration action. Causal combined deterioration is combined

deterioration in which one deterioration process makes the other deterioration process happen, or combined deterioration in which the manifestation of one deterioration results in the other deterioration process. In the case of Causal combined deterioration, it is normal for one deterioration action to precede and the other deterioration action to start working with a time lag, and deterioration progression also appear at the time lag.

In Fig. 1, combined deterioration is organized by applying the above three classifications [1].

In the next, we will introduce the previous studies on the combined deterioration of frost damage.

2.2 Combined deterioration between salt and frost damage

In the world, salt damage seriously threatens the safety of RC concrete, and will accelerate the damage of frost damage. Therefore, in the field of concrete durabiliy research, the combined deterioration between salt and frost damage has been brought to attention, and its studies has been conducted extensively. In the next, some of the research reslits will be introduced.

2.2.1 Change in properties of concrete due to salt damage

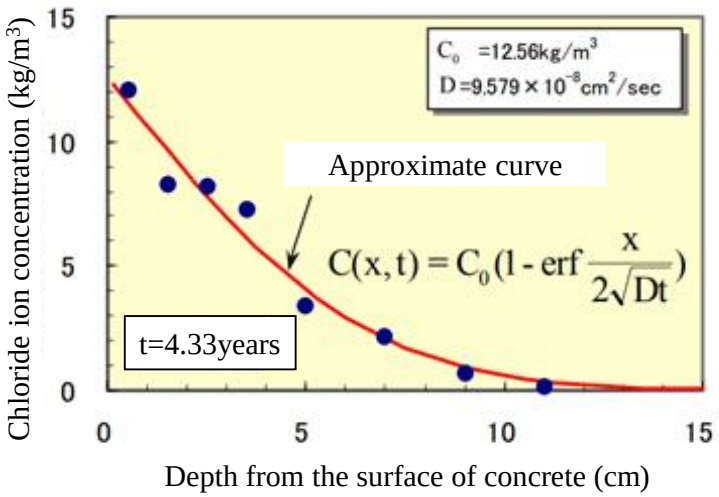

Fig. 2-2 Chloride ion concentration distribution in concrete after 4.33

In according to study [2] of Yu Yokota et al., Fig. 2-2 shows chloride ion concentration distribution in concrete after 4.33 years.From this figure, it is well known that after the concrete is subjected to salt damaged, there is a strong connection between chloride ion concentration and the surface depth of concrete, the concentration tends

to be low with the increasing depth.

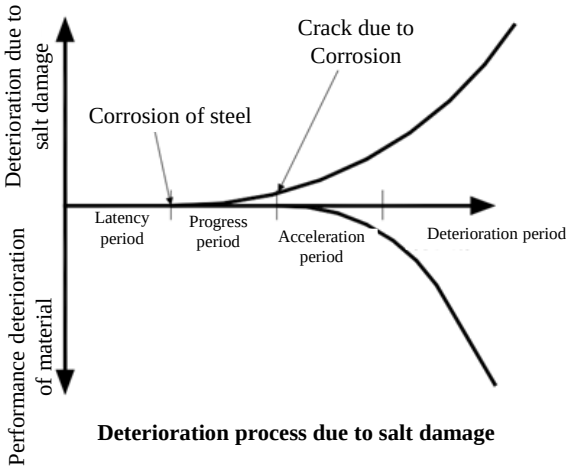

Fig. 2-3 Relationship between deterioration and performance deterioration

Fig. 2-3 shows the relationship between deterioration and performance deterioration [3]. In the figure, chloride ions gradually permeate the concrete, and the incubation period is the period until the chloride ion concentration at the steel covering position reaches the corrosion generation limit concentration of 1.2 kg/m^3. the growth stage is the period in which cracks occur, the acceleration period is the period in which the corrosion rate increases due to the occurrence of corrosion cracks and the performance of the member gradually declines, and the degradation period is the period when the performance of the member decreases significantly due to the increase in the amount of corrosion.

2.2.2 The effect of BFS and FA on the salt damage

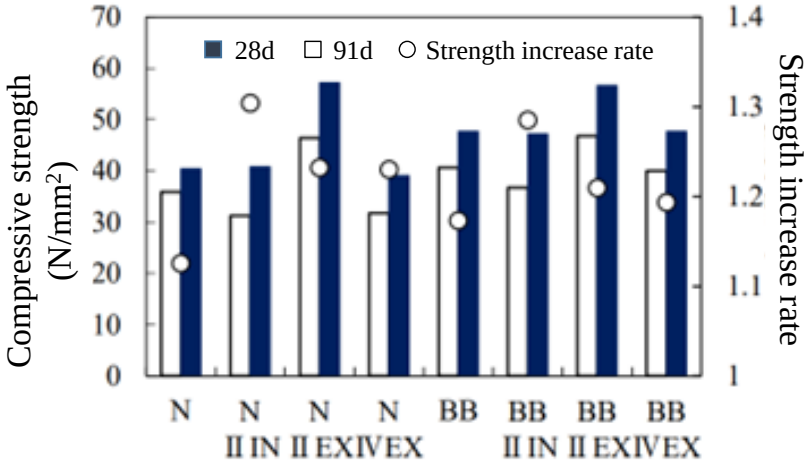

Fig. 2-4 Compressive strength and the strength increase rate of OPC and BFS concrete

In according to study [4] of Kenta Miura et al., Fig. 2-4 shows the compressive strength and the strength increase rate obtained by dividing the 91-day strength by the 28-day strength. Comparing the case of OPC concrete and BFS concrete, BFS concrete has slightly higher strength overall than OPC concrete, regardless of the material age.

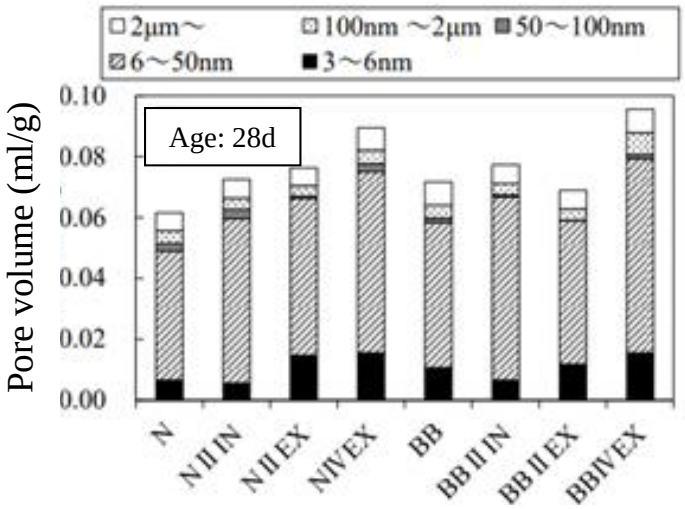

Fig. 2-5 Change in pore structure due to BFS and FA

Fig. 2-5 shows the pore size distribution of mortar sealed and cured up to 91 days. For OPC concrete, concrete using FA has a higher total pore volume than concrete without FA. Comparing the OPC concrete and BFS concrete, the additive of BFS can increase the total pore volume.

2.2.3 Combined deterioration of salt damage and frost damage

2.2.3.1 OPC concrete

Takeda et al. [5] conducted a combined deterioration environment in which salt damage act on OPC concrete using an AE admixture. In order to grasp the durability of concrete in a combined deterioration environment between salt damage and frost damage, we investigated the durability of concrete subjected freeze-thaw action and the penetration of chloride ions.

Fig. 2-6 shows changes in the relative dynamic modulus of elasticity (RDM) of concrete. As a result, the RDM decreases due to freeze-thaw action under salt-supplied environment, and the diffusion coefficient of chloride ions increases. For the case of AE admixture, frost damage resistance was improved well. In addition, the higher the water-cement ratio, the smaller the influence of chloride ions.

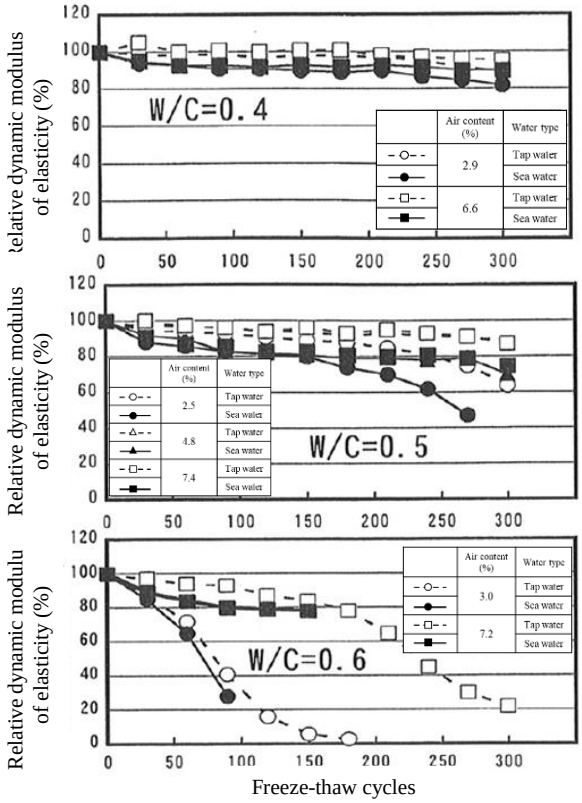

Fig. 2-6 Change in RDM of concrete

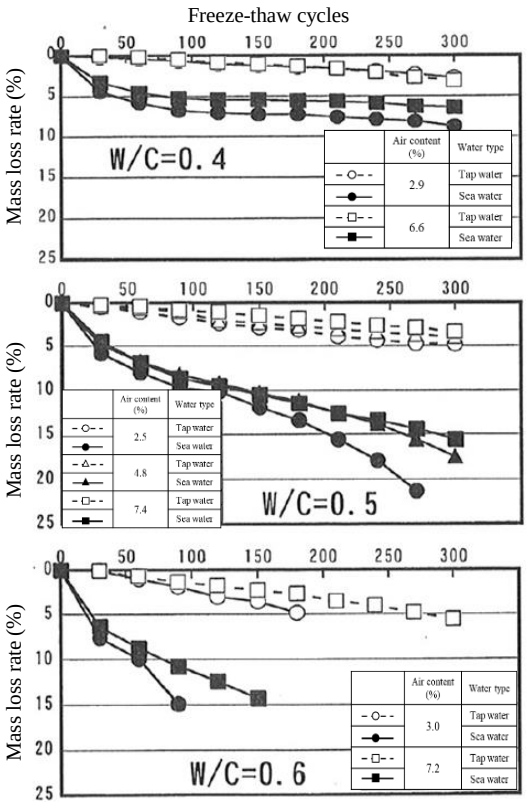

Fig. 2-7 Change in scaling of concrete

Fig. 2-7 shows changes in the mass change rate of concrete. As a result, under salt-supplied environment, when subjected to frost damage, the scaling of surface tends to increase markedly.

2.2.3.1 BFS and FA concrete

In the research by Yasuhiro Koda et al. [6], frost resistance in a salt environment and the additive of FA are investigated.

Fig. 2-8 shows the scaling mass results of concrete. From the figure a, it can be well known that the air content can reduce obviously the scaling mass of concrete, which can confirm the inhibition of scaling due to AE admixture. In other words, entrainment of entrained air is essential for the improvement of frost resistance. In addition, it can be seen that when W/C decreases, the scaling mass tends to decrease. From the figure b, it is obtained that the additive FA increases the scaling mass. From the figure c, BFS also reduces the scaling resistance.

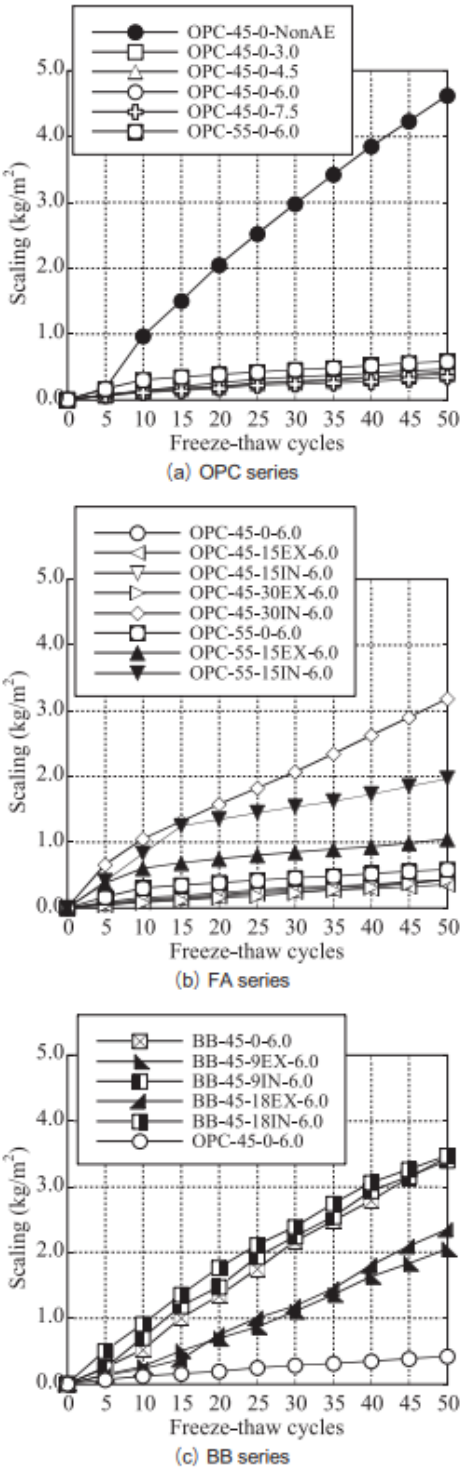

Fig. 2-8 Change in scaling mass of OPC, FA, BFS concrete

2.3 Combined deterioration between carbonation and frost damage

In the studies of frost resistance in recent years, the durability on concrete buildings in an exposed environment have been focused on, and the frost resistance of concrete exposed to carbonation conditions has

aroused public concern worldwide. It has been pointed out that the deterioration of concrete subjected to multi-damage processes could be significantly promoted [7]. Additionally, based on the results of research projects at VTT (VTT is one of Europe's leading research institutions) focusing on coupling deterioration mechanisms, Miguel Ferreira et al. [8] and H. Kuosa et al. [9] pointed that long-term aging with carbonation and drying at RH 65% results in larger frost-salt scaling compared with standard testing where freeze-thaw started soon after 28-day. However, there has been little research on the change in frost resistance of concrete added BFS and fly ash under the carbonation conditions.

In the next the previous studies on carbonation and frost damage will be introduced in detail.

2.3.1 Change in properties of concrete due to carbonation

2.3.1.1 carbonation resistance

OPC concrete

According to the experiment by Tatematsu et al.[10], the carbonation resistance of the cement paste using OPC decreased as the water-cement ratio increased in Fig .2-9.

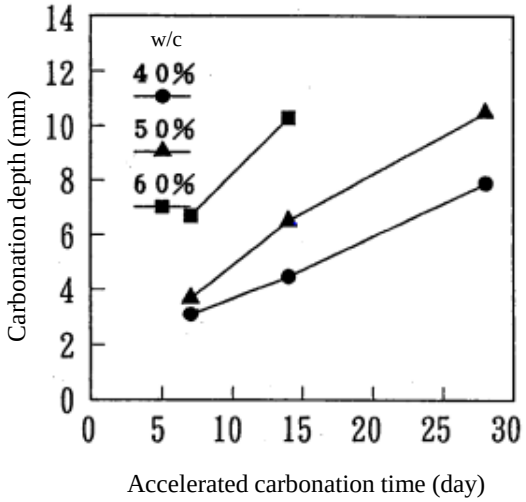

Fig. 2-9 relationship between carbonation depth and water-cement ratio

Fly ash concrete

Huang Ritsu [11] et al. predicted the progress of carbonation of concrete mixed with FA. As a result, from Fig. 2-10 and Fig. 2-11, in the concrete mixed with fly ash, $Ca(OH)_2$ is consumed by the pozzolanic reaction

and the carbonation resistance decreases, but the microstructure becomes denser, the diffusion coefficient decreases, which can explain the carbonation resistance tend to increases.

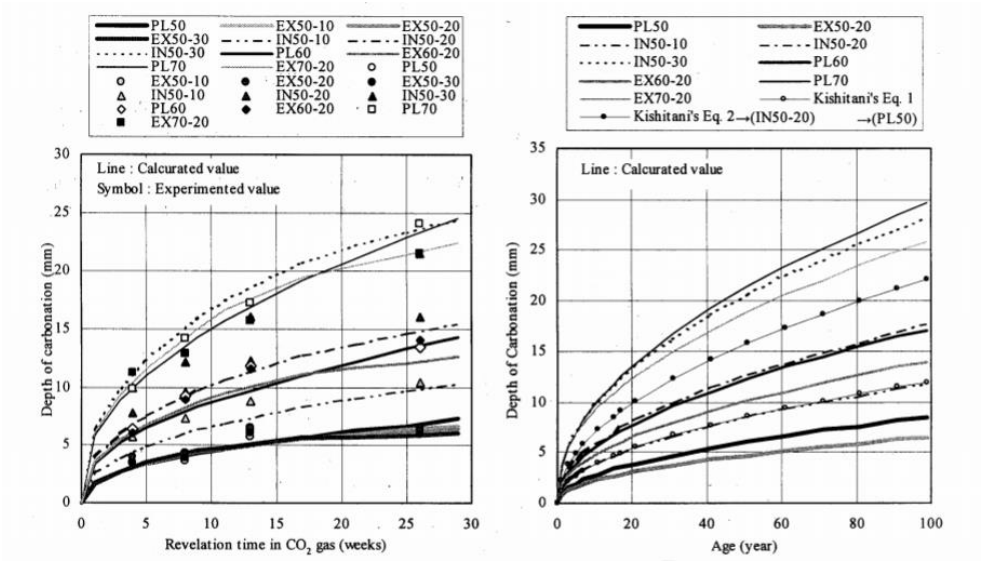

Fig. 2-10 Relationship between accelerated carbonation test results and numerical calculation results

Fig. 2-11 prediction of carbonation progress

BFS concrete

An experiment was conducted by Matsuya [12] to understand the basic physical properties of concrete using BFS. As a result, from Fig. 2-12, it is found that the carbonation resistance of BFS concrete decreased as the replacement ratio of BFS increased.

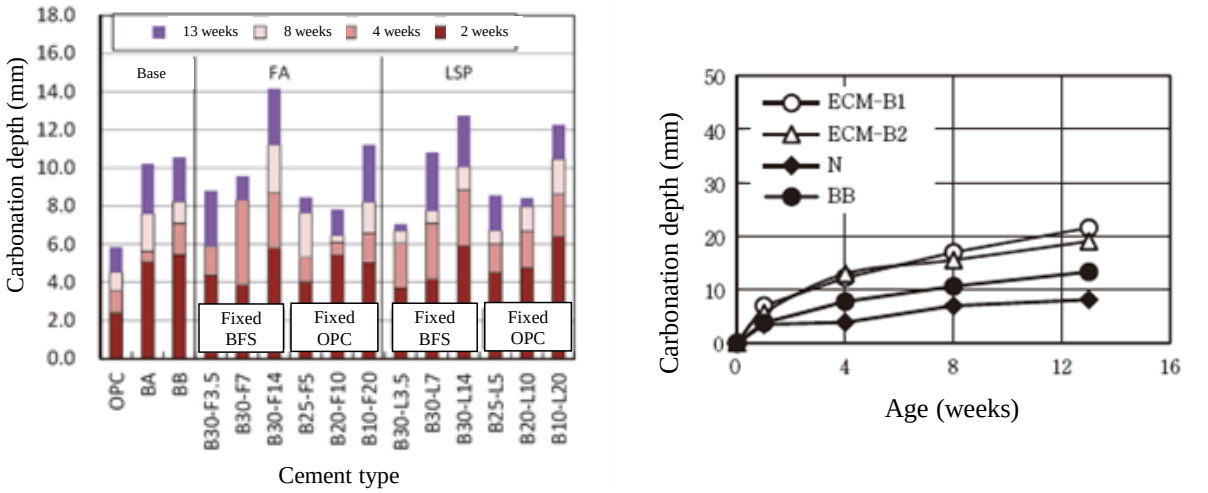

Fig. 2-12 carbonation depth of OPC and BFS concrete

2.2.1.2 Change in pore structure

Figure 2-13 shows the changes in pore structure of OPC and BFS concrete due to carbonation obtained by

Harasawa et al.[13]. From the figure, after water curing, the additive of BFS can increase the pore volume. In addition, for ,OPC and BFS concrete, Carbonation can coarsen the pore structure.

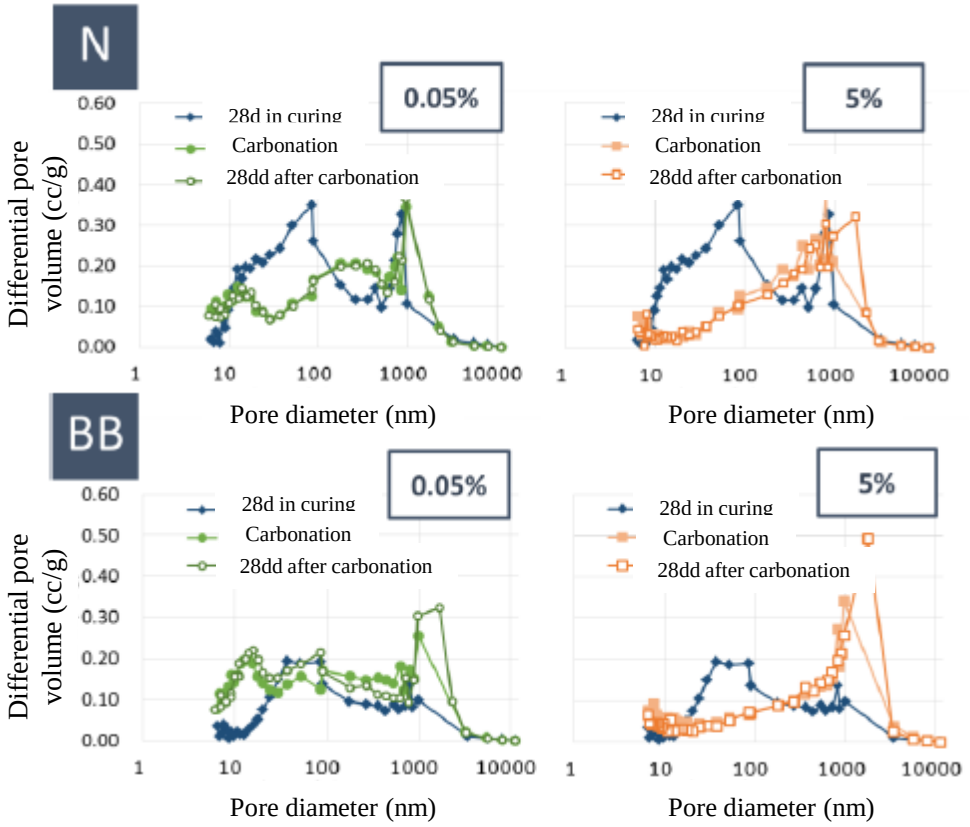

Fig. 2-13 change in pore structure of BFS concrete due to carbonation

For the study of Igarashi et al. [14], Figure 2-14 shows the total pore volume and pore size distribution of FA concrete.

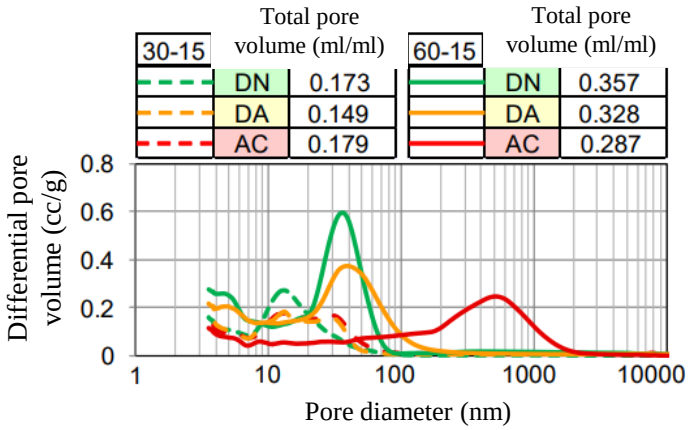

Fig. 2-14 Total pore volume and pore size distribution of FA concrete

From the figure, in the case 30(W/B)-15(FA placement ratio), a slight shift in the peak diameter toward larger diameters due to carbonation is seen in DA (0.3% CO_2) and AC (5% CO_2). Although the total pore

volume decreased in the case of 60-15, the peak diameter shifted toward larger diameters due to carbonation, especially in AC. This agrees with the trend of increasing oxygen diffusion coefficient. In other words, for W/B = 60%, carbonation increased the number of large pores, which increases the oxygen diffusion coefficient.

2.2.1.3 Changes in hydration products

Carbonation components of hardened cement are said to be mainly calcium hydroxide and C-S-H. the change in amount of calcium hydroxide due to carbonation is introduced in the next.

Figure 2-15 shows the change in calcium hydroxide content due to carbonation of OPC concrete obtained by Toyoura et al.[15]. The amount of calcium hydroxide decreases due to carbonation.

Before carbonation, calcium hydroxide and C-S-H are dissolved in the water on the pore surface, and carbon dioxide in the air also dissolves in the water on the pore surface. Calcium carbonate is produced in water. In addition, since the solubility of calcium hydroxide is higher than that of C-S-H, calcium hydroxide tends to be carbonated easily .

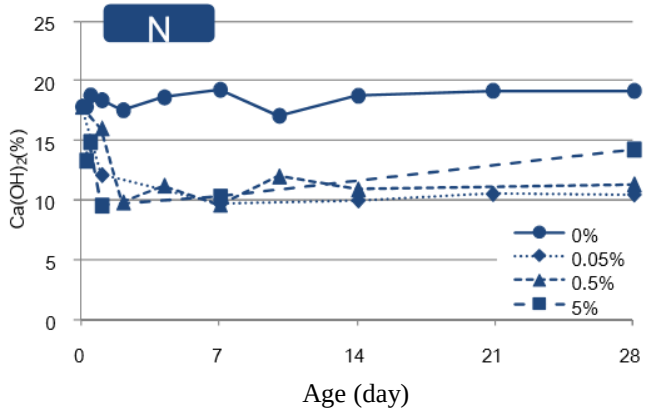

Fig. 2-15 change in $Ca(OH)_2$ due to carbonation

Change in C-S-H due to carbonation.

As an example, the carbonation reaction equation of C-S-H with a Ca/Si ratio of 1.4 and an H_2O/Si ratio of 1.9 is shown below. Due to carbonation, C-S-H is decomposed into $CaCO_3$ and SiO_2 as shown in eq. 1, or C-S-H is partially decomposed along with the generation of $CaCO_3$ as shown in eq. 2. C-S-H with a ratio of 1 or more may transform into low Ca/Si ratio C-S-H (C-S-H with a Ca/Si ratio of 1 or less). The difference between them is H_2CO_3, and the more H_2CO_3 generated can accelerate the decomposition of C-S-H.

$$1.4CaO \cdot SiO2 \cdot 1.9H2O + 1.4H2CO3 \rightarrow 1.4CaCO3 + SiO2 + 3.3H2O \quad \ldots [1]$$

$$1.4CaO \cdot SiO2 \cdot 1.9H2O + xH2CO3 \rightarrow (1.4 - x)\ CaO \cdot SiO2 \cdot 1.9H2O + xCaCO3 + xH2O \quad \ldots [2]$$

Figure 2-16 shows the ratio of low Ca/Si ratio C-S-H and high Ca/Si ratio C-S-H due to carbonation of C-S-H with a Ca/Si ratio of 1.4 in corroding to Ishida et al. [16]. From these results, it is understood that carbonation of C-S-H reduces the Ca/Si ratio, and SiO_2 is generated.

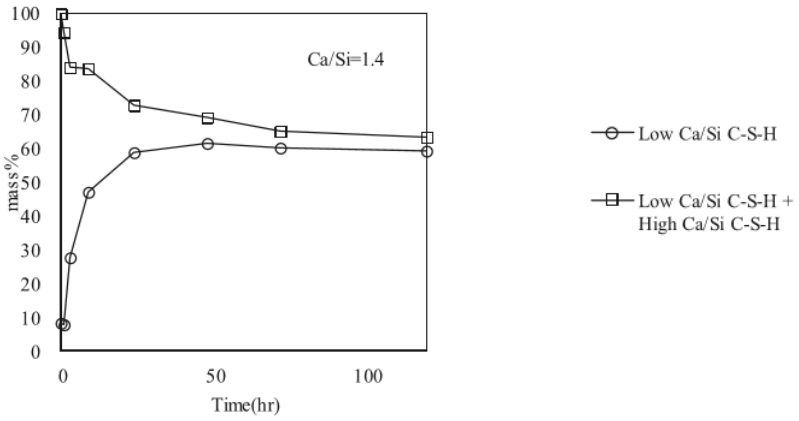

Fig. 2-16 change in hydration due to carbonation of C-S-H

Calcium carbonate by C-S-H with different Ca/Si ratios

Fig. 2-17 shows the amount of calcium carbonate produced by C-S-H with different Ca/Si ratios by Ito et al. [17]. It can be seen that the higher the Ca/Si ratio, the greater the amount of calcium carbonate produced by C-S-H.

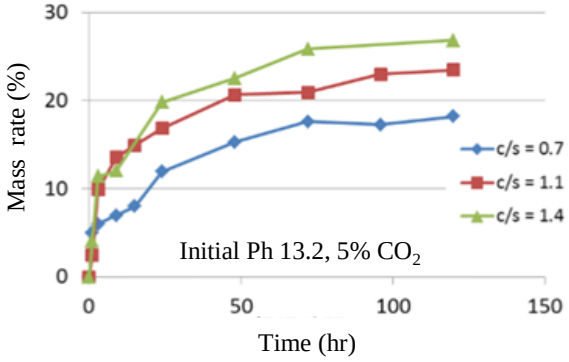

Fig. 2-17 The amount of calcium carbonate produced by C-S-H with different Ca/Si ratios

2.3.2 Combined deterioration of concrete between carbonation and frost damage

2.3.2.1 OPC concrete

Takeda et al. [3] investigated the change in frost resistance after carbonation of concrete and change in

carbonation after freeze-thaw of concrete of concrete to grasp the combined deterioration between frost damage and carbonation of OPC concrete using an AE admixture. For the results of carbonation after freeze-thaw as shown in Fig. 2-18, the greater the degree of frost damage deterioration, the lower the carbonation resistance. The higher the water-cement ratio, the more pronounced it becomes. In addition, as shown in Fig. 1-3-12, the change in frost resistance due to carbonation was not observed in the freeze-thaw test of carbonation concrete.

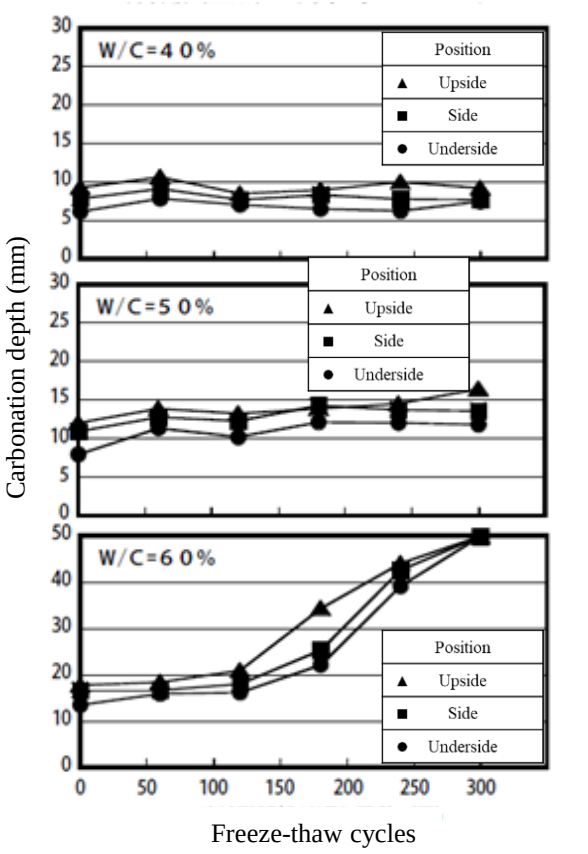

Fig. 2-18 Change in carbonation after freeze-thaw

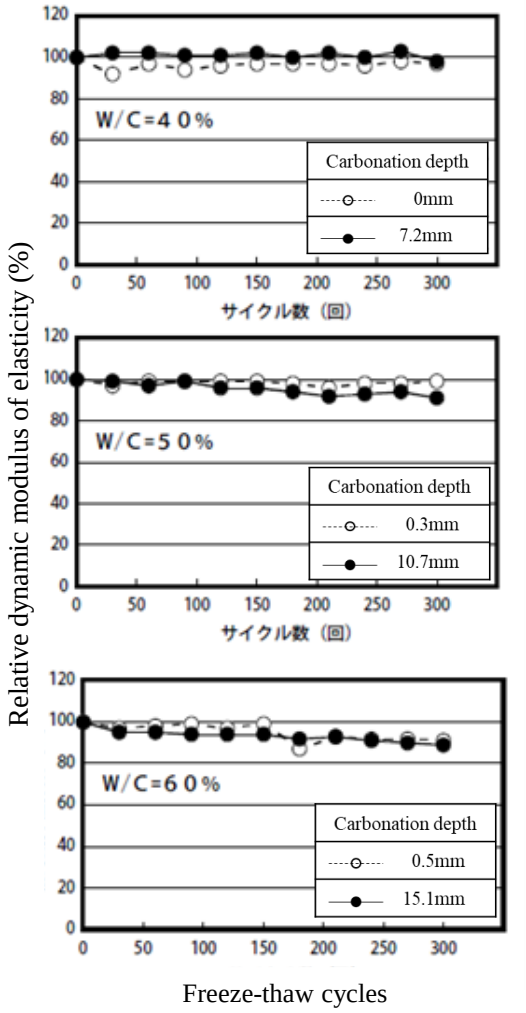

Fig. 2-19 change in frost resistance after carbonation

2.2.2.2 BFS and FA concrete

There has been little research on the change in frost resistance of concrete added BFS and fly ash under the carbonation conditions. Therefore, it is essential to experimentally assess the combined deterioration of carbonation and freeze-thaw resistance of BFS and fly ash concrete. In addition, the use of air-entraining (AE)

admixture is an effective countermeasure against frost damage, so it is extremely important to confirm the effect of the AE admixture on BFS and fly ash concrete.

Therefore, in the CHAPTER 3 and CHAPTER 4 of this study, the experimental program is designed to assess combined deterioration of carbonation and freeze-thaw resistance of BFS and fly ash concrete with different replacement ratio within the range of JIS R 5211 and JIS R 5213. The influence of fly ash or BFS with different replacement ratio on the mechanical properties, carbonation resistance and freeze–thaw resistance of concrete is evaluated.

2.4 Combined deterioration between ASR and frost damage

The dangers of ASR have only been discovered in recent years. And ASR seriously endangers the safety of concrete. At present, the research on ASR mainly focuses on the hazard of single ASR. But ASR can create cracks. This will greatly accelerate the freezing damage, which has aroused everyone's concern. Research on combined deterioration between ASR and frost damage has been started, but still very few. With the popularity of BFS and FA, which have a significant inhibitory effect on ASR. the effect of BFS and FS on the combined deterioration between ASR and frost damage is also aroused the interest of all.

In the next the previous studies on ASR and frost damage will be introduced in detail.

2.4.1 changes in properties of concrete due to ASR

In the "maintenance and management guidelines for alkali-aggregate reaction of highway bridges", continuous cracks of 1 mm or more occurred in the bridge substructure (T-type pier) due to the progress of ASR in Fig. 2-20.

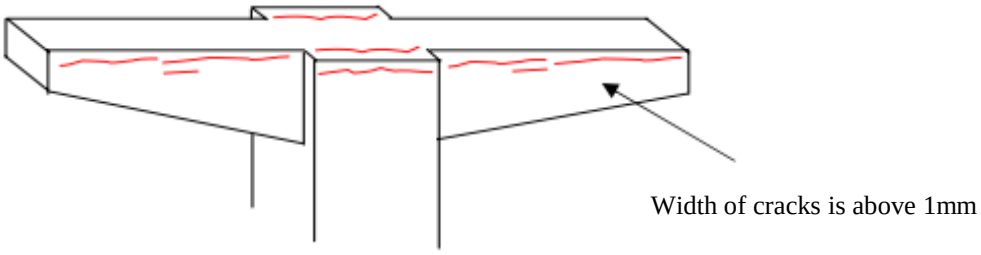

Fig. 2-20. Cracks due to ASR

Kobayashi et al.'s study [19] described the cracks due to ASR.

Fig. 2-21 ASR gel and cracks due to ASR

In Fig. 2-21 cracks and ASR gel due to ASR are seen.

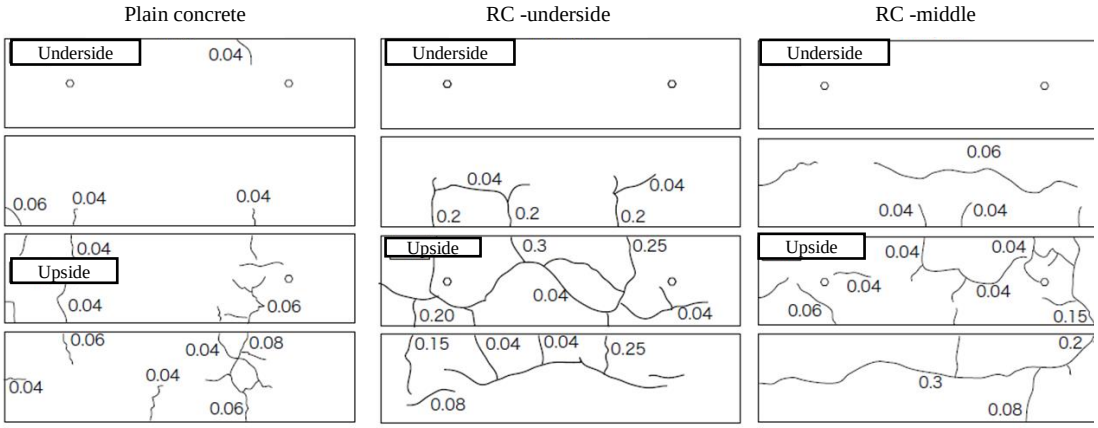

Fig. 2-22 Cracks distribute due to ASR

Fig. 2-22 shows the cracks distribute of concrete after 240 days of ASR. At this stage, cracks with a maximum width of 0.3 mm were formed. In addition, when comparing the unreinforced concrete and the RC concrete, it seems that cracks in the member axial direction are predominant in the RC concrete.

In Takagi et al.'s study [12], the deterioration of mechanical properties of concrete subjected to ASR was investigated.

Fig. 2-22 shows the change in e expansion due to ASR. from the figure, it can be well known that the expansion increases due to ASR, and the high the water-cement ratio can reduce the ASR resistance, which is due to the easier diffusion of OH- ions and water inside the concrete.

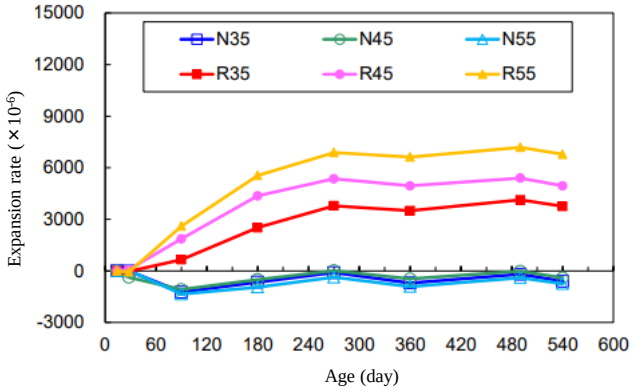

Fig. 2-22 change in expansion rate due to ASR

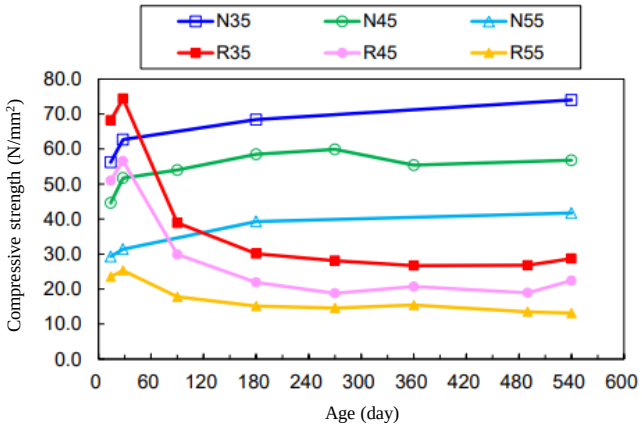

Fig. 2-23 change in compressive strength due to ASR

Fig. 2-23 shows the change in compressive strength. from the figure, when subjected to ASR, the compressive strength of concrete tend to decrease, which is because of cracks due to ASR.

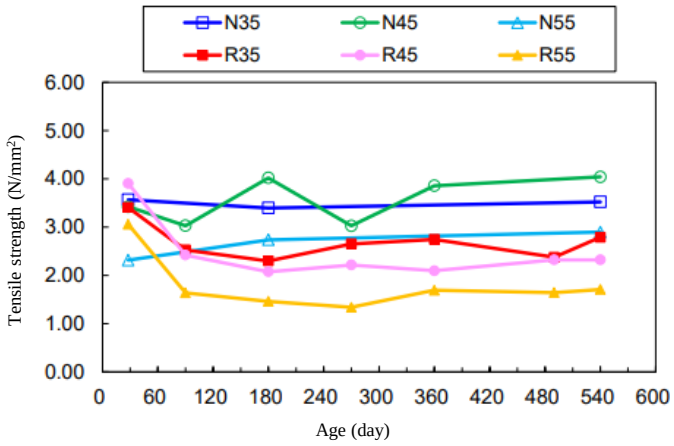

Fig. 2-24 change in tensile strength due to ASR

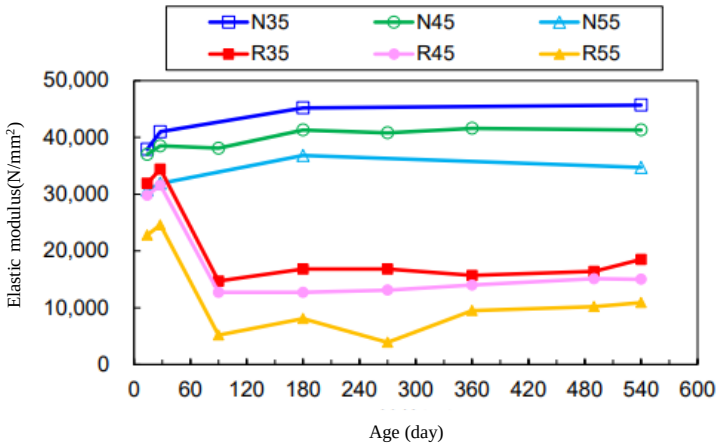

Fig. 2-25 change in elastic modulus due to ASR

Fig. 2-24 and Fig. 2-25 show the changes in tensile strength and elastic modulus of concrete. The tensile strength and elastic modulus of concrete tend to decrease due to ASR.

2.4.2 Combined deterioration of concrete between ASR and frost damage

2.4.2.1 OPC concrete

In Koichi Kobayashi et al.'s study [19], an experimental study was conducted on the combined deterioration between ASR and frost damage.

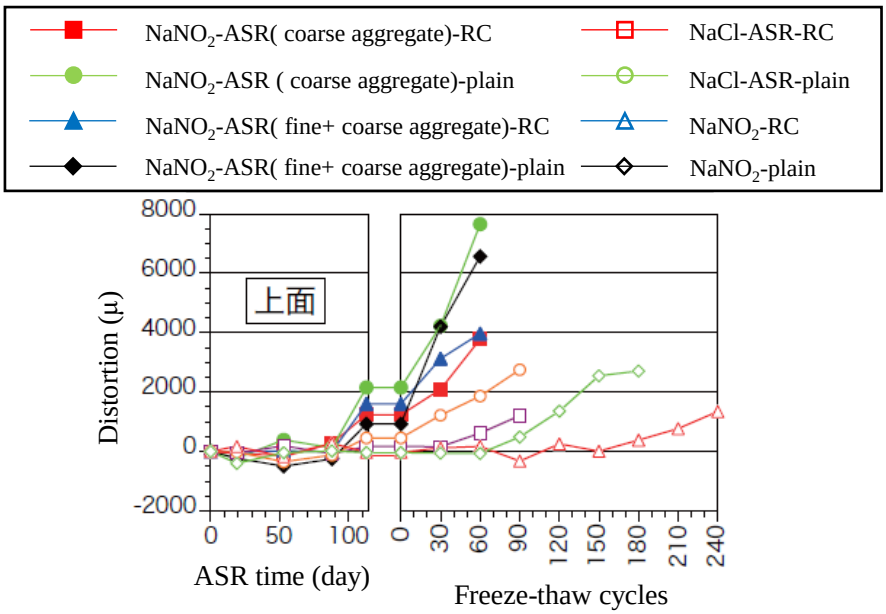

Fig. 2-26 change in expansion due to freeze-thaw after ASR

Figure 10 shows the expansion of concrete subject to freeze-thaw after ASR. For ASR concrete, the average

expansion of the upper and lower surfaces of the concrete was about 750 to 1500m due to ASR deterioration. After that, the expansion increased rapidly due to repeated freeze-thaw, and the expansion Strain reached 3000-6000μ after 60 or 90 cycles freeze-thaw.

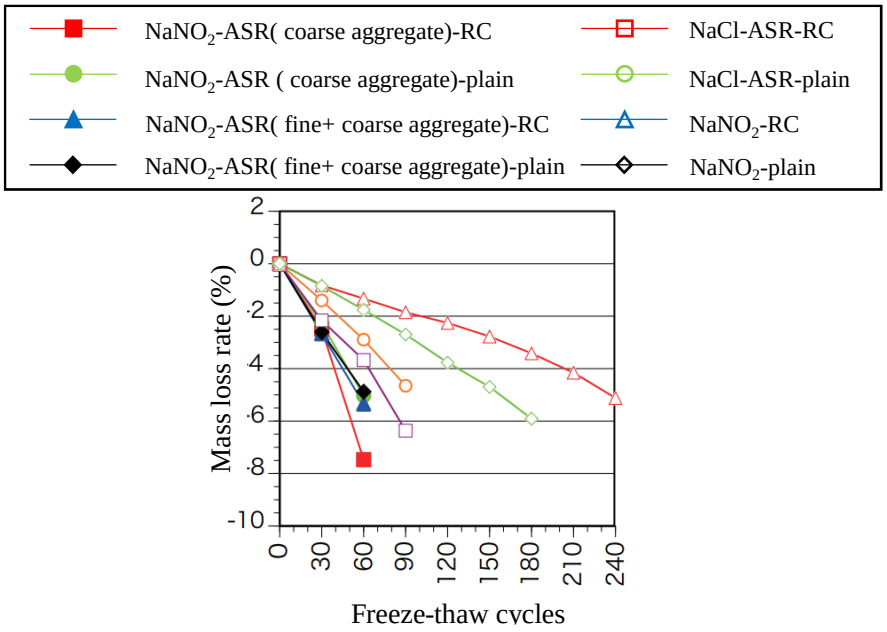

Fig. 2-27 Mass loss due to freeze-thaw of concrete subject to ASR

Fig. 2-27 shows the change in the concrete mass due to repeated freeze-thaw. Regardless of the use of ASR aggregates, all concrete eventually suffered severe scaling. However, when the ASR aggregate was used, scaling occurred on almost the entire surface of the concrete due to first 30 cycles freeze-thaw, whereas when the ASR aggregate was not used, it was observed that the scaling due to freeze-thaw tends to be less.

In addition, Gong et al. [20] investigated the expansion behaviors and mechanical deteriorations of concrete subject to combined deterioration between ASR and frost damage.

For Non-AE concrete, frost resistance is reduced by ASR of concrete with low W/C levels. While, for concrete with high W/C, ASR decreases deterioration due to freeze-thaw. For low W/C concrete, pore volume is decreased due to low W/C to lead to make concrete have low permeability. When a large amount of ASR gel produced due to ASR, which can cause many cracks. After that, the intrusion of water promotes frost damage. For high W/C concrete: concrete has a large pore volume and a high permeability. When subject to ASR, A large amount of ASR gel fills the pores, resulting in less cracking, which can reduce the intrusion of water to reduce the frost damage.

For AE concrete, frost damage is promoted by ASR at all levels, however, the lower the W/C, the greater the effect of ASR. for low W/C concrete: concrete have a low pore volume and low permeability, when subjected to ASR, a large amount of ASR gel produces, which causes many cracks. After that, the intrusion of water promotes frost damage. For high W/C concrete: concrete have a large pore volume and high permeability. concrete has a large pore volume and a high permeability. When subject to ASR, A large amount of ASR gel fills the pores, resulting in less cracking, so there was smaller effect on frost damage.

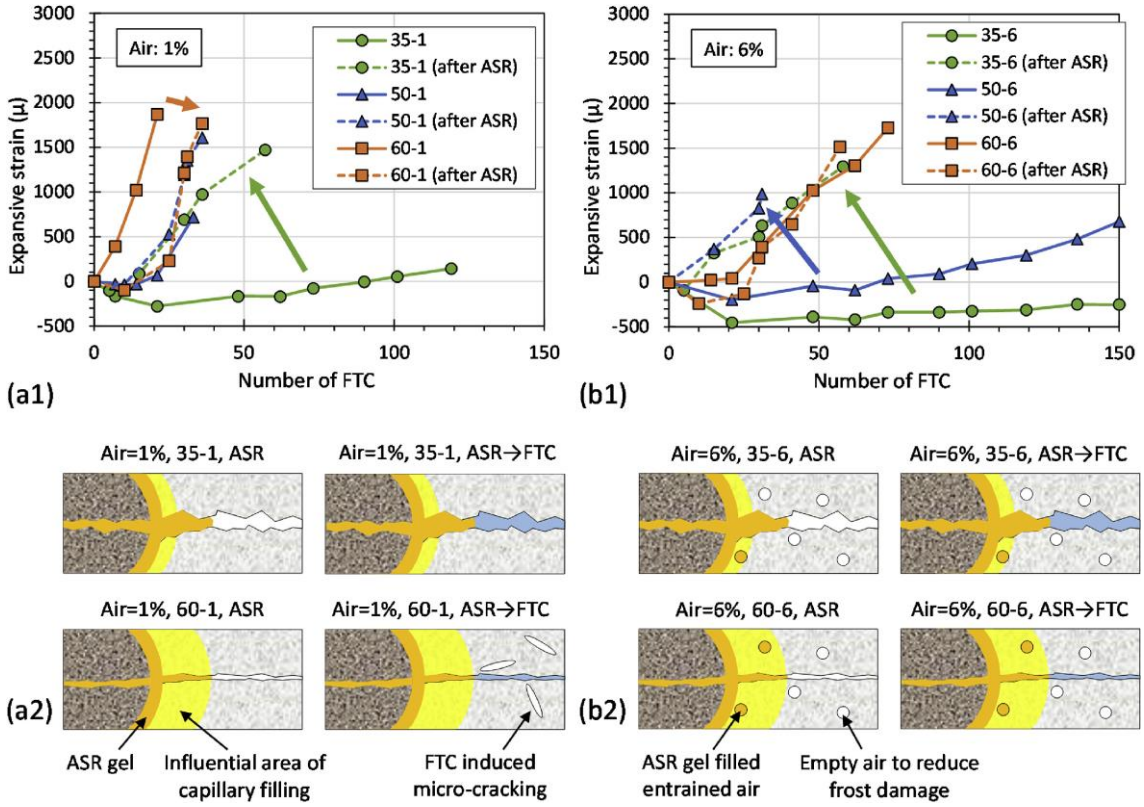

Fig. 2-27 mechanism of combined deterioration between ASR and frost damage

2.4.2.2 BFS and FA concrete

In the world, there has been little research on combined deterioration of concrete between ASR and frost damage containing BFS and fly ash. Therefore, it is essential to experimentally assess the combined deterioration between ASR and frost damage of BFS and fly ash concrete. In addition, the concrete will crack due to ASR, which will reduce the frost resistance regardless of AE admixture, so based on the real environment, the effect of BFS and FA on the combined deterioration of AE concrete will investigated in the in the CHAPTER 5 of this study.

2.5 Summary

For combined deterioration on frost damage of concrete, there mainly are 3 types of combined deterioration, they are combined deterioration between salt damage and frost damage (S&F), combined deterioration between carbonation and frost damage (C&F), combined deterioration between ASR and frost damage (A&F). the S&F of concrete has been studied extensively in the world, and its changes due to the use of BFS and FA have also been investigated well. However, there has been less research the C&F and A&F of concrete in the world. Even, the C&F and A&F of concrete using BFS and FA have been little studied. Due to previous studies, it can be well known that the pore structure, air content, water content and cracks of concrete is related closely to combined deterioration of concrete. The additive of BFS and FA can change the the pore structure, air content, water content and cracks of concrete, which will change the combined deterioration of concrete. It is necessary to make clear their relationship.

Therefore, the experimental program in this study was designed to assess the influence of BFS and FA on combined deterioration between carbonation and frost damage, between ASR and frost damage. The influence of BFS and FA on the mechanical properties, carbonation resistance ASR resistance and frost resistance of concrete were evaluated. Furthermore, the effects of carbonation and ASR on the frost damage of concrete were investigated.

References:

1. Toyoaki Miyagawa et al., Evaluation of Composite Degraded Concrete Structures and Maintenance Planning Research Committee Report, Concrete Engineering Annual Proceedings.Vol.23. No.1, 2001

2. Masaru Yokota et al., Prediction of deterioration of concrete with corroded reinforcing bars due to salt damage, Proceedings of the Japan Concrete Institute, Vol.26, No.1, 2004

3. Japan Society of Civil Engineers: Concrete Standard Specifications [Maintenance], pp99.2001.1.

4. Kenta Miura et al., Fundamental study on resistance to salt damage and neutralization of concrete using blast furnace cement and fly ash, Proceedings of the Japan Concrete Institute Vol.36, No.1, 2014

５. Takeda et al. Durability of concrete subjected to combined slat attack and freezing and thawing action, , Obayashi Technical Research Institute, No.64 2002

6. Koda et al. Influence of air concrete and fly ash on frost resistance of concrete exposed to chloride, Cement Science and Concrete Technology, vol. 68

7.Wei S, Ru M, Xin L and Changwen M, "Effect of chloride salt, freeze–thaw cycling and externally applied load on the performance of the concrete", Cement and Concrete Research, Vol. 32, Issue 12, 2002, pp. 1859-1864.

8.Miguel F, Hannele K, Markku L and Erika H, "Concrete performance subject to coupled deterioration in cold environments", Nuclear Engineering and Design, Vol. 323, 2017, pp. 228-234.

9.H. Kuosa, R. M. Ferreira, E. Holt, M. Leivo and E. Vesikari, "Effect of coupled deterioration by freeze–thaw, carbonation and chlorides on concrete service life", Cement and Concrete Composites, Vol. 47, 2014, pp. 32-40.

10. Hidenobu Tatematsu et al., Formation of ferrite in carbonation of cement hydrate, Concrete Engineering Annual Proceedings, Vol,14No,1,1992

11.Hwang et al. Prediction model of carbonation progress rate of concrete using fly ash, J. Struct. Constr., AIJ, No. 541, 9-15, Mar, 2001

12. Matsuka et al. Low－carbon concrete using ground granulated blast-furnace slag and fly ash, Cement

Science and Concrete Technology, No. 64, pp. 295-302, 2010

13. Yoko Harasawa et al.: Effects of different carbonation environments on pore properties and carbonation products, Proceedings of the Japan Concrete Institute, Vol.36, pp. 808-813, 2014

14. Tomoka Igarashi et al., Carbonation and mass transfer resistance of hardened cementitious materials using fly ash, The 67th Annual Conference of the Japan Society of Civil Engineers, 2012.9

15. Eri Toyomura et al.: A Study on Carbonation Mechanism under Environments with Different Carbon Dioxide Concentrations, Annual Proceedings of Concrete Engineering, Vol.35, No.1, pp.769-774, 2013

16. Ishida et al. Effects of carbon dioxide gas concentration of carbonation of C-S-H, Cement Science and Concrete Technology, Vol.63, pp. 347-353, 2009

17. Ito et al. Fundamental Study on Carbonation of C-S-H with Different Ca/Si Ratios

18. Nobunori Takeda et al.: A study on the durability of concrete subjected to the combined action of freeze-thaw and neutralization, Proceedings of the Annual Concrete Institute, 24-1,735-740,2002

19. Kobyashi et al. Example of composite deterioration of RC slab caused by ASR and frost attack in mountainous cold area and its verification test, Journal of Japan Society of Civil Engineers, Vol. 70, No. 3, 320-335, 2014

20. Yusuke Takagi et al., Decrease in compressive strength of concrete deteriorated by ASR and effect of accelerated curing, Proceedings of the Japan Concrete Institute, Vol.39, No.1, 2017

21. Gong et al. Mechanical properties of concrete with smeared cracking by alkali-silica reaction and freeze-thaw cycles, Cement and Concrete Composites 111 (2020) 103623

Chapter 3

A STUDY ON THE CHANGE IN FROST RESISTANCE AND PORE STRUCTURE OF CONCRETE CONTAINING bLAST FURNACE SLAG UNDER THE CARBONATION CONDITIONS

3.1 Overview

A global “climate and environmental emergency” had been declared in 2019, and it is intended to control the greenhouse gas emissions. From the previous study [1], it is pointed out that cement production accounts for 7.4% of the global CO2 emission, approximately. Therefore, in civil engineering realm, in order to establish a sustainable society with low carbon, it is expected that mineral admixtures, such as blast furnace slag (BFS) and fly ash, are increasingly used as concrete material from the viewpoint of reducing environmental load, in which the reduction of CO2 emission and effective utilization of industrial byproducts were carried out [2], [3]. S. Hesami et al. [4] found that the combination of limestone powder and coal waste ash can result in the concrete with higher mechanical properties, and E. Aprianti et al. [5] pointed out that supplementary cementitious materials can be used as cementitious material to reduce the CO2 emission. For the previous studies [6], [7], [8], it can be well-known that: generally, the concrete using BFS, fly ash or copper slag has better durability and long-term mechanical properties than ordinary Portland cement (OPC) concrete. Besides, it is reported in the study [9]: carbonated BFS is used to mitigate the climatic change impact as a carbon dioxide capture, utilization, and storage (CCUS) technology as reported. BFS cement is classified into three categories according to the Japan Industrial Standards (JIS) R 5211: type A, B and C, which BFS content from 5 to 30%, 30 to 60% and 60 to 70% by weight, respectively. Compared to OPC, there are some advantages such as low heat generation and high long-term strength, but disadvantages such as a delay in early-age strength and low carbonation resistance using BFS cement [10].

Furthermore, the durability of concrete has always been attracted wide attention in the construction field because it is connected with safety, economy and sustainability. Concrete in cold region is subjected to the frost damage, which causes cracks to destroy the structure of concrete, and the performance of concrete is dropped. J. Qiu et al. [11] established a freeze–thaw damage constitutive model and B. Gérar et al. [12] studied the effect of cracks on the properties of concrete, which can be caused by the frost damage. Zhao et al. [13] and Chung et al. [14] pointed out that the freeze-thaw repeated can increase the chloride diffusion coefficients and the relative chloride ion penetration depths of concrete. Kurihashi et al. [15] concluded that the frost damage can decrease the impact resistance of RC beams. Due to a long-term exposure to air, with intrusion of

CO2 into concrete, the alkalinity of concrete is reduced to cause that it will became easy to corrode for steel in concrete [16], [17], which also reduces the durability of reinforced concrete.

From the previous studies, in which the carbonation resistance and frost resistance of concrete have been investigated, it is well-known that the carbonation coefficient is related to the 28-day compressive strength [18]. Liu et al. [19] pointed out that carbonation depth can be assessed though temperature, CO2 concentration and relative humidity. In addition, R. Neves et al. [20] claimed that carbonation resistance is indirect calculated with Torrent air permeability test under carbonation conditions by carbonation concentration, temperature and relative humidity. And, C. Andrade et al. [21] pointed out that the CO2 uptake depends on the CaO content in cement, and is controlled by the humidity in the pores. Besides, Y. dan et al. [22] confirmed that a higher compressive strength can reduce carbonation of concrete. Carbonation of cement paste can cause a change in porosity and pore structure [23]. Moreover, it is confirmed that frost resistance of concrete strongly depends on the capillary porosity value [24]. The assessment of frost resistance of concrete is impacted significantly on by different freezing regimes. Slow freezing rate is more destructive for scaling damage than rapid freezing rate [25].

With the expansion of BFS concrete, most of the previous studies have particularly focused on the durability, such as carbonation or frost resistance of BFS concrete. From previous studies [26], [27], [28], the pore structure, durability and mechanical properties of concrete are changed with the use of BFS, and the k-value concept is proposed for the addition of BFS. However, there are the different k-value due to property and the production conditions, it is cautious to set up from the safety criteria [29]. In addition, it is pointed out that carbonation depth increases with an increase of BFS added [30]. And, Miguel et al. [31] confirmed that there are different correlations between the carbonation coefficient and BFS content for mortars due to curing time. Elke Gruyaert et al. [30] found that the long-wet curing can increase significantly the carbonation resistance of BFS concrete. Zhang et al. [32] stated that the frost resistance decreases as the BFS replacement ratio increases. The deterioration of concrete that is subjected to multi-damage processes could be promoted significantly [13], [33]. Additionally, based on the results of research projects at VTT (VTT is one of Europe's leading research institutions) focusing on coupling deterioration mechanisms [34], [35], M. Ferreira et al. [36] and H. Kuosa et

al. [37] pointed that a large frost-salt scaling after freeze-thaw test will be caused due to long-term ageing with carbonation and drying at 65% relative humidity. However, there has been little research on the change in frost resistance of concrete added mineral admixture under the carbonation conditions. Therefore, it is essential to experimentally assess the combined deterioration of carbonation and frost resistance of BFS cement hardened.

Zhang et al. [32] previously studied the combined deterioration by freeze–thaw and carbonation of mortar incorporating BFS, and pointed out that: The compressive strength of mortar tends to decrease with an increase of BFS replacement ratio from 0 to 45%. The frost resistance and carbonation resistance both decreased due to BFS added. The scaling mass of carbonated mortar is less than that of the non-carbonated ones. However, the water content in the concrete is one of the most important factors of frost damage, the change of water content due to carbonation and its influence on frost damage have not been mentioned in Zhang's study, and deterioration process due to water has still not been forecast. In addition, air entrainment with an AE admixture is effective as a countermeasure against freezing damage of carbonated concrete in cold regions, so it is extremely important to confirm the effect of the AE admixture on BFS concrete. It is well known that frost damage is closely related to the microstructure [38], and it is essential to evaluate the influence of pore structure and hydration product, which is conducive to grasp the combined deterioration of carbonation on frost resistance of concrete.

Therefore, the experimental program in this study was designed to assess the influence of carbonation on frost resistance of BFS concrete with different BFS replacement ratio within the range of JIS R 5211. The influence of BFS as cement replacement on the mechanical properties, carbonation resistance and frost resistance of concrete were evaluated. Furthermore, the effects of carbonation on the frost damage of concrete were investigated, and the changes in pore structure and hydration product under the carbonation conditions were also measured, which is used to assess the change of frost resistance of carbonated concrete.

3.2 Experimental

3.2.1 Materials

The cement used in this experiment was the ordinary Portland cement based on the JIS R 5210 [39] in Japan

(Nippon steel cement corporation, Muroran, Japan). The cement was denoted as N with a specific gravity of 3.17 g/cm^3. BFS Blaine4000 based on JIS A 6206 [40] (Nippon steel cement corporation, Muroran, Japan) with a specific gravity of 2.91 g/cm^3 was used to replace cement at 15% (BFS cement Type A: BA), 45% (BFS cement Type B: BB), and 65% (BFS cement Type C: BC) by weight of cement. The chemical compositions and physical properties of OPC and BFS Blaine4000 are shown in Table 1. Shiraoi land sand with a surface-dry density of 2.67g/cm^3 and a water absorption of 1.57%, was used as the fine aggregate in this experiment. And Shikiu River andesite with the nominal maximum size of 20mm was used as the coarse aggregate and had a surface-dry density of 2.57g/cm^3 and a water absorption of 2.98%. In this study, an AE water-reducing admixture is used to increase air entrainment as a chemical admixture.

Table 1. Chemical compositions (wt.%) and physical properties of OPC and BFS

	Blaine Fineness (cm^2/g)	Chemical Composition (%)								
		SiO_2	Al_2O_3	Fe_2O_3	CaO	MgO	K_2O	Na_2O	SO_3	TiO_2
OPC	3390	21.37	5.5	2.79	64.25	2.06	0.42	0.29	1.9	0.27
BFS Blaine4000	3930	34.03	14.36	0.83	43.28	6.51	0.31	0.18	-	0.46

3.2.2 Experimental program

3.2.2.1 Experiment of BFS concrete

The experimental program of BFS concrete is shown in Table 2.

Table 2. Experimental program of concrete

Cement type	Cement replacement ratios (%)	Objective		Experimental items
		Air (%)	Slump (cm)	
BFS	0 15(Type A) 45(Type B) 65(Type C)	1.0±1.0 or 4.5±1.5	18±2	Compressive Strength test Freeze-Thaw in water test RILEM / CIF test Water content distribution test

Table 3. The mixture proportions and fresh properties of concrete

Symbol	w/b (%)	s/a (%)	Binder (%)		Materials contents (kg/m^3)					AE water-reducing admixture (ml/m^3)	Fresh properties	
			OPC	BFS	W	OPC	BFS	S	G		Air (%)	SL (cm)
Non-AE-N	55	44.7	100	0	204	371	0	769	988	0	2.0	19.6
Non-AE-BA			85	15	202	312	55	770	990		1.8	18.7
Non-AE-BB			55	45	200	200	164	770	990		1.5	18.6
Non-AE-BC			35	65	198	126	234	772	992		1.4	18.2
AE-N			100	0	184	335	0	761	973	836	4.1	19.0
AE-BA			85	15	180	278	49	771	975	818	4.5	18.3
AE-BB			55	45	178	178	146	772	975	809	4.6	18.6
AE-BC			35	65	176	112	208	774	997	800	3.8	18.2

In this experiment, in order to investigate the influence of carbonation on frost resistance of BFS concrete, the basic mechanical properties of BFS concrete with different BFS replacement ratio were tested at the material age of 4 weeks, and the contrast of combined deterioration was investigated using the concrete test specimens, which were subjected to carbonation curing (20℃, 60% relative humidity, CO_2 concentration 5%) and air curing (20℃, 60% relative humidity) for the same period, respectively.

The compressive strength test was conducted at the material age of 4 weeks in water curing, and the freeze-thaw in water test, RILEM / CIF test and water content distribution test were carried out at the material age of 4 weeks in which concrete was cured in water, and 21 weeks in which concrete was cured in water for 4 weeks, in air for 4 weeks (in order to dry the concrete before accelerating carbonation test), and in air or carbonation for 13 weeks.

The mixture proportions and fresh properties of concrete are shown in Table 3. BFS concrete specimens were prepared with 55% water-to-binder ratio (w/b) and 44.7% sand-to-aggregate ratio (s/a), in which slump was controlled at 18±2cm, and air content was controlled at 4.5±1.5% with chemical admixture (AE concrete), or at 1.0±1.0% without chemical admixture (Non-AE concrete).

3.2.2.2 Additional experiments on the microstructure of hardened BFS cement paste

It is well known to all that the formation of the microstructure in the concrete mainly is by hydration reaction of cement. Therefore, in this study, in order to better observe the change of microstructure due to

carbonation to investigate the deterioration process of frost damage of carbonated concrete, the microstructure of hardened BFS cement paste was carried out. In this experiment, material is the same as BFS concrete experiments.

The experimental program of hardened BFS cement paste is shown in Table 4, the curing condition was performed on the same condition with BFS concrete experiment.

Table 4. The experimental program of cement paste

Symbol	w/b [%]	Binder [%]		Mixing and retaining time[h]	Curing		Experimental items
		OPC	BFS		Standard curing	Environmental condition	
N	65	100	0	7	Water curing for 4 weeks	Air curing or carbonation curing for 13weeks	MIP method TG-DTA XRD
BA		85	15				
BB		55	45				
BC		35	65				

BFS cement paste, in which BFS replacement ratio is 0% (N), 15% (BA), 45% (BB), 65% (BC) respectively, were prepared without chemical admixture. In order to accelerate carbonation of cement paste, water-to-binder ratio is set to 0.65, which is higher than 0.55 of concrete, and in order to suppress material separation, kneading was performed once an hour, and a sample was prepared after 7 hours. The Mercury intrusion porosimetry (MIP) method, Thermogravimetry-differential thermal analysis (TG-DTA) test and X-ray diffraction analysis (XRD) were carried out after the curing in water, air and carbonation, respectively.

3.2.3 Experimental method

3.2.3.1 Compressive strength test

According to JIS A 1108, the compressive strength test was carried out at the material age of 28 days. Three test specimens, which had a dimension of φ100×200mm, were polished to a flat surface, and were applied firm pressure by compression. The maximum loads until three specimens were damaged were recorded, respectively. The compressive strength was obtained by dividing the maximum load by the cross-sectional area of the

specimen, and the measured value was the average value of the three specimens.

3.2.3.2 Accelerated carbonation test

According to JIS A 1153, the accelerating carbonation test was carried out using the test specimens of φ100×200 mm at the material age of 8 weeks (concrete is cured in water for 4 weeks, and dried for 4 weeks in air). The carbonation depth was measured by spraying the phenolphthalein indicator to the broken concrete surfaces when concrete was cured in air or in carbonation condition for 13 weeks. The carbonation speed coefficient was calculated from the carbonation depth using the following equation [41], [42]:

$$x = k\sqrt{t} \qquad \text{Eq. (1)}$$

Where, x is the depth of carbonation (mm); t is the time at which carbonation has taken place (week); and k is the carbonation speed coefficient (mm・weeks$^{-0.5}$).

3.2.3.3 Freeze-thaw in water test

The dynamic modulus of elasticity was calculated by making test specimens of 75×75×400mm maintain the minimal temperature of -18℃ and the maximal temperature of 5℃, which is based on the JIS A 1148 A method [43]. The resonant frequency of sample was measured before freeze-thaw, and was measured every 6-cycle until 30 cycles, and then was measured every 30-cycle until 300 cycles or it was broken. The relative dynamic modulus of elasticity was calculated using the following equation:

$$P_n = \frac{f_n^{\,2}}{f_0^{\,2}} \times 100\% \qquad \text{Eq. (2)}$$

Where, P_n is the dynamic modulus of elasticity after n cycles of freeze-thaw (%); f_n is the resonant frequency after n cycles of freeze-thaw (Hz); f_0 is the resonant frequency at 0 cycle of freeze-thaw (Hz);

The frost resistance is the measure of the durability factor, which is obtained when the relative dynamic modulus of elasticity the test specimen falls to less than 60% or the specimen is subjected to 300 cycles.

3.2.3.4 RILEM/CIF test

The one-side freeze-thaw test (RILEM/CIF test), in which RILEM method [44] was measured, is used to evaluate frost damage of concrete with a marginal water saturation. In this test, the side surface of the test specimens of φ100×200 mm is sealed by the aluminum tape with butyl rubber, and absorbing water in the bottom surface is performed for 7 days in a constant temperature room at 20°C and 60% RH. And water absorption was measured every day. After that the one-side freeze-thaw test was carried out keeping the bottom surface absorbing water in a chamber, where the minimal temperature was maintained at -20°C for 3 hours and the maximal temperature was maintained at 20°C for 1 hour with a temperature gradient of ± 10°C/hour, until 56 cycles. Water absorption and scaling mass were measured per 6 cycles.

3.2.3.5 Water content distribution test

In order to grasp the change of water content in concrete due to carbonation, the water content was measured according to JIS A 1476. The side surface of the test specimens of φ100×200 mm was sealed with the aluminum tape by butyl rubber. Absorbing water in the bottom surface is performed for 28 days. After absorbing water, the test specimens were cut at intervals of 25mm (0-25mm, 30-55mm, 60-85mm, 90-115mm, 120-145mm, 150-200mm) from the water absorbing surface as follows.

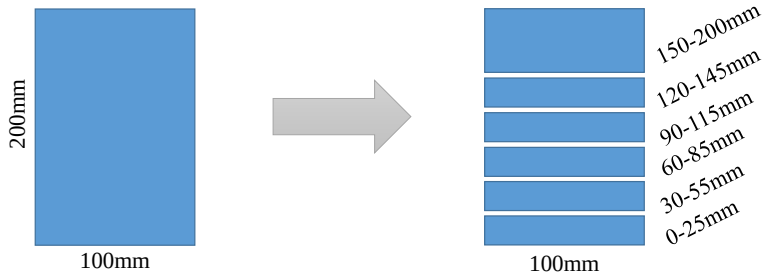

And each sample was weighed immediately after cutting to avoid the effect of drying. This mass before drying is expressed in "m". And after be dried for 48 hours at 105°C, the each sample was weighed and the mass is expressed in "m_0". The water content is calculated using the following equation:

$$\text{water content } [\%] = \frac{m - m_0}{m_0} \times 100\% \qquad \text{Eq. (3)}$$

3.2.3.6 Microstructure test

The hardened BFS cement paste was cut into 5mm cubes, and was stopped hydration reaction in the ethanol for 1 week, and then was dried for 1 day by the F-dry method. The pore structure was determined using the 5mm cubes by the Mercury intrusion porosimetry (MIP) method, which is used to measure the pore size distribution and cumulative pore volume for cement-based materials [45], [46], [47], according to JIS R 1655.

3.2.3.7 TG-DTA test

At the material age in TG-DTA test, the specimen was cut into 5mm cubes, then was pretreated as MIP method. The measurement specimen was heated up to 1000 °C with a heating rate of 10 ° C/min in a filled Nitrogen environment. The amount of calcium hydroxide and calcium carbonate was calculated from the thermogravimetric change in the range of 370 to 450 °C and 550 to 800 °C. In addition, from the consumption obtained by the amount of calcium hydroxide before and after carbonation, the amount of calcium carbonate by calcium hydroxide was calculated, and the other amounts of calcium carbonate were attributed to be by C-S-H.

3.2.3.8 X-ray diffraction analysis (XRD)

The samples were pretreated as MIP method and TG-DTA before XRD analysis, and were ground to fine sand in 30 seconds using a vibration mill. The analyses of hydration product were determined by the XRD analysis. The evaluated components in this study were calcite, vaterite, calcium hydroxide, silica, and the same diffraction intensity as Borges [48] was used for the measurement. Although the amount of the component cannot be quantified from this data, it can be relatively judged that the higher the peak of diffraction intensity, the larger the component.

3.3 Results and discussion

3.3.1 The effect of compressive strength on carbonation speed

The relationships between 28-day compressive strength and BFS replacement ratio of concrete are shown in Fig. 1.

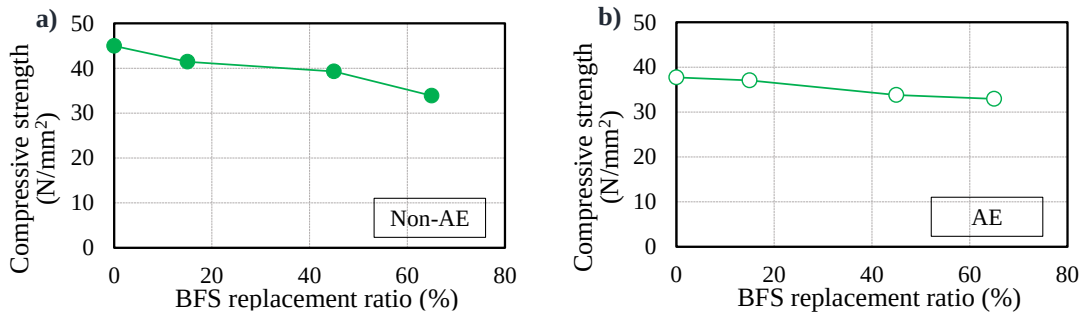

Fig. 1. Compressive strength results at 28 days.

In the previous study [32], Zhang pointed out that in the mortar, with an increase in BFS replacement ratio the compressive strength decreases. From Fig. 1, it is seen that the compressive strength of concrete decreased as the BFS replacement ratio increased. The more BFS replacement ratio, the less the quantity of OPC, and with the decrease of hydration of cement, the reduction of 28d-age compressive strength can be predicted. In addition, it is pointed that an interfusion of AE admixture into concrete can cause a reduction of its strength due to the increased porosity [49]. Comparing the cases of Non-AE and AE in Fig. 1, under the same replacement ratio, the compressive strength of Non-AE concrete is higher than the one of AE, which is the same as the previous study.

Fig. 2 shows the carbonation depth of BFS concretes. The carbonation depth tended to increase as BFS replacement ratio increased for each curing whether AE or Non-AE concrete, which is the same as results of previous study [32]. In the case of Non-AE concrete, it is shown that the carbonation depth of BB and BC had a significant increase than N and BA due to carbonation.

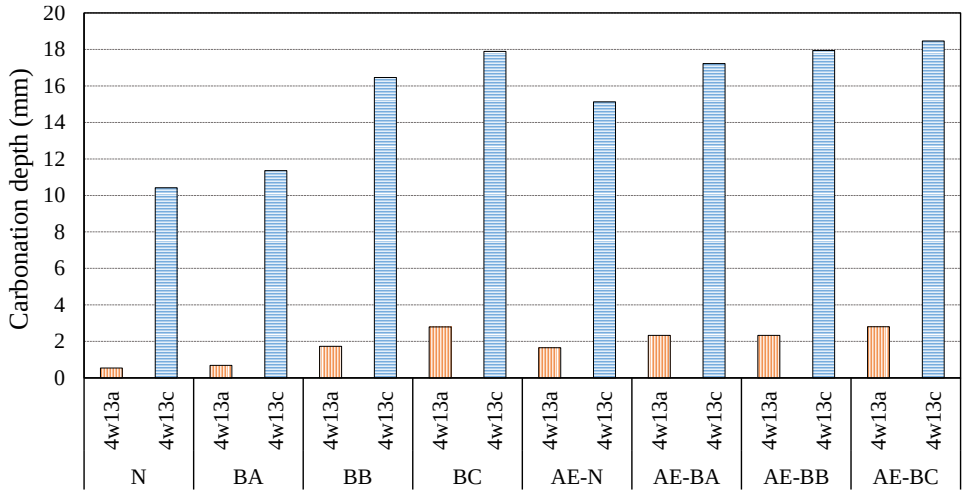

Fig. 2. Carbonation depth of BFS concrete (4w13a: air curing for 13 weeks after water curing, 4w13c: carbonation curing for 13 weeks after water curing)

In this study, the relationship between the carbonation speed coefficient and the compressive strength for the cases of 4w13a and 4w13c would be investigated in Fig. 3a and Fig. 3b, respectively. From the study of carbonation [50], it is pointed out that: for prediction of carbonation behavior, the compressive strength of concrete at the time of initial exposure to carbonation are crucial, and when the compressive strength increases, the carbonation resistance tends to be high. In Fig 3, The R^2 value with 0.9053 for 4w13a and 0.8714 for 4w13c signified that there is a direct correlation between the carbonation speed coefficient and the compressive strength. M. A. Sanjuán et al. [42] deduced that 7-15 days of accelerated carbonation (4-5% CO_2, 50-60% RH) is equivalent to 1 year of natural carbonation. In according to Eq. (1), the carbonation speed coefficient under accelerated carbonation is 5-7 times the carbonation speed coefficient under natural carbonation. From Fig. 3a, the correlation curve between K_a (the carbonation speed coefficient under air curing), and the compressive strength (F_c) could be obtained as the following equation:

$$Ka = -0.0554Fc + 2.5998 \quad \text{Eq. (4)}$$

Where, K_a is the carbonation speed coefficient under air curing (mm・weeks$^{-0.5}$), and F_c is the compressive strength (N/mm^2).

And for the study [42] of M. A. Sanjuán et. al., although BFS concrete had not been studied, fly ash concrete had been studied, and it is indicated that when the carbonation speed coefficient of fly ash concrete under natural carbonation is 7.89 or 4.93 mm/ year$^{0.5}$, the carbonation speed coefficient of fly ash concrete under accelerated carbonation (for 5% CO_2) is 26.85 or 21.91 mm/ year$^{0.5}$, and is less than 5 time the carbonation speed coefficient under natural carbonation. Be analogous to fly ash concrete, from Eq. (4), K'_c of BFS concrete (the carbonation speed coefficient under carbonation curing) in this study can be deduced as 5 times of K_a:

$$K'c = -0.277Fc + 12.999 \quad \text{Eq. (5)}$$

Where, K'_c is the carbonation speed coefficient under carbonation curing deduced from K_a (mm・weeks$^{-0.5}$), and F_c is the compressive strength (N/mm^2).

In Fig. 3b, the correlation curve between K_c (the carbonation speed coefficient under carbonation curing) and F_c can be obtained:

$$Kc = -0.1923Fc + 11.566 \quad \text{Eq. (6)}$$

Where, K_c is the carbonation speed coefficient under carbonation curing (mm · weeks$^{-0.5}$), and F_c is the compressive strength (N/mm^2).

Comparing with K'$_c$, there is a small gap between K_c and K'$_c$, and K_c is slighty less than K'$_c$, which implied that under accelerated carbonation conditions the carbonation speed coefficient of BFS concrete can be predicted by the compressive strength. The carbonation speed coefficient tended to increase as compressive strength decreased; which may be due to that with a low speed of hydration reaction as BFS placement ratio increased, the densification of concrete is delayed and calcium hydroxide (CH) in the concrete was consumed due to latent hydraulic property of BFS to lead to lower the pH of concrete. Furthermore, it had become easy for the intrusion of CO_2 into concrete through the capillary pore that was not densified yet. This result is the same as the previous study [50].

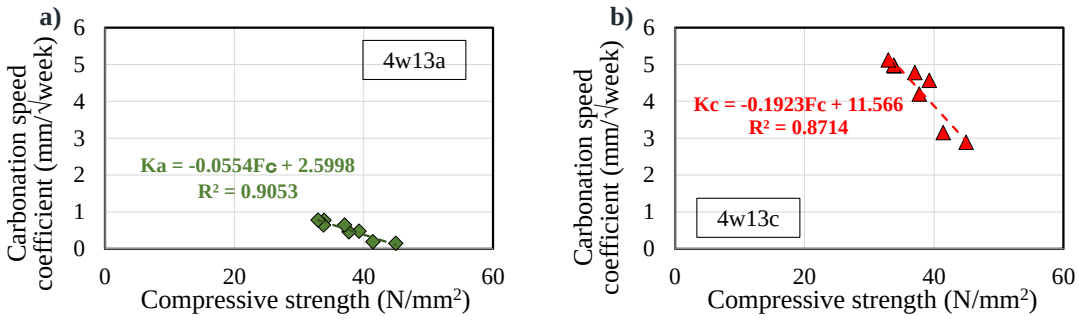

Fig. 3. Change of carbonation speed coefficient (4w13a: air curing for 13 weeks after water curing, 4w13c: carbonation curing for 13 weeks after water curing).

3.3.2 The change of frost resistance and scaling resistance due to carbonation

The changes of relative dynamic modulus of elasticity of concrete without AE admixture in the freeze-thaw test are shown in Fig. 4. Fig. 4a, Fig. 4b, Fig. 4c and Fig. 4d show the change of relative dynamic modulus of elasticity of N, BA, BB and BC, respectively.

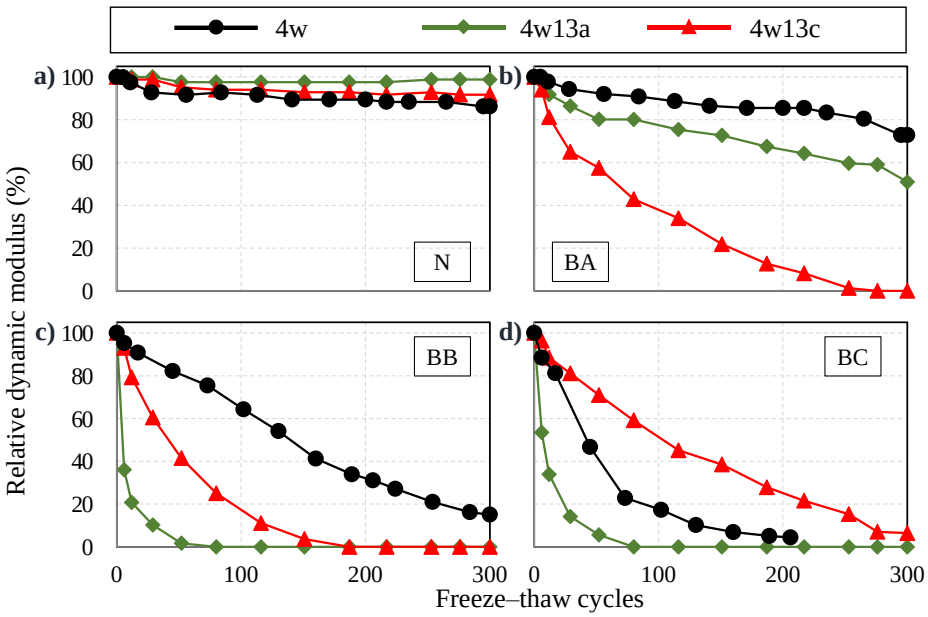

Fig. 4. Relative dynamic modulus of elasticity result of concrete in the case of Non-AE (4w: water curing for 4 weeks, 4w13a: air curing for 13 weeks after water curing, 4w13c: carbonation curing for 13 weeks after water curing).

From the previous studies [32], [51], it can be well-known that the use of BFS can decrease the frost resistance of concrete. For the case of water curing in Fig. 4, the results show that: the higher BFS replacement ratio, the more the deterioration of concrete, which is in general agreement with the previous research. This may be attributed to that with the increase of BFS replacement ratio, less hydration of cement was carried out to lead to increase the capillary pore. In Fig. 4a, comparing with the cases after water curing, little deterioration occurred even at 300 cycles for N by air curing or carbonation curing after water curing. The deterioration was promoted for BA in Fig. 4b and BB in Fig. 4c due to air curing and carbonation curing, while for BC in Fig. 4d, the deterioration was promoted due to air curing, and was inhibited due to carbonation curing. For the specimens with a same material age, compared to the cases after air curing, the deterioration in N and BA was promoted, while the deterioration in BB and BC was inhibited due to carbonation. The changes of relative dynamic modulus of elasticity of concrete with AE admixture in the freeze-thaw test are given in Fig. 5.

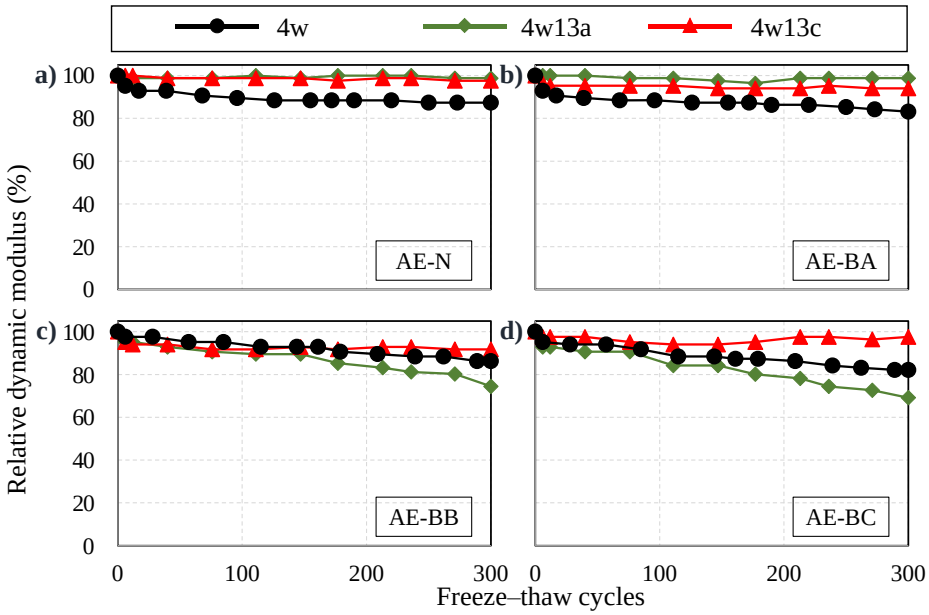

Fig. 5. Relative dynamic modulus of elasticity result of concrete in the case of AE (4w: water curing for 4 weeks, 4w13a: air curing for 13 weeks after water curing, 4w13c: carbonation curing for 13 weeks after water curing).

For the case after water curing in Fig. 5, little change was observed on the dynamic modulus of elasticity of concrete as BFS replacement ratio increased, and the dynamic modulus of elasticity was maintained to 80 or more due to AE water-reducing admixture. And the frost resistance of concrete performed carbonation curing or air curing after water curing was raised for AE-N in Fig. 5a and AE-BA in Fig. 5b. While for AE-BB in Fig. 5c and AE-BC in Fig. 5d, the frost resistance was raised due to carbonation curing, and was reduced due to air curing. In addition, comparing the cases after air curing and carbonation curing, which have a same material age, the frost resistance was little changed for AE-N and AE-BA, and was raised for AE- BB and AE-BC due to carbonation.

Fig. 6 shows the changes in durability factor of concrete. For the case without AE, it is shown that in all curing the higher the BFS replacement ratio, the lower durability factor. After specimens were subjected to carbonation curing or air curing after water curing for 4weeks, the durability factor of N was stayed above 80, while the durability factor of BA and BB had fallen. And the durability factor of BC was less than 20 no matter which curing condition. Comparing the cases after air curing and carbonation curing with a same material age, the durability factor of N was decreased slightly, and the durability factor of BA was reduced due to carbonation,

while for BB and BC, the durability factor was increased due to carbonation.

For the case with AE, the durability factor of concrete in all curing was maintained a high value, which is because air entrainment is increased due to AE water-reducing admixture. And in the case after air curing, durability factor of AE-BB and AE-BC tend to be lower than AE-N and AE-BA, but still higher than 60.

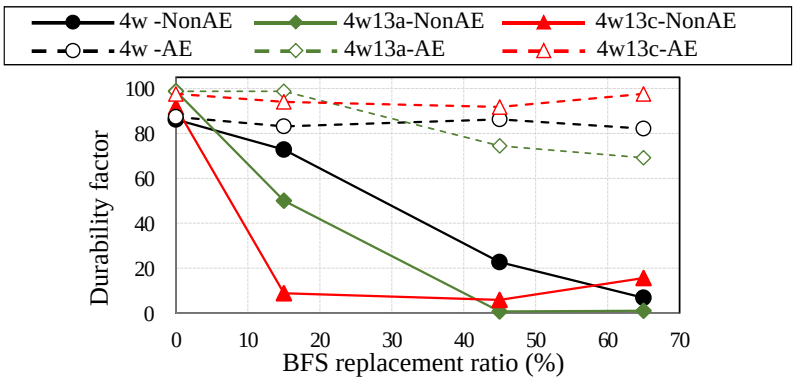

Fig. 6. Changes of durability factor of concrete (4w: water curing for 4 weeks, 4w13a: air curing for 13 weeks after water curing, 4w13c: carbonation curing for 13 weeks after water curing).

The changes of the scaling mass of concrete without AE water-reducing admixture due to freeze-thaw cycles in CIF test are shown in Fig. 7. In Fig. 7a, it can be seen that a high scaling resistance for N in all curing, after freeze-thaw, the scaling mass was maintained a low level, and even if concretes were subjected to air curing or carbonation curing after water curing, the scaling mass had not been increased. For the case of water curing in Fig. 7, the scaling mass tended to increase with an increase of the BFS replacement ratio. The scaling mass of concrete had no change for N in Fig. 7a and BA in Fig. 7b by performed air curing after water curing. The scaling mass was significantly increased for BB in Fig. 7c and BC in Fig. 7d due to air curing, while there was no obvious change on the scaling mass for BB and BC due to carbonation curing. Comparing the cases after air curing and carbonation curing with a same material age, the scaling mass had no significant change for N and BA, and was decreased for BB and BC due to carbonation.

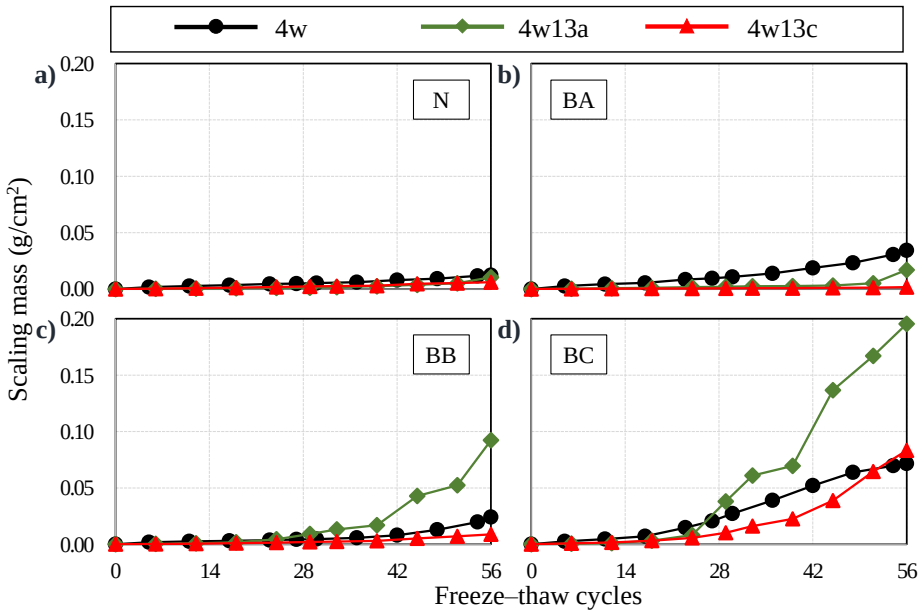

Fig. 7. Scaling mass results of concrete of Non-AE (4w: water curing for 4 weeks, 4w13a: air curing for 13 weeks after water curing, 4w13c: carbonation curing for 13 weeks after water curing).

The changes of the scaling mass at 56 cycles due to curing in CIF test are shown in Fig. 8. Comparing the cases of Non-AE and AE, it was confirmed that the scaling was inhibited due to AE admixture. For the case of Non-AE concrete, the scaling mass was increased as the BFS replacement ratio increased under the same curing. And on the basis of the case after water curing for 4 weeks, the scaling mass was increased by performing air curing, while the scaling was inhibited by performing carbonation curing. Besides, comparing the cases after air curing and carbonation curing, the scaling mass of concrete was inhibited due to carbonation. In addition, with the increase of BFS replacement ratio, the scaling mass was more lowered due to carbonation.

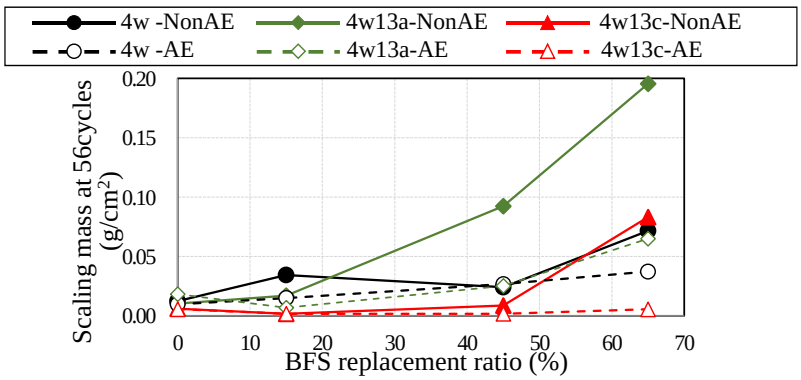

Fig. 8. Relationship between scaling mass at 56 cycles and BFS replacement ratio (4w: water curing for 4 weeks, 4w13a: air curing for 13 weeks after water curing, 4w13c: carbonation curing for 13 weeks after water curing).

3.3.3 The changes in water absorption and water content distribution due to carbonation

The changes of water absorption of Non-AE concrete in CIF test are shown in Fig. 9. In the process of absorbing water of bottom surface before freeze-thaw, the water absorption was raised slightly by performing carbonation curing or air curing for 13 weeks after water curing. And for both the cases after air curing and carbonation curing, there is no change in water absorption. The water absorption of concrete subjected to freeze-thaw had increased significantly due to Micro-Ice-Lens pump [52]. The water absorption of concrete performed air curing or carbonation curing was higher than the ones after water curing. Comparing the cases after air curing and carbonation curing, the absorbing water was restrained due to carbonation.

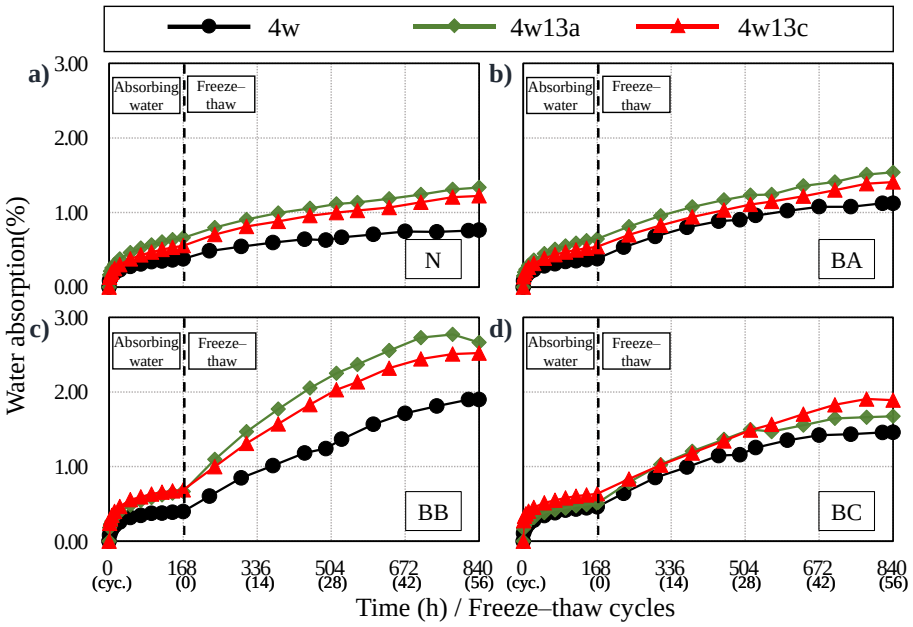

Fig. 9. Change of water absorption in the case of Non-AE (4w: water curing for 4 weeks, 4w13a: air curing for 13 weeks after water curing, 4w13c: carbonation curing for 13 weeks after water curing)

Fig. 10 shows the changes in water content distribution of N and BB after air curing and carbonation curing without AE water-reducing admixture. The water content after absorbing water was measured using the test specimens that were performed air curing or carbonation curing for 13 weeks after water curing, in which the test specimens had not been carbonated in air curing, and had been carbonated after carbonation curing. In Fig. 10a and Fig. 10b, the water content of concrete subjected to freeze-thaw had no marked change for both N non-carbonation and carbonation. However, for non- carbonation BB in Fig. 10c, the water content of concrete, which was subjected to freeze-thaw, increased due to Micro-Ice-Lens pump [52], and the water absorption is maximum in bottom surface. For carbonation BB in Fig. 10d, the water content of bottom surface after freeze-thaw was lower than the non- carbonation ones, while the water content in the middle of concrete tended to increase.

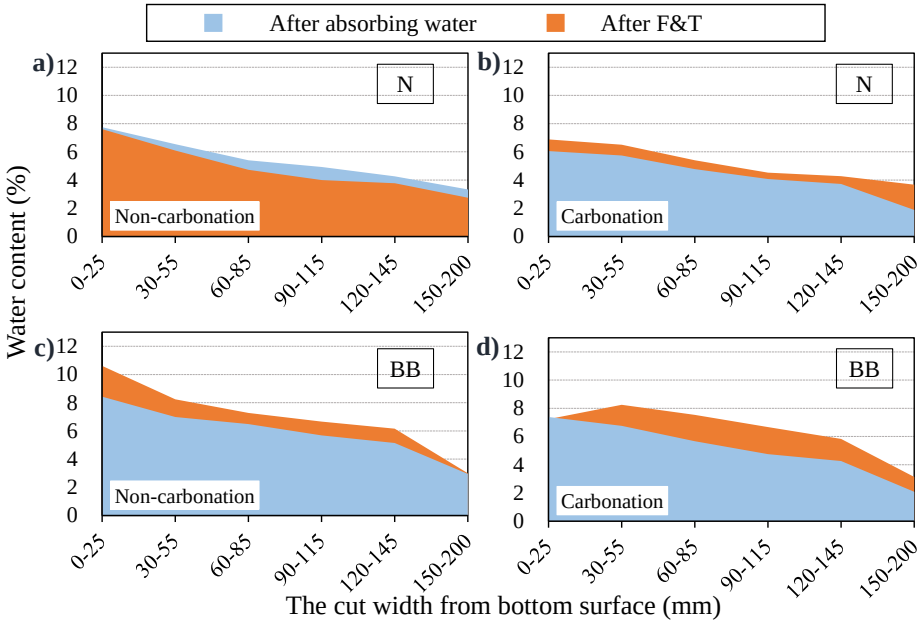

Fig. 10. Change in water content distribution (N, BB) due to carbonation

F&T: Freeze-thaw

3.3.4 The change of pore structure due to carbonation

Fig. 11 shows the cumulative pore volume of hardened BFS cement paste. Comparing the cases after air curing and carbonation curing, the cumulative pore volume tended to decrease due to carbonation for all concrete. In addition, the threshold diameter is one of important parameters characterizing the pore structure, and can be calculated in cumulative or differential curve of MIP results. The threshold diameter is the pore diameter where the pore volume begins to increase [53], [54], which is useful to identify the pore diameter related to various durability of concrete. In Fig. 11 and Fig. 12, the threshold diameters in different curing cases were calculated and were shown in Table 5.

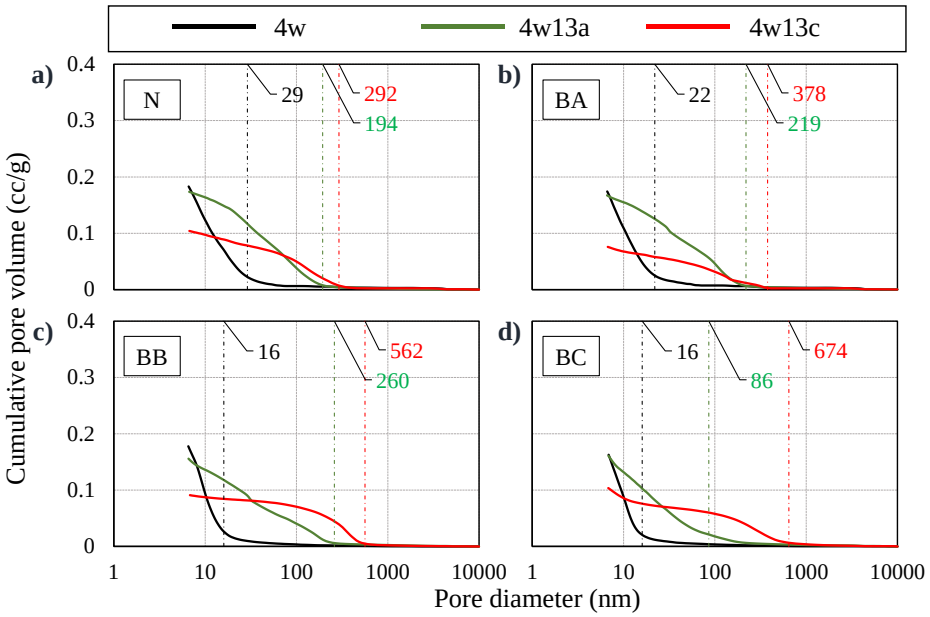

Fig. 11. Cumulative pore volume result of BFS cement paste (4w: water curing for 4 weeks, 4w13a: air curing for 13 weeks after water curing, 4w13c: carbonation curing for 13 weeks after water curing)

Table 5. The threshold diameter in each curing

Sample	The threshold diameter (nm)		
	Water curing	Air curing after water curing	Carbonation curing after water curing
N	29	194	292
BA	22	219	378
BB	16	260	562
BC	16	86	674

Fig. 12 shows the pore size distribution of hardened BFS cement paste. For the case after water curing for 4 weeks, the pore was mainly concentrated in the area below the size of 100nm, which is considered that the pore structure of concrete was densified due to hydration of cement in water curing. There were two pore size distribution peaks near 100nm diameter in the case after air curing. While in the case after carbonation curing, the pore size distribution peak below 150nm disappeared and the one above 150nm shifted to a larger diameter. However, the pore below 150nm in BC had not been densified enough. And the pore size distribution peak shifted to a larger diameter with an increase of BFS replacement ratio. This was considered that it was easier to carbonate for C-S-H to lead to coarsen the pore structure in the hardened BFS cement paste with a low Ca/Si

ratio as BFS replacement ratio increased [55].

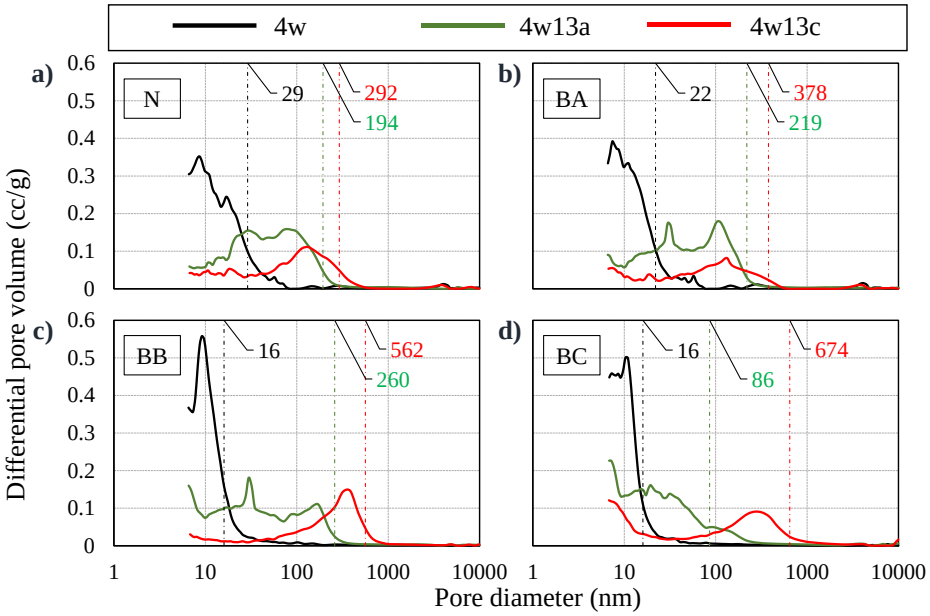

Fig. 12. The pore size distribution of BFS cement paste (4w: water curing for 4 weeks, 4w13a: air curing for 13 weeks after water curing, 4w13c: carbonation curing for 13 weeks after water curing)

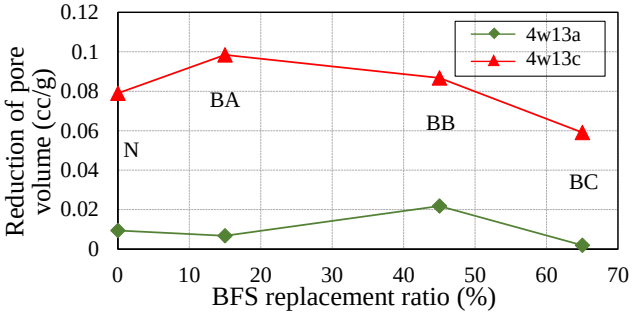

Fig. 13. The reduction of pore volume due to air or carbonation curing (4w13a: air curing for 13 weeks after water curing, 4w13c: carbonation curing for 13 weeks after water curing)

Fig. 13 shows the relationships between the reduction of pore volume due to air or carbonation curing and the BFS replacement ratio. The reduction of pore volume due to air or carbonation curing is a subtraction value which is obtained by subtracting the pore volume of BFS cement paste preforming air curing or carbonation curing for 13 weeks after water curing from the one after water curing for 4 weeks. It is generally said that

carbonation of concrete occurs in capillary. For that reason, it is considered that the pore structure changes due to carbonation occur in capillary pore. In Fig. 13, comparing the reduction due to air curing and carbonation curing, the higher the BFS replacement ratio, the smaller the pore reduction due to carbonation. That was the gap between the reduction due to air curing and carbonation curing. The reason is that the amount of calcium hydroxide (CH) became smaller as the BFS replacement ratio increased, and the densification due to carbonation of CH was reduced. In addition, the reduction of pore volume in N and BA after air curing is less than in BB after air curing because in air curing a small amount of CH is carbonated to densify pore structure for N and BA. However, for BB with a high BFS replacement ratio, the latent hydraulic property of BFS was in progress under the alkaline conditions, which led to densify pore structure.

3.3.5 The change of threshold diameter and permeability due to carbonation

Fig. 14 shows the relationships between the BFS replacement ratio and the threshold diameter. The threshold diameter indicates the minimum pore size that can strongly affect mass transfer in the hardened cement paste. From Fig. 14, it can be seen that the higher the BFS replacement ratio, the larger the change in the threshold diameter due to carbonation, which is owed to that the pore structure was coarsened due to carbonation of C-S-H of hardened BFS cement paste with a lower Ca/Si ratio as the BFS replacement ratio increased.

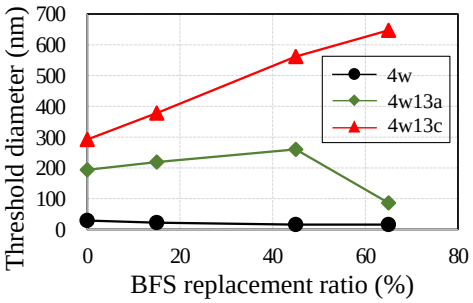

Fig. 14. Relationship between the BFS replacement ratio and the threshold diameter

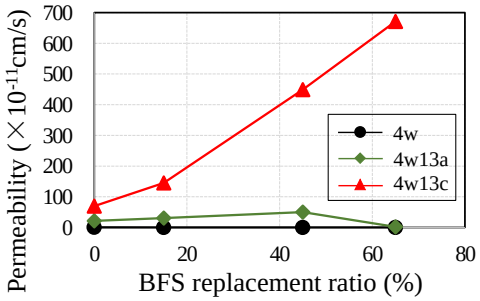

Fig. 15. Relationship between the BFS replacement ratio and permeability

Fig. 15 shows the relationships between the BFS replacement ratio and permeability. Mehta [53] proposed an

equation of the permeability (K: × 10^{-11} cm/s) of hardened cement paste is obtained by threshold diameter (TD: Å) or air volume as following:

$$LnK = 2.85LnTD-18.5 \quad \text{Eq. (7)}$$

In Fig. 15, the permeability figured out by Equation 7 became huger due to carbonation, moreover, the increment of permeability increased with the increase of BFS replacement ratio. In other words, it can be said that in the hardened BFS cement paste, permeability was raised to cause that the water was difficult to absorb and the water in pore was easy to dry due to carbonation. Aoyama [56] confirmed that in carbonated concrete, the water absorption decreases, and both the evaporation rate and water penetration quantity increase. In the carbonation area of concrete, it is difficult to absorb water, and the pore structure is in a state of moisture dissipation. While, in the non-carbonation area of concrete, the pore is in a state of saturation due to absorbing water, which made it become difficult to move for the water in pore. It can explain that the water content in the middle of concrete tended to increase, and was higher than the ones of bottom carbonated surface in Fig. 10. It is taken into consideration that this phenomenon is related to the increase in the proportion of large pore due to carbonation. In addition, Endo [57] also found that the lower the permeability, the higher the scaling mass, from which it can be explained that the scaling resistance of BFS concrete was improved due to the carbonation.

3.3.6 The change of hydration produces of BFS cement with different curing

Fig. 16 shows the amount of CH and calcium carbonate (CC) produced in water curing (w), air curing (a), carbonation curing (c), respectively. For the case after water curing for 4 weeks, the production amount of CH in the hardened cement paste was reduced with the increase of BFS replacement ratio, which may be due to that cement quantity decreased and the hydration reaction was slowed due to BFS added [10]. In addition, the amount of CC tended to decrease with the increase of BFS replacement ratio for the case after carbonation curing. This is because the total amount of calcium is reduced with an increase of BFS added.

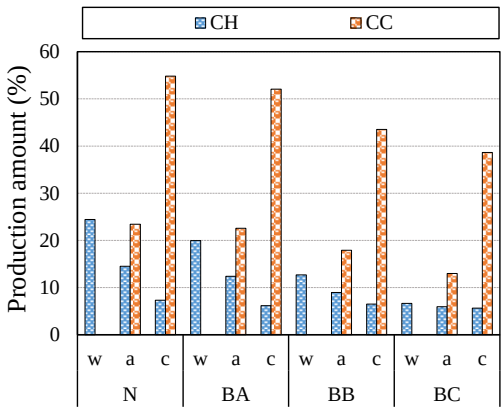

Fig. 16. Production amount of CH and CC.

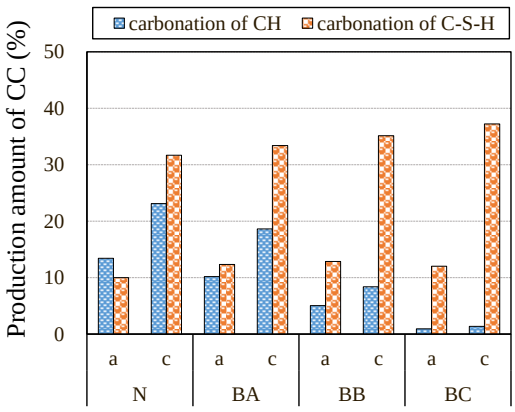

Fig. 17. Amount of CC by carbonation of CH and C-S-H.

Fig. 17 shows the production amount of CC by carbonation of CH and C-S-H, respectively. For both the cases after air curing and carbonation curing, the higher the BFS replacement ratio, the lower the amount of CC by carbonation of CH. While, the amount of CC by carbonation of C-S-H tend to increase with an increase of BFS replacement ratio. This can explain that the pore size distribution peak shifted to a larger diameter with an increase of BFS replacement ratio. In particular, little CH was carbonated, and CC mainly was by carbonation of C-S-H in BC, and this is why the densification of pore structure below 150nm is slowed for BC. In addition, in the previous study [58], it is reported that when the hardened cement paste has a low Ca/Si ratio, the amount of CC by carbonation of C-S-H increases. And this tendency is sufficiently confirmed in this study.

Fig. 18 shows the changes in diffraction intensity due to different curing obtained by X-ray diffraction. In Fig. 18, the peak of CH (2θ=18, 33.9, 47) in N was higher than in BB. In addition, vaterite (peak of V, 2θ=25, 27, 33, 44, 50.5, 56) and calcite (peak of C, 2θ=29, 39) were the polymorph of CC. And for the case after carbonation curing, the diffraction intensity of calcite in N was higher, while the diffraction intensity of vaterite in BB tended to be higher. This is due to that calcite was mainly produced in the carbonation of CH, and vaterite is mainly produced in the carbonation of C-S-H. The case of BB4w13c shows that there was a peak of CH even after carbonation curing for 13 weeks, which indicated that CH is not completely carbonated. It is the same as the result of production amount of CH in Fig. 16.

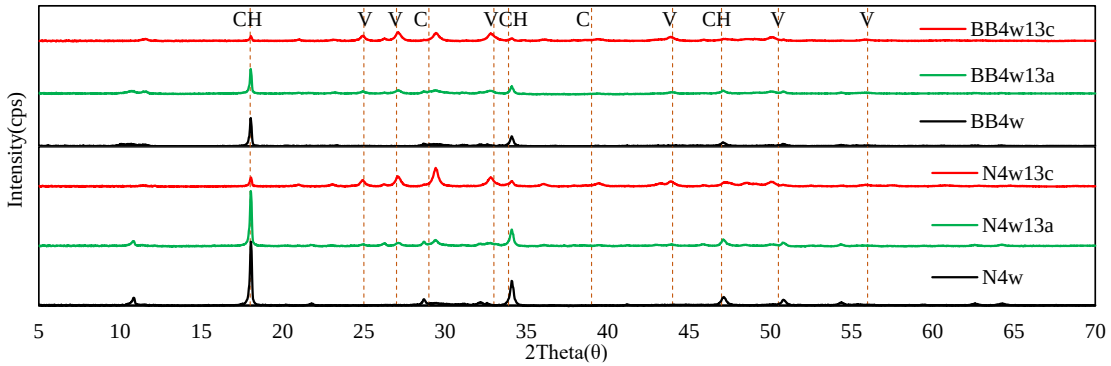

Fig. 18. Change in diffraction intensity obtained by X-ray diffraction.

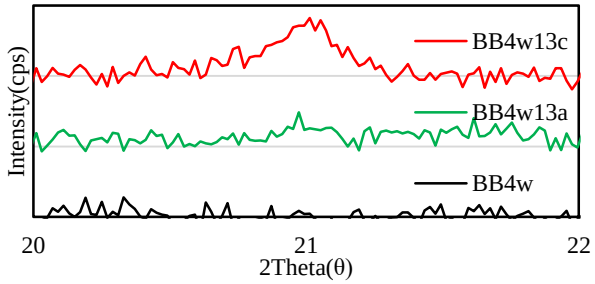

Fig. 19. Change in diffraction intensity of silica (SiO_2) in BB.

The changes in the diffraction intensity of silica (SiO_2) in BB are shown in Fig. 19. It is given that in Fig. 19: the diffraction intensity of SiO_2 increased due to carbonation. The C-S-H in BFS cement had a lower Ca/Si ratio than N, which caused that SiO_2 was easily separated out by carbonation of C-S-H. It can be proved that a large shift of the threshold diameter and a tendency of coarsening of the pore structure due to carbonation mainly was caused by carbonation of C-S-H.

3.3.7 Deterioration process of frost damage of concrete due to carbonation

Fig. 20 shows the deterioration process of frost damage of carbonated concrete. In Fig. 20a, under the carbonation conditions, due to carbonation of C-S-H in BFS concrete with a low Ca/Si ratio, the proportion of large pore increased, and permeability of concrete surface was raised to lead to lower the water content, which caused that scaling, which is an important characteristics of frost damage, was inhibited. In addition, for the freeze-thaw test in Fig. 20b, in the carbonation area of concrete, the water absorption was lowered to cause the

frost damage was suppressed. While, for the non-carbonation area, in which the pore was in a state of saturation, a significant deterioration due to freeze-thaw was expected due to a higher water content than the carbonated concrete surface. Therefore, for N and BA with a low BFS replacement ratio, in which the carbonation depth was small, and water content in the middle of concrete increased to lead to lower the frost resistance. And for BB and BC, which had a high BFS replacement ratio, the section size of the test specimens was 7.5×7.5cm, and the carbonation depth was 1.9cm. Three quarters of the area of concrete was carbonated to lead to decrease the water content of concrete, which could improve the frost resistance of concrete. Furthermore, there was a higher water content in inside concrete, it is expected that the inside of concrete was more vulnerable to frost damage, which caused that the surface area with a certain thickness would be scaled due to freeze-thaw condition.

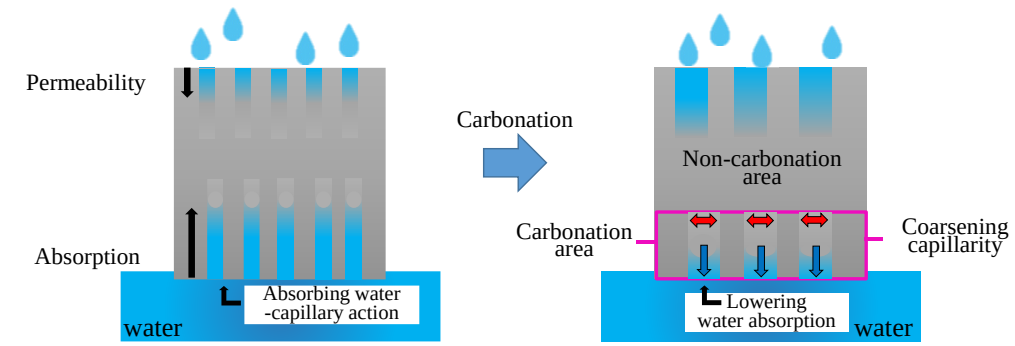

a) Deterioration process on scaling in CIF test

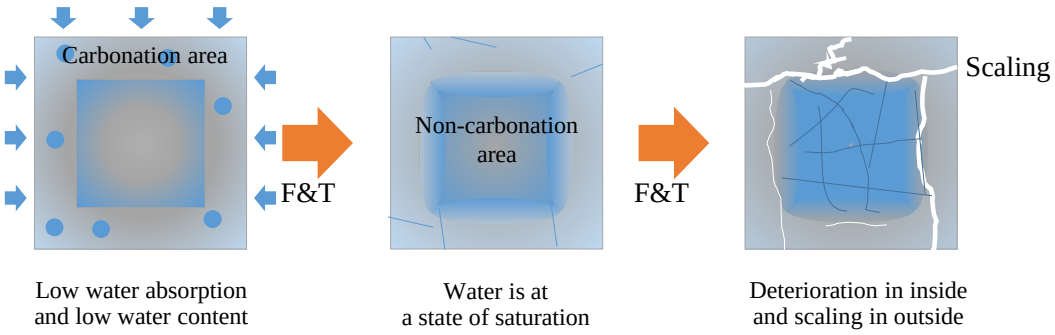

b) Deterioration process in freeze-thaw test (F&T: freeze-thaw)

Fig. 20. Deterioration process of frost damage in carbonated concrete

3.4 Conclusion

In this paper, the effects of carbonation on the frost resistance of the concrete with different BFS replacement

ratio were investigated. As a result, the following conclusions were obtained:

1) Under the same curing, carbonation resistance and scaling resistance decrease with the increasing BFS replacement ratio. The frost durability tends to decrease as BFS replacement ratio increases in Non-AE concrete.

2) With an increase of BFS replacement ratio, the production amount of CC in the hardened cement pastes by carbonation of CH tends to decrease even close to zero in BC, which causes that pore structure below 150nm in BC is not densified enough. And the one by carbonation of C-S-H tends to increase, which lead to the pore size distribution peak shifts to a larger diameter.

3) Under the carbonation conditions, carbonation of C-S-H gives a rise to the increase in the proportion of large pore, which brought about that permeability of concrete is raised and scaling is inhibited.

4) The frost resistance of N and BA with a low BFS replacement ratio tends to decrease, and the one of BB and BC, which has a high BFS replacement ratio, tends to increase due to carbonation. It is expected that the surface area with a certain thickness in the carbonated concrete will be scaled due to freeze-thaw condition.

References:

[1] M. Ángel Sanjuán, C. Andrade, Mora and A. Zaragoza, Carbon Dioxide Uptake by Cement-Based Materials: A Spanish Case Study, Appl. Sci. 10 (2020), doi.org/10.3390/app10010339

[2] Cement Technology Roadmap 2009: Carbon emissions reductions up to 2050, International Energy Agency, (2009), https://doi.org/10.1787/9789264088061-en

[3] G.M. Stefanovic, G.D. Vuckovic, M.M. Stojiljkovic, M.B. Trifunovic, CO2 reduction options in cement industry: the Novi Popovac case, Thermal Science, 14 (2010), pp. 671-679, doi.org/10.2298/TSCI091211014S

[4] S. Hesami, A. Modarres, M. Soltaninejad, H. Madani, Mechanical properties of roller compacted concrete pavement containing coal waste and limestone powder as partial replacements of cement. Constr. Build. Mater, 111 (2016), pp.625–636, doi.org/10.1016/j.conbuildmat.2016.02.116

[5] E. Aprianti, P. Shafigh, S. Bahri, J.N. Farahani, Supplementary cementitious materials origin from agricultural wastes—a review, Constr. Build. Mater, 74 (2015), pp. 176–187, doi.org/10.1016/j.conbuildmat.2014.10.010

[6] W. Zhang, Y. Hama, S. Na, Drying shrinkage and microstructure characteristics of mortar incorporating ground granulated blast furnace slag and shrinkage reducing admixture, Constr. Build. Mater, 93 (2015), pp.267–277, doi.org/10.1016/j.conbuildmat.2015.05.103

[7] S. Na, Y. Hama, M. Taniguchi, O. Katsura, T. Sagawa, M. Zakaria, Experimental investigation on reaction rate and self-healing ability in fly ash blended cement mixtures, Journal of Advanced Concrete Technology, 10 (2012), pp. 240–253, doi.org/10.3151/jact.10.240

[8] W.A. Moura, J.P. Goncalves, M.B.L. Lime, Copper slag waste as a supplementary cementing material to concrete, J Mater Sci, 42 (2007), pp. 2226–2230, doi.org/10.1007/s10853-006-0997-4

[9] M. A. Sanjuán, C. Argiz, P. Mora and A. Zaragoza, Carbon Dioxide Uptake in the Roadmap 2050 of the Spanish Cement Industry, Energies, 13 (2020), doi.org/10.3390/en13133452,

[10] E. Özbay, M. Erdemir and H. Durmuş, Utilization and efficiency of ground granulated blast furnace

slag on concrete properties – A review, Constr. Build. Mater, 105 (2016), pp. 423-424, doi.org/10.1016/j.conbuildmat.2015.12.153

[11] J. Qiu, Y. Zhou, N. I. Vatin, X. Guan, S. Sultanov, K. Khemarak, Damage constitutive model of coal gangue concrete under freeze-thaw cycles, Constr. Build. Mater, 264 (2020), doi.org/10.1016/j.conbuildmat.2020.120720

[12] B. Gérard, J. Marchand, Influence of cracking on the diffusion properties of cement-based materials: part I: influence of continuous cracks on the steady-state regime, Cem. Concr. Res., 30 (2000), pp. 37-43, doi.org/10.1016/S0008-8846(99)00201-X

[13] J. Zhao, G. Cai, D. Gao, S. Zhao, Influences of freeze–thaw cycle and curing time on chloride ion penetration resistance of Sulphoaluminate cement concrete, Constr. Build. Mater, 53 (2014), pp. 305-311, doi.org/10.1016/j.conbuildmat.2013.11.110

[14] C. Chung, C.S. Shon, Y.S. Kim, Chloride ion diffusivity of fly ash and silica fume concretes exposed to freeze–thaw cycles, Constr. Build. Mater, 24 (2010), pp. 1739-1745, doi.org/10.1016/j.conbuildmat.2010.02.015

[15] Y. Kurihashi, H. Konno, Y. Hama, Effects of frost-damaged reinforced concrete beams on their impact resistance behavior, Constr. Build. Mater, 274 (2021), doi.org/10.1016/j.conbuildmat.2020.122089

[16] J. A. Gonzalez, J. S. Algaba and C. Andrade, Corrosion of Reinforcing Bars in Carbonated Concrete, British Corrosion Journal, 15 (1980), pp. 135-139, doi.org/10.1179/bcj.1980.15.3.135

[17] M. Stefanoni, U. Angst and B. Elsener, Corrosion rate of carbon steel in carbonated concrete – A critical review, Cement and Concrete Research, 103 (2018), pp. 35-48, doi.org/10.1016/j.cemconres.2017.10.007

[18] Fe. Lollini, E. Redaelli, Carbonation of blended cement concretes after 12 years of natural exposure, Constr. Build. Mater, 276 (2021), doi.org/10.1016/j.conbuildmat.2020.122122.

[19] P. Liu, Z. Yua, Y. Chen, Carbonation depth model and carbonated acceleration rate of concrete under different environment, Cem. Concr. Com., 114 (2020),

doi.org/10.1016/j.cemconcomp.2020.103736

[20] R. Neves, B. Sena da Fonseca, F. Branco, J. de Brito, A. Castela, M. F. Montemor, Assessing concrete carbonation resistance through air permeability measurements, Constr. Build. Mater, 82 (2015), pp. 304-309, doi.org/10.1016/j.conbuildmat.2015.02.075

[21] C. Andrade and M. Á. Sanjuán, Updating Carbon Storage Capacity of Spanish Cements, Sustainability, 10 (2018), doi.org/10.3390/su10124806

[22] Y. Dan, T. Iyoda, Y. Ohtsuka, Y. Sagawa, and H. Hamada, The relationship between curing condition and durability on concrete using blast-furnace slag cement, J-STAGE, 65 (2009), pp. 431-441, doi.org/10.2208/jsceje.65.431, (in Japanese)

[23] B. Šavija, M. Luković, Carbonation of cement paste: Understanding, challenges, and opportunities, Constr. Build. Mater, 117 (2016), pp. 285-301,
doi.org/10.1016/j.conbuildmat.2016.04.138

[24] L. Dvorkin, Design estimation of concrete frost resistance, Constr. Build. Mater, 211 (2019), pp. 779-784, doi.org/10.1016/j.conbuildmat.2019.03.108

[25] Y. Şahin, Y. Akkaya, M. A. Taşdemir, Effects of freezing conditions on the frost resistance and microstructure of concrete, Constr. Build. Mater, 270 (2021),
doi.org/10.1016/j.conbuildmat.2020.121458

[26] E. Gruyaert, M. Maes, N. De Belie, Performance of BFS concrete: k-Value concept versus equivalent performance concept, Constr. Build. Mater, 47 (2013), pp. 441-455, doi.org/10.1016/j.conbuildmat.2013.05.006

[27] K. Abdelli, M. Tahlaiti, R. Belarbi, M. N. Oudjit, Influence of the pozzolanic reactivity of the Blast Furnace Slag (BFS) and metakaolin on mortars, Energy Procedia, 139 (2017), pp. 224-229, doi.org/10.1016/j.egypro.2017.11.200

[28] K. M. Lee, H. K. Lee, S. H. Lee, G. Y. Kim, Autogenous shrinkage of concrete containing granulated blast-furnace slag, Cem. Concr. Res., 36 (2006), pp. 1279-1285,
doi.org/10.1016/j.cemconres.2006.01.005

[29] M. A. Sanjuán, A. Piñeiro, O. Rodríguez, Ground granulated blast furnace slag efficiency coefficient (k value) in concrete. Applications and limits, Materiales de Construcción, 61 (2011), pp. 303-313, doi.org/10.3989/mc.2011.60410

[30] E. Gruyaert, P. V. Heede and N. D. Belie, Carbonation of slag concrete: Effect of the cement replacement level and curing on the carbonation coefficient – Effect of carbonation on the pore structure, Cem. Concr. Com.,35 (2013), pp. 38-48, doi.org/10.1016/j.cemconcomp.2012.08.024

[31] M. Á. Sanjuán, E. Estévez and C. Argiz, Carbon Dioxide Absorption by Blast-Furnace Slag Mortars in Function of the Curing Intensity, Energies, 12 (2019), doi.org/10.3390/en12122346

[32] W. Zhang, S. Na, J. Kim, H. Choi, Y. Hama, Evaluation of the combined deterioration by freeze–thaw and carbonation of mortar incorporating BFS, limestone powder and calcium sulfate, Mater. Struct., 50 (2017), doi.org/10.1617/s11527-017-1039-1

[33] W. Sun, R. Mu, X. Luo, C. Miao, Effect of chloride salt, freeze–thaw cycling and externally applied load on the performance of the concrete, Cem. Concr. Res., 32 (2002), pp. 1859-1864, doi.org/10.1016/S0008-8846(02)00769-X

[34] R.M. Ferreira, H. Kuosa and L. Makkonen, Performance & Durability of Concrete in Extreme Cold Environment, CSLA Project-Task 1. Literature Review: VTT Research Report. VTT-R-073643-12 (2012)

[35] CSLA (Concrete Service Life Assessment, 2012–2015) Leivo et al., 2011a, Ferreira et al., 2012

[36] M. Ferreira, H. Kuosa, M. Leivo, E. Holt, Concrete performance subject to coupled deterioration in cold environments, Nuclear Engineering and Design, 323 (2017), pp. 228-234, doi.org/10.1016/j.nucengdes.2016.10.021

[37] H. Kuosa, R. M. Ferreira, E. Holt, M. Leivo, E. Vesikari, Effect of coupled deterioration by freeze–thaw, carbonation and chlorides on concrete service life, Cem. Concr. Com., 47 (2014), pp. 32-40, doi.org/10.1016/j.cemconcomp.2013.10.008

[38] E. Kamada, O. Senbu, M. Tabata, Hirokazu, Statistical investigation concerning the effects of pore structure on the frost resistance of concrete, J. Struct. Constr. Eng., AIJ, 487 (1996), pp.1-9, doi.org/10.3130/aijs.61.1_9, (in Japanese)

[39] Japanese Industrial Standard Committee, Portland cement; JIS R 5210, Japanese Standards Association, Tokyo, Japan, 2019.

[40] Japanese Industrial Standard Committee, Ground granulated blast-furnace slag for Concrete; JIS A 6206; Japanese Standards Association, Tokyo, Japan, 2013.

[41] M. A. Sanjuán, C. Andrade, and M. Cheyrezy, Concrete carbonation tests in natural and accelerated conditions, Advances in Cement Research, 15 (2003), pp. 171-180, doi.org/10.1680/adcr.2003.15.4.171

[42] C. Pade and M. Guimaraes, The CO2 uptake of concrete in a 100 year perspective, Cem. Concr. Res., 37 (2007), pp. 1348-1356, doi.org/10.1016/j.cemconres.2007.06.009

[43] Japanese Industrial Standard Committee, Method of Test for Resistance of Concrete of Freezing and Thawing, JIS A 1148, Japanese Standards Association, Tokyo, Japan, (2010).

[44] RILEM Recommendation TC 176-IDC, Test method of frost resistance of concrete, Materials and Structures, 34 (2001), pp. 515-531,

[45] W. Zhang, Y. Hama, S. Na, Drying shrinkage and microstructure characteristics of mortar incorporating ground granulated blast furnace slag and shrinkage reducing admixture, Constr. Build. Mater, 93 (2015), pp. 267–277, doi.org/10.1016/j.conbuildmat.2015.05.103

[46] O. Kayyali, Mercury intrusion porosimetry of concrete aggregate. Mater. Struct., 18 (1985), pp. 259–262

[47] W. Zhang, M. Zakaria, Y. Hama, Influence of aggregate materials characteristics on the drying shrinkage properties of mortar and concrete, Constr. Build. Mater, 49 (2013), pp. 500–510, doi.org/10.1016/j.conbuildmat.2013.08.069

[48] H.R. P. Borges, O. J. Costa, B. N. Milestone, J. C. Lynsdale, E. R. Streatfield, Carbonation of CH and C-S-H in composite cement pastes containing high amounts, Cem. Concr. Res., 40 (2010), 284-292, doi.org/10.1016/j.cemconres.2009.10.020

[49] T.L. Thomas, The effects of air content, water-cement ratio, and aggregate type on the flexural fatigue strength of plain concrete (Ph.D. thesis), Iowa State University, (1979)

[50] S.O.Ekolu, A review on effects of curing, sheltering, and CO2 concentration upon natural carbonation of concrete, Constr. Build. Mater, 127 (2016), pp. 306-320, doi.org/10.1016/j.conbuildmat.2016.09.056

[51] M. Yamazaki, O. Chiho, T. Hasegawa, Study on frost resistance of concrete applied blast-furnace slag fine aggregate, Cement Science and Concrete Technology,.65 (2011), pp. 406-412, doi.org/10.14250/cement.65.406, (in Japanese)

[52] M. J. Setzer, Micro-Ice-Lens Formation in Porous Solid, Journal of Colloid and Interface Science, 243 (2001), pp. 193-201, doi.org/10.1006/jcis.2001.7828

[53] P.K. Mehta, D. Manmohan, Pore Size Distribution and Permeability of Hardened Cement, 7th International Congress Chemistry Cement l Paris, 3 (1980), pp.7.1-7.5

[54] N. X. Quy, J. Kim, Y. Hama, Effect of 10-Year Outdoor Exposure and Curing Conditions on the Pore Structure Characteristics of Hardened Cement Mortar, Journal of Advanced Concrete Technology, Journal of Advanced Concrete Technology, 16 (2018), pp. 461-475, doi.org/10.3151/jact.16.461

[55] Y. Harasawa, Effects of different carbonation conditions on pore properties and carbonation products, Proceedings of the Japan Concrete Institute, 36 (2014), pp. 808-813, (in Japanese)

[56] M. Aoyama, Study on the mechanism of salt transfer in the carbonation area, Proceedings of the Japan Concrete Institute, 35 (1) (2013), (in Japanese)

[57] H. Endo, Study on Durability Design Method for Control of Scaling due to Combined Action by Freeze-Thaw and Chloride, Doctorate Thesis, Hokkaido University, 2011

[58] Y. Aono, B. Matushita, S. Juno, Y. Hama, Changes in pore structure of cement paste due to repeated dry and wet conditions, Proceedings of the Japan Concrete Institute, 29 (2007), pp.993-998, (in Japanese)

Chapter 4

EVALUATIONS OF FROST AND SCALING RESISTANCE OF FLY ASH CONCRETE IN TERMS OF CHANGES IN WATER ABSORPTION AND PORE STRUCTURE UNDER THE ACCELERATED CARBONATION CONDITIONS

4.1 Overview

In cold region, the frost damage often occurs in the winter construction of concrete, which seriously threatens the performance and structural safety of concrete [1]. The other concrete deteriorations such as salt damage, carbonation, and alkali-silica reaction are also related closely to the durability of concrete [2], [3], [4]. So far, the single deterioration mechanism is mainly studied in almost previous studies and the results have been accumulated substantially. However, for the actual concrete structures, it is not possible to suffer a single deterioration only. In general, for the cause of deterioration in a concrete structure, a deterioration phenomenon called combined deterioration [5], [6], [7] is often seen, in which the deterioration characteristics generated by the interaction of different deterioration phenomenon cannot be evaluated by adding two and more single deterioration model.

For concrete in cold region, the frost damage due to freeze-thaw repeated is the main degradation phenomenon, and is inevitable in winter. Therefore, in order to study the durability of concrete, the frost resistance of concrete has been focused on, and has been studied extensively. From the previous studies, it is well-known that the frost damage of concrete has a close relationship with the water in pore structure [8], and is caused by the huge expansion stress due to 9% expansion of ice formation when the water in concrete is frozen [9], [10]. Besides, as we know, the pore structure is decisive in the mechanical and durability properties of concrete. Kamada et al. [11] and Quy et al. [12], [13] claimed that frost resistance of concrete is related closely to pore volume in diameter from 40 to 2000 nm. Similarly, it is confirmed that frost resistance of concrete is determined by the capillary porosity value, and the frost resistance decreases with the increase of capillary porosity [14]. However, the effect of gel porosity on frost resistance of concrete has not been proven.

Based on the combined deterioration, the frost damage of concrete subjected to other deterioration phenomenon has received much attention in recent years. For most of concrete structures, carbonation is in presses to reduce the pH of concrete with intrusion of CO2 into concrete due to a long-term exposure to air. For carbonation of concrete, it is concluded that in some studies [15], [16]: carbonation results a densification of the pore structure, which is depended on by the frost damage. From the studies on the frost resistance of carbonated

concrete [17], [18], it is well known that natural carbonation curing results a larger frost-salt scaling, however, Duo Zhang et al. [19] confirmed that accelerated carbonation curing improved scaling resistance of concrete. Takeda et al. [20] concluded that for ordinary Portland cement (OPC) concrete, frost damage has little effect on the progress of carbonation of concrete, and there is little change in frost damage due to carbonation. Zhang et al. [21] pointed out that for blast furnace slag (BFS) mortar, the freeze-thaw repeated results a reduce of carbonation resistance, and the scaling mass loss decreases due to carbonation of concrete.

On the other hand, the atmospheric CO2 concentration has been increased and lead to the greenhouse effect that global temperatures increase, and a global “climate and environmental emergency” had been declared in 2019 to rise the challenge of climate change [22]. It has become a global trend to limit and reduce carbon dioxide emissions. The study [23] shows that the CO2 emissions due to cement manufactured accounts for 8% of all in the world, approximately. Therefore, in recent years, in the trend of CO2 emission reduction, fly ash (FA) are used more widely to reduce the cement consumption in the field of building materials, and the use of FA can result in a concrete with better durability [24]. In Japan, according to the Japan Industrial Standards (JIS) R 5213 [25], FA cement is classified into type A, in which FA replacement ratio is from 5 to 10%, type B, in which FA replacement ratio is from 10 to 20%, and type C, in which FA replacement ratio is from 20 to 30%, respectively. With the expansion of the use of FA, the property of FA concrete is studied. From the previous studies [26], [27], it is known that the additive of FA can change the microstructure, durability and mechanical properties of concrete. Comparing with OPC concrete [28], [29], [30], FA concrete has low heat generation and a high long-term strength, however, the use of FA results a delay in early-age strength. Carbonation or frost resistance of concrete also are reduced due to FA added [31], [32], [33]. Besides, using FA can improve water-tightness and reduce air entraining for concrete [31]. Under the trend of FA popularization in the world, in order to grasp the durability of FA concrete, it is necessary to evaluate the effect of FA on the combined deterioration between carbonation and frost damage of concrete. However, little research on combined deterioration of FA concrete has been studied.

Therefore, in this paper, the change in frost resistance of concrete with different FA replacement ratios under

the carbonation conditions was studied. In addition, it is well-known that the frost resistance has a close relationship with air content of concrete [34]. In order to lessen the effects of frost damage on concrete, AE additive is often added to increase the volume of air in the mixture. In addition to this, the influence that the AE admixture had on the overall degradation was investigated.

4.2 Experimental program

4.2.1 Experimental program

Experiments were carried out using concrete specimens as shown in Table 1. FA concrete specimens with 0.55 water-to-binder ratio (W/B) and 0.447 sand-to-aggregate ratio (s/a) were used. The slump was controlled at 18±2cm, and air content was controlled at 1.0±1.0% for Non-AE concrete, or at 4.5±1.5% for AE concrete based on the JIS A 6204 [34]. AE admixture named 'MasterAir® 785' was used to improve air content of FA concrete. However, according to JIS A 6204 [35], an AE admixture named 'MasterAir® 101' is used in AE-N. The ordinary Portland cement based on the JIS R 5210 [36] (Nippon steel cement corporation, Muroran, Japan) with a specific gravity of 3.17 g/cm^3 and the fly ash based on the JIS A 6201 [37] (Hokkaido Electric Power corporation, Tomakomai, Japan) with a specific gravity of 2.91 g/cm^3 were used in this study. The chemical compositions and physical properties of OPC and FA are shown in Table 2. FA cement Type A, Type B and Type C were denoted as FA_A, FA_B and FA_C, which contained FA with a replacement ratio at 7.5%, 15%, and 25%, respectively. Shiraoi land sand with surface-dry density of 2.67 g/cm^3 and a water absorption of 1.57% was used as the fine aggregate. Shikiu River andesite with a surface-dry density of 2.57 g/cm^3 and a water absorption of 2.98% was used as the coarse aggregate. This coarse aggregate had a nominal maximum size of 20 mm.

In this study, the basic mechanical properties containing compressive strength, frost resistance and scaling resistance were tested after 4 weeks of water curing. In order to investigate the effect of carbonation of concrete, according to JIS A 1153 [38], the concrete specimens are curing in water until the material age of 4 weeks, and are curing in air (20℃, 60%RH) until the material age of 8 weeks. After that, concrete specimens were subjected to carbonation curing (20℃, 60%RH, 5.0%CO_2 concentration) and air curing (20℃, 60%RH) for 13 weeks. The

experimental items were conducted once after air and carbonation curing.

For the microstructure test, the porosity was calculated by the Archimedes method and the pore size distribution was determined by the mercury intrusion porosimetry (MIP) method [39]. The MIP method was tested using mortar, which was obtained by performing wet screening to remove coarse aggregate in fresh concrete.

The mix proportions and fresh properties of concrete are shown in Table 3.

Table 1. Experimental design

Type	FA replacement ratios (%)	Objective		Curing		Experimental items
		Air content (%)	Slump (cm)	Standard curing	Curing condition	
FA concrete	0 7.5(Type A) 15(Type B) 25(Type C)	1.0 (Non-AE) or 4.5 (AE)	18	Water curing for 4 weeks	Air curing or carbonation curing for 13 weeks	Compressive strength test Accelerated carbonation test Freeze-Thaw test RILEM / CIF test Microstructure test

Table 2. Chemical compositions and physical properties of OPC and FA

Binder type	Blaine fineness (cm^2/g)	Chemical composition (wt.%)								
		SiO_2	Al_2O_3	Fe_2O_3	CaO	MgO	K_2O	Na_2O	SO_3	LOI
OPC	3390	21.4	5.5	2.8	64.3	3.1	0.4	0.3	1.9	0.56
FA	4010	57.75	23.65	5.75	3.75	1.1	-	-	1.05	1.8

Table 3. Mix proportions and fresh properties of concrete

Symbol	W/B (%)	s/a (%)	Binder (%)		Materials contents (kg/m^3)					AE admixture (ml/m^3)	Fresh properties	
			OPC	FA	W	OPC	FA	S	G		Air (%)	SL (cm)
N	55	44.7	100	0	204	371	0	801	991	0	0.4	17.9
FA_A			92.5	7.5	193	325	26	818	1012		0.4	18.0
FA_B			85	15	193	298	53	813	1006		0.2	18.5
FA_C			75	25	193	263	88	808	999		0.2	17.8
AE-N			100	0	184	335	0	779	991	13	4.8	18.6
AE-FA_A			92.5	7.5	185	311	25	785	971	101	5.2	19.7
AE-FA_B			85	15	181	280	49	788	975	148	5.6	19.7
AE-FA_C			75	25	178	242	81	790	977	194	5.3	19.5

4.2.2 Test method

4.2.2.1 Compressive strength test

According to JIS A 1108 [40], the compressive strength test was conducted using three test specimens with dimension of φ100×200mm after 28 days of water curing. The maximum loads (P) until three specimens were damaged were tested and the compressive strength was calculated by the following equation:

$$f_c = \frac{P}{\pi \times \left(\frac{d}{2}\right)^2} \quad \text{Eq. (1)}$$

where, f_c is the compressive strength (N/mm^2); P is the maximum load (N); and d is the diameter of concrete specimen (mm).

The compressive strength of concrete was the average value of the three specimens.

4.2.2.2 Accelerated carbonation test

According to JIS A 1153 [37], the test specimens of accelerated carbonation test were conducted at the material age of 8 weeks (4 weeks in water and were dried for 4 weeks in air). And then the specimens were cured for 13 weeks in a chamber with a carbonation concentration of 5% at 20℃ and 60% relative humidity. The carbonation depth was measured by spraying the split concrete with a phenolphthalein indicator. The carbonation speed coefficient was obtained by the following equation [41], [42]:

$$x = k\sqrt{t} \quad \text{Eq. (2)}$$

where, x is the depth of carbonation (mm); t is the time at which carbonation has taken place (week); and k is the carbonation speed coefficient (mm・weeks$^{-0.5}$).

4.2.2.3 Freeze-thaw in water test

According to JIS A 1148 A [43], the test specimens were subjected to freeze-thaw in water in a chamber, where the temperature was maintained the minimal temperature of -18℃ and the maximal temperature of 5℃. The resonant frequency of specimens was measured before freeze -thaw in water test, and then was measured every 30-cycle when subject to freeze-thaw until 300 cycles or it was broken. The relative dynamic modulus of elasticity was calculated using the following equation:

$$P_n = \frac{{f_n}^2}{{f_0}^2} \times 100\% \quad \text{Eq. (3)}$$

where, P_n is the dynamic modulus of elasticity after n cycles of freeze-thaw (%); f_n is the resonant

frequency after n cycles of freeze-thaw (Hz); f_0 is the resonant frequency at 0 cycles of freeze-thaw (Hz);

The durability factor was obtained by the following equation:

$$DF = (P \times N)/M \quad \text{Eq. (4)}$$

where, DF is durability factor of concrete; P is the dynamic modulus of elasticity after N cycles (%); N is the small number between the number of cycles after that the relative elastic modulus becomes 60% and 300 cycles; M is 300 cycles;

4.2.2.4 RILEM / CIF test

Based on the RILEM method [44], in order to evaluate scaling resistance of concrete, the RILEM/CIF test was conducted using the test specimens of φ100×200 mm. Before this test, the test specimens were dried in air for 2 weeks, and then the side surface of the specimens was sealed by the aluminum tape with butyl rubber, and absorbing water in the bottom surface was performed for 7 days before freeze-thaw. Starting from absorbing water, the mass of test specimens was recorded daily and the water absorption was calculated. After that, the bottom surface of specimens, which was kept absorbing water in a chamber, was subjected to freeze-thaw. The temperature was maintained at -20℃ to 20℃. The water absorption and scaling mass were tested per 6 cycles when subjected to freeze-thaw. The scaling mass (Un) is the mass dropped per unit area. The dropped mass (m) due to freeze-thaw were determined by dried at 105℃ for 24h, and the scaling mass was calculated by the following equation:

$$U_n = \frac{m}{\pi \times \left(\frac{d}{2}\right)^2} \quad \text{Eq. (5)}$$

where, U_n is the scaling mass (g/mm^2); m is the dropped mass due to freeze-thaw (g); and d is the diameter of concrete specimen (mm).

The cumulative scaling mass is the sum of all scaling mass until n cycles.

4.2.2.5 Microstructure test

For the Archimedes method, the test specimens of φ100 × 200 mm were cut into cylinders with a thick of 20 mm evenly. The cylinders were placed into the water to absorb water in an evacuated chamber for 1 week. After

that, the cylinders were dried at 40℃ for 3 weeks and at 105 ℃ for 2 days (the water content in capillary pore is considered to escape for the drying of 40℃, and the water content in gel pore will escape for the drying of 105℃).

For MIP method, the pore size distribution was determined using mortar in accordance with the JIS R 1655 [39]. The mortar specimens of 40×40×160mm were cut into 5mm cubes at age of 4 weeks, and were curing in air and carbonation condition. Before test, the mortar cubes were stopped hydration reaction in the ethanol for 1 week, and then were dried by the F-dry method. Besides, in order to avoid the effect of material separation, the specimen was cut into cubes excluding 5 mm from the surface of mortar.

4.3 Experiment result and discussion

4.3.1 The effect of compressive strength on carbonation process

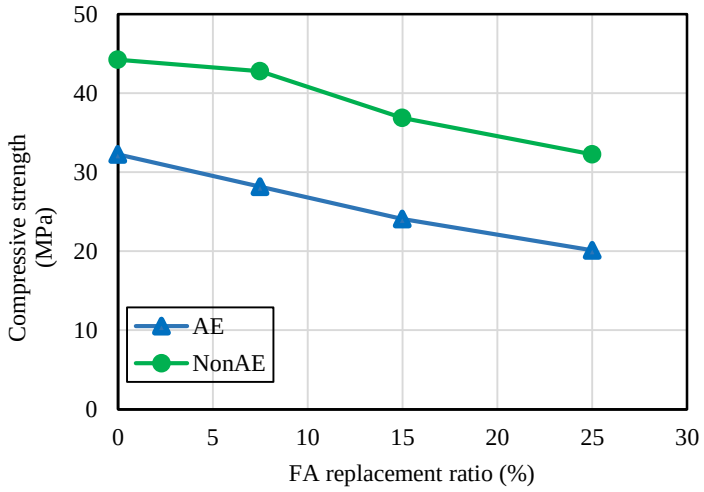

Fig. 4-1. Compressive strength result at 28-day

The relationships between compressive strength and FA replacement ratio of concrete are shown in Fig. 4-1. It can be seen that the compressive strength of both AE and Non-AE concrete decreased as the FA replacement ratio increased. This is due to the more FA replacement ratio, the less the quantity of OPC will led to decrease of hydration of cement, and reduce the compressive strength of concrete at 28-day. In the previous study [45], it is found that when the AE admixture is used as concrete additive, the compressive strength of concrete can be

reduced by the increased porosity. Comparing the cases of Non-AE and AE, under the same FA replacement ratio, the compressive strength of AE concrete was reduced due to an interfusion of AE admixture, which is consistent with the previous study [45].

Fig. 4-2 shows the carbonation depths of all AE and Non-AE concretes. For the cases of carbonation curing after water curing (4w13c), the carbonation depth tended to increase when FA replacement ratio increased whether AE or Non-AE concrete, which is in good agreement with the results of previous study [31]. And indeed, the results of AE concrete were higher than the ones of Non-AE concrete under the same FA replacement ratio, which is due to a higher air-entraining property caused by AE admixture.

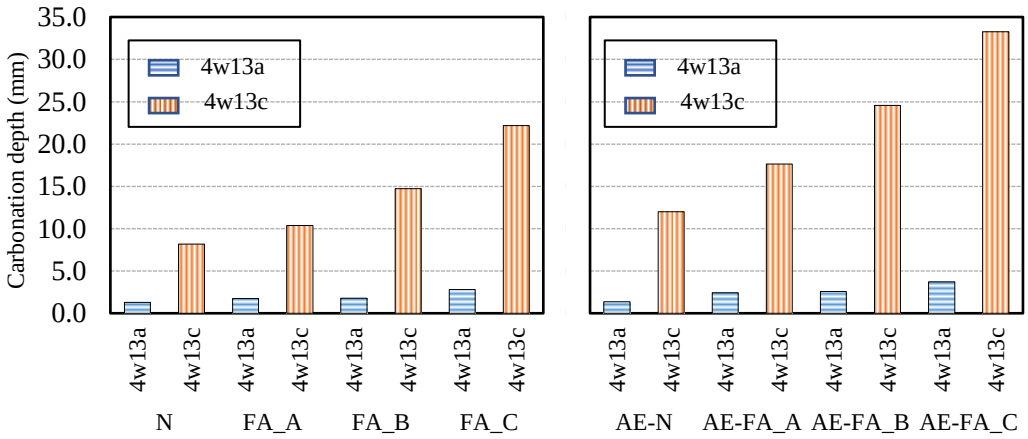

Fig. 4-2. Carbonation depth of FA concrete

In previous study [32], it is confirmed that there is a close relationship between the carbonation depth of natural carbonation and accelerated carbonation for FA concrete, and the natural carbonation depth can be predicted from the accelerated carbonation depth using the following equation:

$$D_{n,t} = A \times D_a \times \sqrt{t} \qquad \text{Eq. (6)}$$

where, $D_{n,t}$ is the carbonation depth of concrete normal exposed in natural environment for t months, D_a is the carbonation depth of the same concrete tested in the accelerated carbonation chamber for one month (mm), t is the exposure time in a real environment (months), A is the slope of the relationship, which is dependent on

the environmental conditions.

From Eq. (5), it can be known that for the same environmental conditions and exposure time, there is a linear relationship between the carbonation depth of natural carbonation and accelerated carbonation. In this study, the relationship between the carbonation depth in air and carbonation curing are shown in Fig. 4-3. From the R^2 value with 0.933, it can be obtained that the carbonation depth in case of air curing (4w13a) can be predicted by in case of carbonation curing (4w13c).

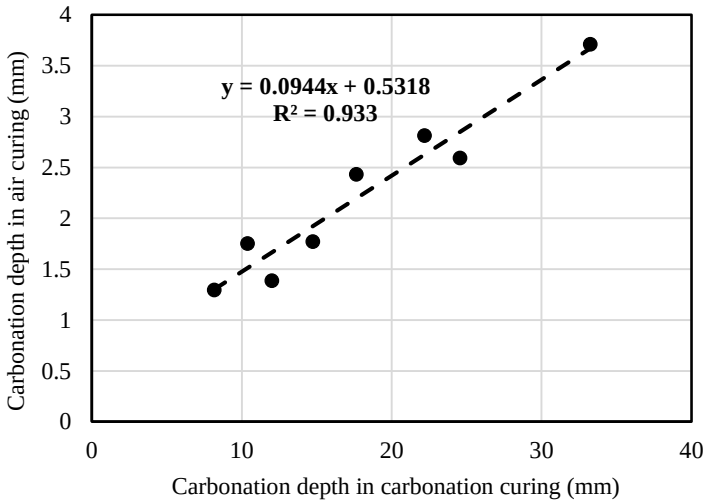

Fig. 4-3. Relationship between carbonation depth in air and carbonation curing

It also is pointed out that in previous study [32], the carbonation coefficient of FA concrete is related strongly to its 28-day compressive strength. The relationships between the carbonation speed coefficient in air (4w13a) and carbonation (4w13c) curing and the compressive strength in this study are shown in Fig. 4-4.

In Fig. 4-4, for the case of 4w13c, the R^2 value with 0.8101 signified that there was a good correlation between the carbonation speed coefficient and the compressive strength. The lower the compressive strength, the larger the carbonation speed coefficient, which is similar to result of previous study [32]. With the increasing FA replacement ratio, the hydration reaction of cement was decreased to lead to reduce the densification of concrete, which increase the capillary pores, and then it was easier for intrusion of CO_2 into concrete to accelerate the carbonation of concrete. While for the case of 4w13a, the R^2 value with 0.672 was lower than the one of 4w13c,

which might signify that for the case of 4w13a, the correlation between the carbonation speed coefficient and the compressive strength is lower than the case of 4w13c. However, from the previous study [32], it is believed that there is a strong relationship between them, which may be because the carbonation speed coefficient is obtained from 24 months natural carbonation curing. While, in this study, air curing was performed for 13 weeks, which maybe lead to carbonation of concrete slowly progressed, and carbonation depth was very small. Therefore, it is difficult to predict correlation exponent exactly.

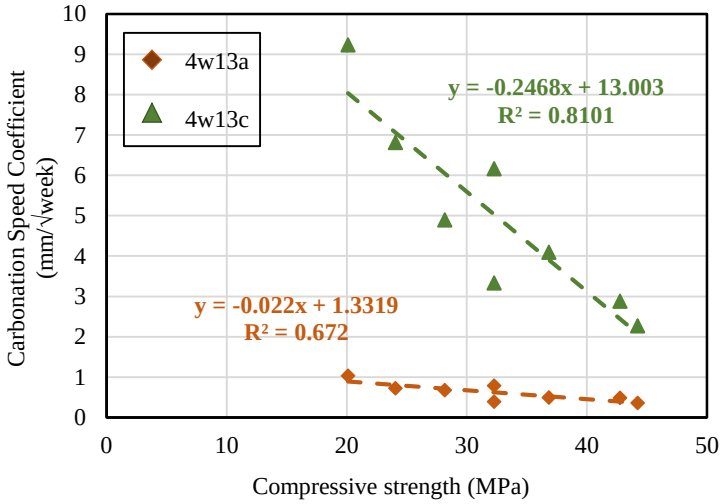

Fig. 4-4. Relationship between the carbonation speed coefficient and the compressive strength

From Fig. 4-2, it can be well-known that the carbonation depth in air curing for Non-AE concrete is less than 3mm, even for AE concrete, which is carbonated easily, the carbonation depth is less than 4mm. The carbonation depth in air curing is less than 1/25 in length of concrete (100mm), which can be considered that carbonation of concrete can be ignored in air curing. While, carbonation of concrete was obviously carried out in carbonation curing. Therefore, by comparing the results in air and carbonation curing, the effect of carbonation of concrete can be investigated.

4.3.2 The change of frost and scaling resistance due to carbonation

4.3.2.1 The frost and scaling resistance of concrete after 4 weeks of water curing

The changes of relative dynamic modulus of elasticity (RDME) of AE and Non-AE concrete after 4 weeks of water curing due to freeze-thaw cycles in the freeze-thaw test are shown in Fig. 4-5. For the case of Non-AE, it can be seen that due to freeze-thaw cycles, the RDME of concrete tended to decrease for all concrete, and the deterioration of concrete was promoted with the increase of FA replacement ratio. The reason may be that the capillary pore increased due to the increase FA replacement ratio. For the case of AE, little change was observed on the RDME due to freeze-thaw cycles for all concrete. The high frost resistance due to AE admixture could be confirmed in this study.

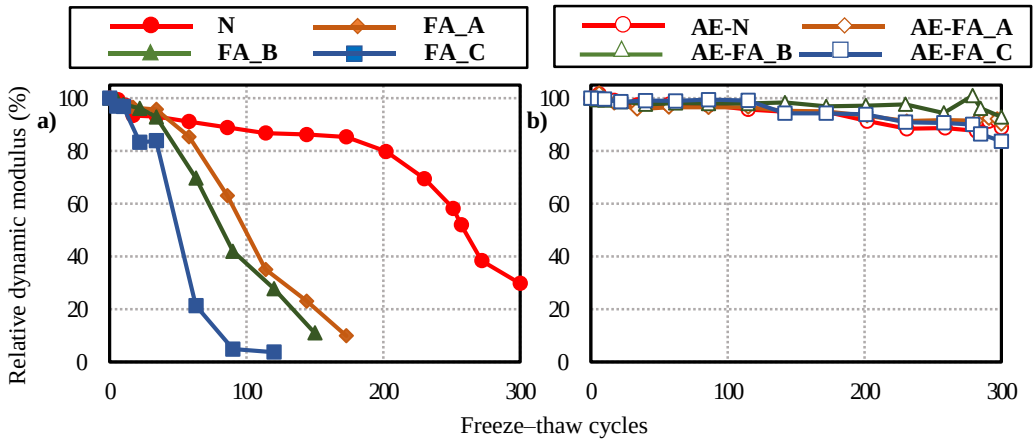

Fig. 4-5. Relative dynamic modulus of elasticity results of all FA concrete after water curing (4w)
a): Non-AE concrete; b): AE concrete

Fig.4-6 shows the changes of the cumulative scaling mass in AE and Non-AE concrete after 4 weeks of water curing due to freeze-thaw cycles in CIF test. Compared to AE concrete, the scaling mass in Non-AE concrete slightly increased, but was less 0.05 g/cm^2. Therefore, it is evident that there is no sensible increase in the scaling mass due to freeze-thaw for all concrete after water curing.

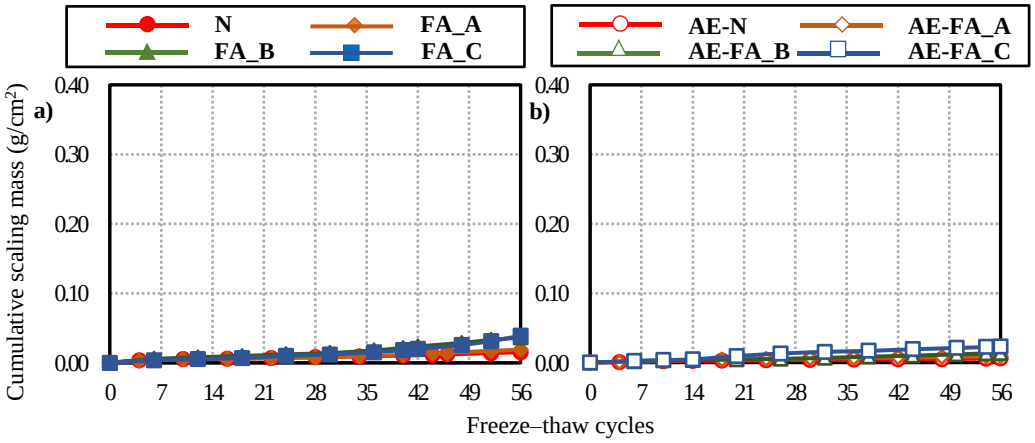

Fig. 4-6. Scaling mass results of all FA concrete after water curing (4w)

a): Non-AE concrete; b): AE concrete

4.3.2.2 The frost and scaling resistance of concrete in air and carbonation curing after water curing

The changes of RDME due to freeze-thaw cycles of AE and Non-AE concrete in the freeze-thaw test are shown in Fig. 4-7. Fig. 4-7a and Fig. 4-7b show the RDME of Non-AE concrete in air (4w13a) and carbonation (4w13c) curing after water curing (4w), respectively. For the case of 4w13a, the RDME of concrete had fallen to less than 60% since 36 cycles for FA_A, FA_B, and FA_C, and there are little change on them with the increase of FA replacement ratio. Compared to the results in the case of 4w (see Fig. 5a), the deterioration was progressed for all concrete due to air curing. For the case of 4w13c, there was a same trend on the RDME in the case of 4w13a. Comparing with the cases of 4w13a and 4w13c, there is little change on the RDME of concrete due to carbonation of concrete.

Fig. 7c and Fig. 7d show the RDME of AE concrete in air (4w13a) and carbonation (4w13c) curing after water curing (4w), respectively. For both 4w13a and 4w13c, comparing with the case of 4w (see Fig. 4-5b), the RDME had not been decreased due to air curing or carbonation curing after water curing, and all samples were kept at a high level due to AE admixture. Therefore, it can be said that the effect of carbonation on frost resistance can be ignored for AE concrete.

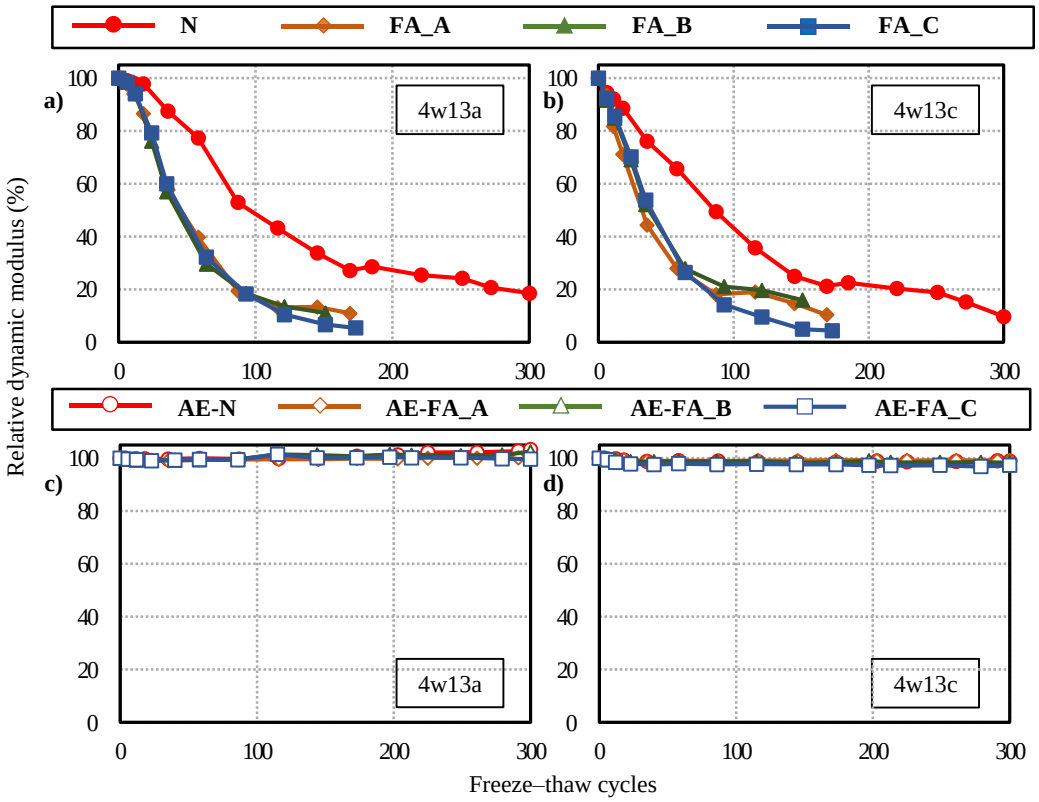

Fig. 4-7. RDME results of all FA concrete in the cases of air (4w13a) and carbonation (4w13c) curing

a), b): Non-AE concrete; c), d): AE concrete

The changes of the cumulative scaling mass due to freeze-thaw cycles of AE and Non-AE concrete in the CIF test are shown in Fig. 4-8. Fig. 4-8a and Fig. 4-8b show the cumulative scaling mass of Non-AE concrete in air (4w13a) and carbonation (4w13c) curing after water curing (4w), respectively. For the case of 4w13a, the cumulative scaling mass significantly increased with the increase FA replacement ratio. While for the case of 4w13c, scaling mass was kept a low level, and there was no increase for N, FA_A and FA_B, with an increase of FA replacement ratio. However, for FA_C, although the cumulative scaling mass had not increased due to freeze-thaw until 30-cycle, the cumulative scaling mass significantly increased since 36-cycle. Comparing with the results of 4w (see Fig. 4-6a), for the case of 4w13a, the cumulative scaling mass was increased due to air curing. For the case of 4w13c, the cumulative scaling mass in N, FA_A and FA_B was decreased slightly due to carbonation curing, while for FA_C, it was significantly increased due to carbonation curing. Comparing the

cases of 4w13a and 4w13c with a same material age, it can be seen that the cumulative scaling mass could be restrained due to carbonation of concrete.

Fig. 4-8c and Fig. 4-8d show the cumulative scaling mass in the cases of 4w13a and 4w13c of AE concrete, respectively. Compared to the cases of Non-AE, it can be obtained that scaling mass was restrained due to AE admixture. For both the cases of 4w13a and 4w13c, comparing with the results of 4w (see Fig. 4-6b), the cumulative scaling mass had not been changed obviously due to air curing or carbonation curing, and the all ones were kept at a low level due to AE admixture. Therefore, it also can be said that the effect of carbonation on scaling resistance can be ignored for AE concrete.

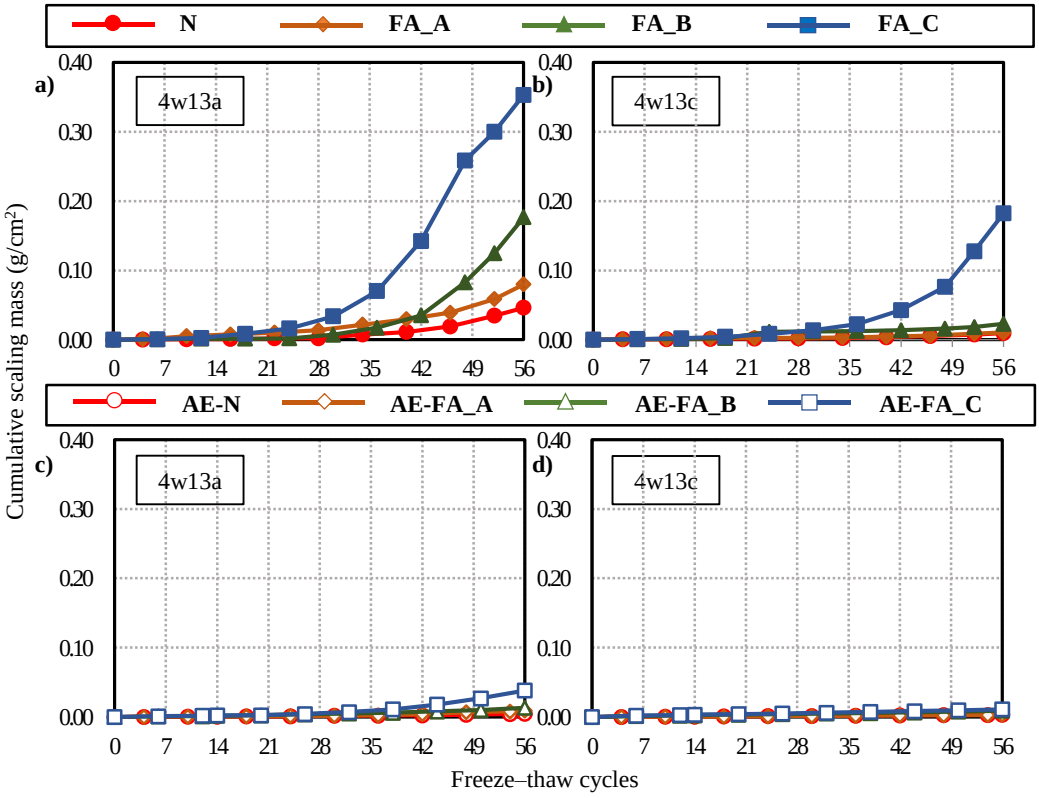

Fig. 4-8. Scaling mass results of all FA concrete in the cases of air (4w13a) and carbonation (4w13c) curing

a), b): Non-AE concrete; c), d): AE concrete

4.3.2.3 The changes in durability factor and scaling mass due to carbonation

Fig.4-9 shows the changes in durability factor of AE and Non-AE concrete due to FA replacement ratios. Fig. 4-9a shows the durability factor results obtain from the freeze-thaw test in Non-AE concrete. As seen in Fig. 4-9a, the durability factor decreased when the FA replacement ratio increased for all curing conditions. Based on the case of 4w, the durability factor for N, FA_A and FA_B in the cases of both 4w13a and 4w13c had dropped a little due to air and carbonation curing, while, though there was no change in the durability factor due to curing condition for FA_C, the durability factor of FA_C in all curing were less than 10. It can be said that the durability factor was reduce due to the next curing stage in air after water curing, regardless of CO_2 exposure conditions, which is because drying of concrete results to coarsen of pore structure remarkably [46]. Comparing the cases of 4w13a and 4w13c, there was no obvious gap between them, and it can be said that the durability factor is not influenced by carbonation of concrete in Non-AE concrete.

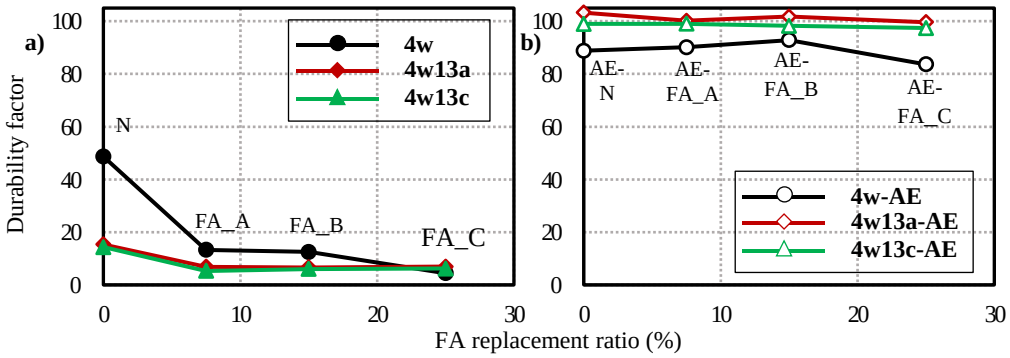

Fig. 4-9. Change of durability factor due to FA replacement ratio (4w: water curing for 4 weeks, 4w13a: air curing for 13 weeks after water curing, 4w13c: carbonation curing for 13 weeks after water curing)

a): Non-AE concrete; b): AE concrete

Fig. 4-9b shows the durability factor results obtain from the freeze-thaw test in AE concrete. The durability factor of AE concrete was maintained a high value above 80 in all curing conditions, regardless of FA replacement ratio. This is because the high air content due to AE additive can improve the frost damage of FA concrete. Based on the case of 4w, for the cases of 4w13a and 4w13c, the durability factors were lightly improved due to the following curing for 13 weeks, regardless of air or carbonation curing. In addition, comparing the cases of 4w13a and 4w13c, it can be seen that there is little gap between the durability factors. Therefore, it can be said that the durability factor was not influenced by carbonation of concrete for AE concrete.

Fig.4-10a and Fig. 4-10b show the changes in the cumulative scaling mass at 56-cycle of Non-AE and AE concrete due to FA replacement ratios, respectively. It is shown that the cumulative scaling mass at 56-cycle increased as FA replacement ratio increased under the same curing condition. And comparing the results of Non-AE and AE concrete, it was confirmed that the scaling was inhibited by AE admixture. In Fig. 10a, for the case of 4w13a of Non-AE concrete, comparing with the case of 4w, the scaling mass increased due to air curing, and the higher the FA replacement ratio, the more the scaling mass increased. For the case of 4w13c, comparing with the case of 4w, the scaling mass was slightly inhibited due to carbonation curing in N, FA_A and FA_B. However, the scaling mass of FA_C increased obviously due to carbonation curing. Besides, comparing the cases of 4w13a and 4w13c, the scaling mass of concrete was decreased due to carbonation of concrete, and the scaling resistance increased by carbonation was raised with the increase FA replacement ratio.

In Fig. 4-10b, the scaling mass was kept at a low value in all curing conditions, and there was no obvious gap between the cases of 4w13a and 4w13c. The scaling mass was not influenced by carbonation of concrete for AE concrete.

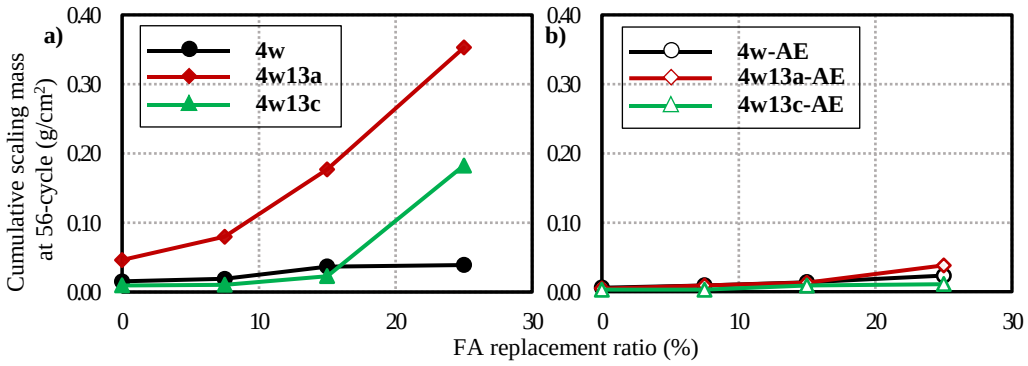

Fig. 4-10. Change of scaling mass due to FA replacement ratio (4w: water curing for 4 weeks, 4w13a: air curing for 13 weeks after water curing, 4w13c: carbonation curing for 13 weeks after water curing)
a): Non-AE concrete; b): AE concrete

Based on the above, it is well-known that the frost and scaling resistance in AE concrete are raised by AE

admixture, and are not influenced by carbonation of concrete, regardless of FA replacement ratio. Therefore, the effect of carbonation on the frost and scaling resistance in Non-AE concrete can be investigated from the view of water absorption and pore structure in the next section.

4.3.3 The change of water absorption due to carbonation

4.3.3.1 The water absorption of concrete after 4 weeks (4w) of water curing

Fig. 4-11 shows the water absorption of Non-AE concrete of 4w in CIF test. It can be seen that in the process of absorbing water of bottom surface before freeze-thaw, there is little gap between the water absorption for N, FA_A and FA_B. For FA_C, the water absorption was the highest, but was less than 1%. When FA concrete was subjected to freeze-thaw, the water absorption increased due to freeze-thaw for all concrete.

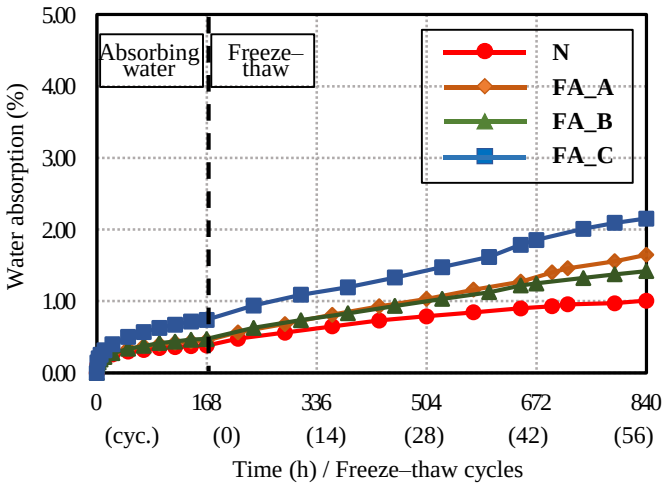

Fig. 4-11. Results of water absorption in Non-AE concrete after water curing (4w)

4.3.3.2 The water absorption of concrete in air (4w13a) and carbonation (4w13c) curing after water curing (4w)

Fig. 4-12a and Fig. 4-12b show the water absorption of Non-AE concrete of 4w13a and 4w13c in CIF test. For both 4w13a and 4w13c, in the process of absorbing water of bottom surface before freeze-thaw, the water absorption depended on the cement type, and increased with the increase FA replacement ratio. Comparing the

cases of 4w13a and 4w13c, there was no obvious change in the water absorption before freeze-thaw, and it can be said that the water absorption before freeze-thaw was not influenced by carbonation of concrete. While, when subjected to freeze-thaw, carbonation of concrete reduced the water absorption [47] [48].

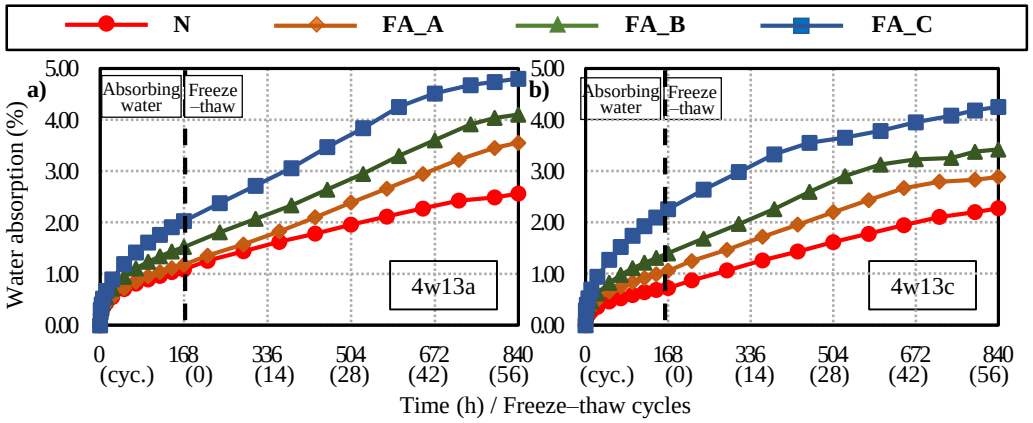

Fig. 4-12. Results of water absorption in the cases of air (4w13a) and carbonation (4w13c) curing

4.3.4 The change of pore structure due to carbonation

4.3.4.1 The pore structure of concrete after water curing for 4 weeks (4w)

Fig. 4-13a and Fig. 4-13b show the cumulative pore volume and the pore size distribution of Non-AE concrete after water curing, respectively. The data in Fig. 4-13a reveal that there was little change in the cumulative pore volume of N, FA_A and FA_B, and the one of FA_C was the higher than the others, which is similar to the trend of water absorption. In Fig. 13b, the size of pore was mainly concentrated in the area below 100 nm, this is due to the hydration reaction of concrete densified the pore structure of concrete in water curing. In addition, it can be observed in the pore size distribution curve that the critical pore entry diameter, which is the pore diameter where the steepest slope of the cumulative curve is recorded [12], was not changed when the FA replacement ratio increased in case of N, FA_A and FA_B, however, the one of FA_C with a highest FA replacement ratio was highest.

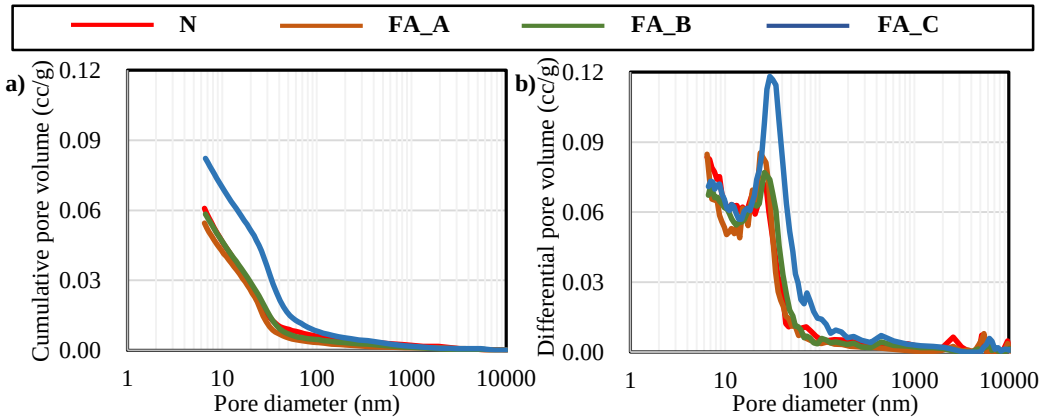

Fig. 4-13. Cumulative pore volume and Pore size distribution result of Non-AE concrete after water curing (4w)

a): Cumulative pore volume; b): Pore size distribution

4.3.4.2 The pore structure of concrete in air (4w13a) and carbonation (4w13c) curing after water curing (4w)

Fig. 4-14a and Fig. 4-14b show the cumulative pore volume of Non-AE concrete in air and carbonation curing, respectively. For both 4w13a and 4w13c, the cumulative pore volume tended to increase with the increase FA replacement ratio. Comparing with the case of 4w (see Fig. 4-13a), for the case of 4w13a, the total pore volume was not changed significant due to air curing, while, for the case of 4w13c, the total pore volume was decreased due to carbonation curing. Comparing the cases of 4w13a and 4w13c, the cumulative pore volume tended to decrease due to carbonation for all concrete.

Fig. 4-14c and Fig. 4-14d show the pore size distribution of Non-AE concrete in air and carbonation curing, respectively. Comparing with the results of 4w (see Fig. 4-13b), for the case of 4w13a, there were two pore size distribution peaks near diameter 100nm, which was because that under the air curing condition, concrete ageing resulted the slow carbonation of CH and C-S-H, which caused a densification of pore structure below 150 nm and coarsening of the pore structure, respectively [49], [50]. For the case of 4w13c, the pore size distribution peak below 150 nm disappeared and the one above 150 nm shifted to a larger diameter due to the full carbonation of CH and C-S-H, respectively. Besides, for both the cases of 4w13a and 4w13c, the pore size distribution peaks

were not changed when the FA replacement ratio increased. However, the critical pore entry diameter raises with the increase FA replacement ratio.

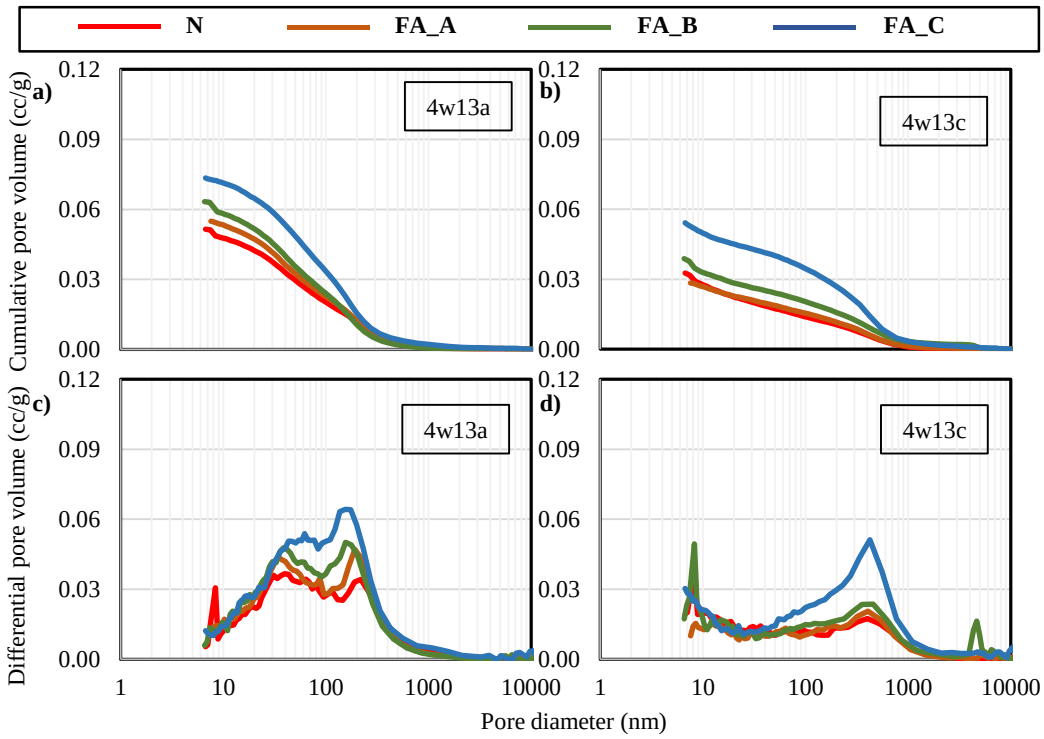

Fig. 4-14. Cumulative pore volume and pore size distribution results of Non-AE concrete in the cases of air (4w13a) and carbonation (4w13c) curing
a), b): Cumulative pore volume; c), d): Pore size distribution

4.3.4.3 The change of porosity of FA concrete for all curing conditions

Fig. 4-15 shows the porosity of Non-AE concrete by the Archimedes method in all curing conditions. Based on the method from Gruyaert et al. [51] and Takahiro et al. [52], the porosity including capillary porosity, gel porosity and total porosity was calculated from the dry weights at 40℃ and 105 ℃. For all the cases of 4w, 4w13a and 4w13c, when the FA replacement ratio increased, the capillary porosity increased but the gel porosity decreased. Comparing with the case of 4w, for the case of 4w13a, the capillary porosity tended to decrease and the gel porosity tended to increased due to air curing. Comparing the cases of 4w13a and 4w13c, both capillary porosity and gel porosity were reduced due to carbonation of concrete. Therefore, it can be said that the porosity

is densified due to carbonation of concrete.

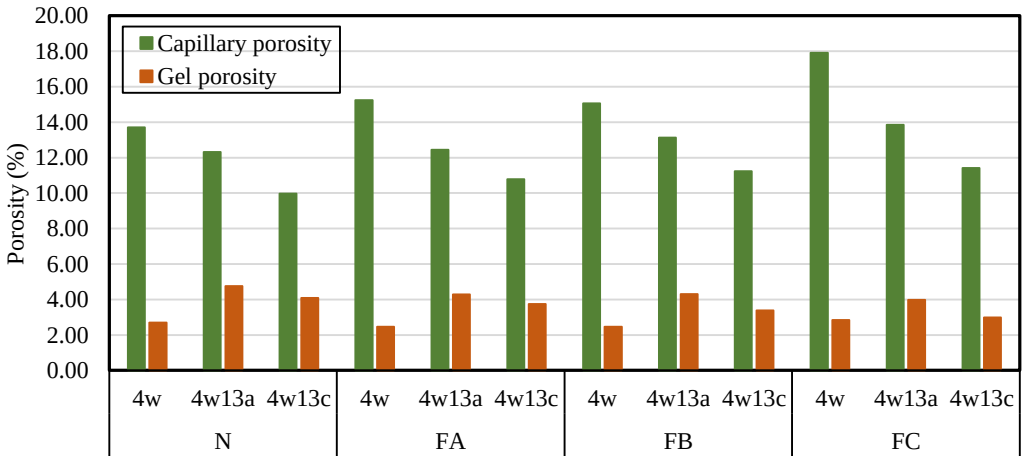

Fig. 4-15. Porosity of Non-AE FA concrete for all curing (4w: water curing for 4 weeks, 4w13a: air curing for 13 weeks after water curing, 4w13c: carbonation curing for 13 weeks after water curing)

4.3.5 Discussion on the water absorption and pore structure

4.3.5.1 Effect of carbonation on frost resistance from the view of water absorption and pore structure

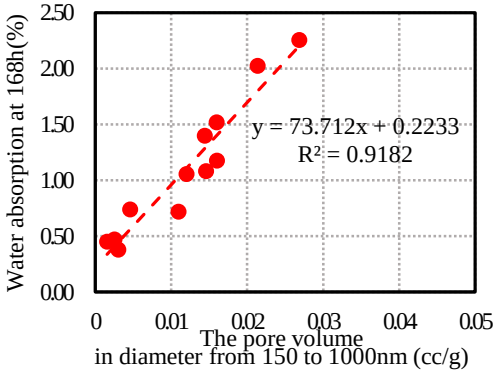

Fig. 4-16. Relationship between the water absorption at 168h and the pore volume in diameter from 150nm to 1000nm

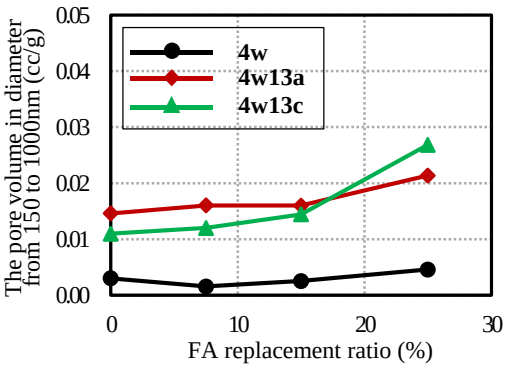

Fig. 4-17. Change of the pore volume in diameter from 150nm to 1000nm due to FA replacement ratio for all curing (4w: water curing for 4 weeks, 4w13a: air curing for 13 weeks after water curing, 4w13c: carbonation curing for 13 weeks after water curing)

Based on the previous studies [53], [54], it is widely known that the water absorption depends on the porosity and pore size of concrete. Fig. 4-16 shows the relationship between the water absorption at 168h in CIF test and the pore volume in diameter from 150 nm to 1000 nm in this study. In Fig. 16, the R^2 value is 0.9182, and it is thought that the water absorption before freeze-thaw has a strong relation with the pore volume in diameter from 150 nm to 1000 nm, and the water absorption increases with the increase pore volume in diameter from 150 nm to 1000 nm. Fig.4-17 shows the change of pore volume in the diameter ranges from 150 nm to 1000 nm due to FA replacement ratio in all curing conditions. Comparing the cases of 4w13a and 4w13c, there is little change on the pore volume in the diameter ranges from 150 nm to 1000 nm due to carbonation, which can explain the water absorption before freeze-thaw is not influenced by carbonation of concrete as in Fig. 12.

It is well-known that the water absorption before freeze-thaw depends on the capillary action of concrete. However, during freeze-thaw process, concrete is in a state of saturation and the water absorption does not increase by capillary action. Setzer Malin et al. [55] pointed out that during cooling the unfrozen water in gel pore flows to ice due to frost shrinkage, which results a high negative pressure in gel pore. If there is absorbable water on the surface, absorbing water due to frost action is more efficient than that due to capillary suction. Therefore, the water absorption due to freeze-thaw is closely related to frost action in gel pore. In order to grasp the effect of gel porosity on the water absorption, a correlation curve between the water absorption due to freeze-thaw and gel porosity is illustrated in Fig. 4-18, in which the water absorption due to freeze-thaw is obtained from the water absorption at 56-cycle subtracting the water absorption at 168h.

In Fig. 4-18, the R^2 value is 0.9278 for the case of 4w13a and is 0.79 for the case of 4w13c, which indicates that water absorption due to freeze-thaw has a good relationship with gel porosity. The water absorption due to freeze-thaw tends to decrease as the gel porosity increases, although the water absorption due to freeze-thaw is mainly by frost action in gel pore. This may be because quantitative water, but not all, in gel pore flows to ice due to frost shrinkage, which results a higher negative pressure with less gel pore.

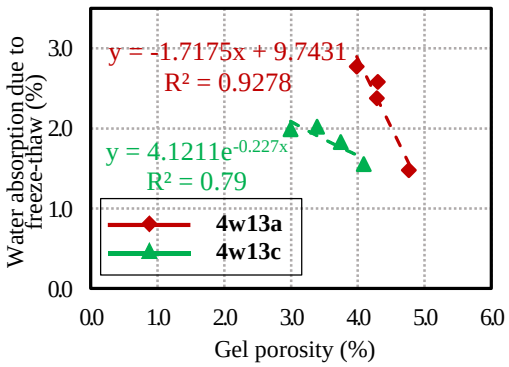

Fig. 4-18. Relationship between water absorption due to freeze-thaw and gel porosity (4w13a: air curing for 13 weeks after water curing, 4w13c: carbonation curing for 13 weeks after water curing)

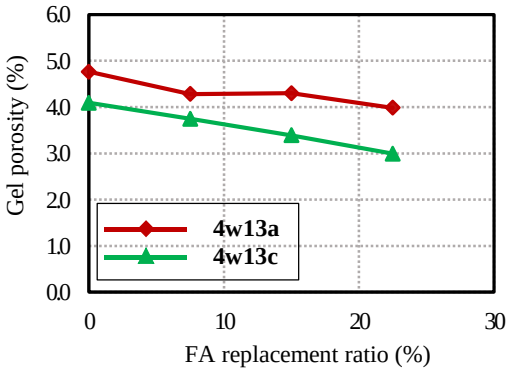

Fig. 4-19. Change in gel porosity due to FA replacement ratio (4w13a: air curing for 13 weeks after water curing, 4w13c: carbonation curing for 13 weeks after water curing)

Fig. 4-19 illustrates the changes in gel porosity due to FA replacement ratio in air (4w13a) and carbonation (4w13c) curing after water curing of Non-AE concrete. For both 4w13a and 4w13c, the gel porosity tends to decrease with the increase FA replacement ratio. It is evident that not only the water absorption is due to capillary action, but also the water absorption is due to freeze-thaw. Furthermore, the water absorption is related to the FA replacement ratio, tends to increase as the FA replacement ratio increases.

From the previous research, it has been noted that the durability of concrete, which strongly depends on the pore size, tends to decrease with the increase pore volume in diameter from 40 to 2000 nm [11], [12], [13]. Fig. 20 shows the changes of pore volume in the diameter ranges from 40 to 2000nm due to FA replacement ratio of Non-AE concrete in all curing conditions. It can be clearly seen from Fig. 4-20 that the pore volume in the diameter ranges from 40 to 2000 nm increases as the FA replacement ratio increases. Furthermore, it is observed that the durability factor of concrete decreases with the increase FA replacement ratio under the same curing condition (see Fig. 4-9). Combining Fig. 4-20 and Fig. 9, it can be concluded that the durability factor of concrete decreases when the pore volume in the diameter ranges from 40 to 2000nm increases also with the increase FA replacement ratio under the same curing conditions. This can be explained that the durability factor decreases when the FA replacement ratio increases as seen in Fig. 4-9. However, comparing the cases of 4w13a

and 4w13c, although the pore volume in the diameter ranges from 40 to 2000 nm increases due to carbonation, the the durability factor of concrete is not changed due to carbonation (see Fig. 4-9). Furthermore, the previous study [56] pointed out that it is difficult to freeze the water in small pore with the diameter below 20 nm, which means the frost resistance increases with the increase of the small pore below 20 nm.

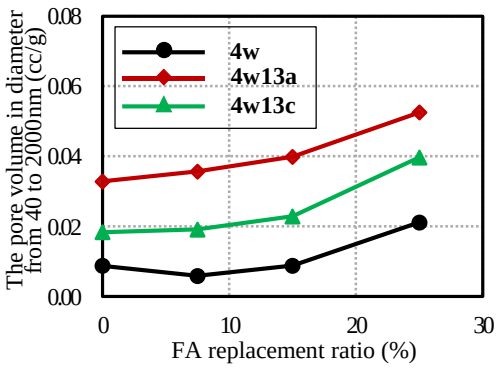

Fig. 4-20. Change of pore volume in diameter from 40 to 2000nm due to FA replacement ratio (4w: water curing for 4 weeks, 4w13a: air curing for 13 weeks after water curing, 4w13c: carbonation curing for 13 weeks after water curing)

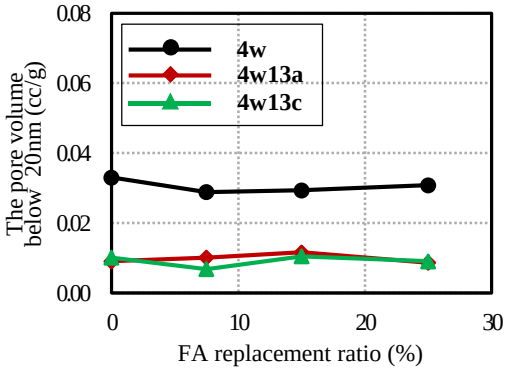

Fig. 4-21. Change of pore volume below 20nm due to FA replacement ratio (4w: water curing for 4 weeks, 4w13a: air curing for 13 weeks after water curing, 4w13c: carbonation curing for 13 weeks after water curing)

Fig. 4-21 shows the the change in pore volume below 20nm due to FA replacement ratio in all curing condition of Non-AE concrete. It could be seen that the pore volume below 20nm decreases due to air and carbonation curing. Therefore, comparing with the case of 4w, air and carbonation curing results an increase in the pore volume in the diameter ranges from 40 to 2000 nm, which can reduce the frost resistance. And the decrease in the pore volume below 20nm also can reduce the frost resistance. This can explain the frost resistance of Non-AE FA concrete is reduced due to air and carbonation curing. From Fig. 4-21, it also can be seen that the pore volume below 20nm is not changed due to carbonation of concrete. However, the reason why the frost resistance is not influenced by carbonation in Fig. 9 can not be explained by the pore volume in diameter from 40 to 2000 nm due to MIP method because the pore structure below 6.5 nm, mainly gel pore, cannot be measured by the MIP method.

Similarly, it is also difficult to freeze the water in gel pore. However, little attention has been paid to the effect of gel pore on the frost resistance. In order to grasp the change of gel pore under the carbonation condition and its effect on the frost resistance, the relationship between the durability factor and the gel porosity of FA concrete is shown in Fig. 4-22.

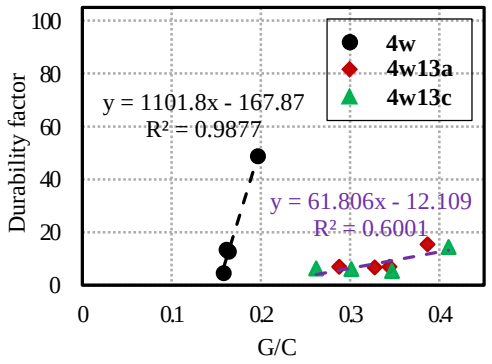

Fig. 4-22. Relationship between durability factor and G/C (4w: water curing for 4 weeks, 4w13a: air curing for 13 weeks after water curing, 4w13c: carbonation curing for 13 weeks after water curing)

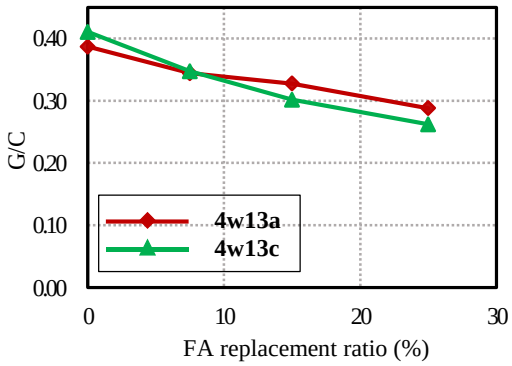

Fig. 4-23. Change of G/C due to FA replacement ratio (4w13a: air curing for 13 weeks after water curing, 4w13c: carbonation curing for 13 weeks after water curing)

Fig. 4-22 shows the relationship between the durability factor and the gel porosity / capillary porosity ratio (G/C). It can be seen that the R^2 value is 0.9877 for the case of 4w, and is 0.6001 for the cases of 4w13a and 4w13c. For the case of 4w, there is a good relationship between the durability factor and G/C, while for the cases of 4w13a and 4w13c, the R^2 value indicates that the durability factor has a certain relationship with G/C. This may be due to all the durability factor in the cases of 4w13a and 4w13c are less than 20. In addition, with the increase of G/C, the durability factor tends to increase in all curing conditions. Therefore, it is clear that the gel pore has a positive effect on the frost resistance. Our current findings expand previous research [14].

Fig. 4-23 shows the change of G/C due to FA replacement ratio in the case of 4w13a and 4w13c. As can be seen from Fig. 4-23, there is little change on G/C between the cases 4w13a and 4w13c, which means the G/C is

not changed by carbonation of FA concrete. This can explain that the durability factor is not influenced by carbonation of concrete. In addition, the G/C tends to decrease with the increase FA replacement ratio, which is the same with the trend of the durability factor tends to decrease when the FA repacement ratio increases as in Fig. 4-9a.

4.3.5.2 Effect of carbonation on scaling resistance from the view of water absorption and pore structure

For the scaling resistance, from Fig. 4-10a and Fig. 4-12, comparing the cases of 4w13a and 4w13c, although the water absorption before freeze-thaw is not influenced by carbonation of concrete, the scaling resistance is enhanced by carbonation of FA concrete. This may be because during freeze-thaw, the water absorption of carbonated concrete is lower than non-carbonated concrete. The changes in water absorption due to FA replacement ratio in the cases of 4w13a and 4w13c of Non-AE concrete are shown in Fig. 4-24. In Fig. 4-24, it can be seen that there is little gap on the reduce range of water absorption due to carbonation with the increase FA replacement ratio. However, in Fig. 4-10a, the improvement of scaling resistance due to carbonation tends to increase when the FA replacement ratio increases.

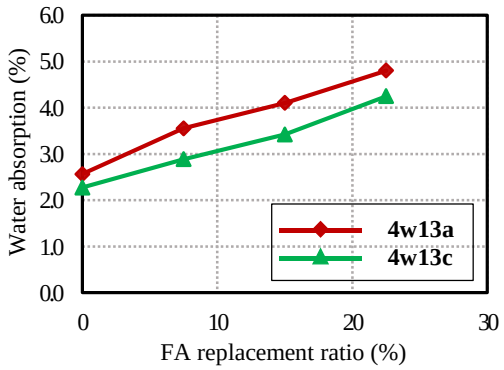

Fig. 4-24. Change in water absorption due to FA replacement ratio (4w13a: air curing for 13 weeks after water curing, 4w13c: carbonation curing for 13 weeks after water curing)

In addition, it is pointed out that the scaling of concrete depends on the pore structure [57], [58], [59]. Endoh et al. [60] confirmed that the scaling of concrete depends on the pore volume above 75nm. Fig. 4-24 shows the

relationship between the cumulative scaling mass at 56-cycle and the pore volume above 75 nm.

From Fig. 4-25, it can be seen that the concrete in which the pore volume above 75 nm is less than 0.015 cc/g, has a high scaling resistance. When the pore volume is more than 0.015 cc/g, the R^2 value with 0.9113 signifies there is a close relationship between scaling resistance and the pore volume above 75 nm, and the scaling mass increase exponentially with the increase of pore volume.

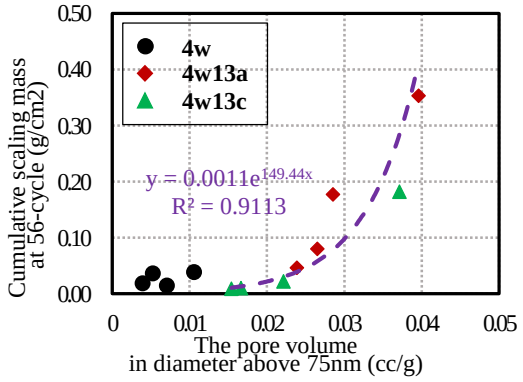

Fig. 4-25. Relationship between the cumulative scaling mass at 56-cycle and the pore volume above 75nm (4w: water curing for 4 weeks, 4w13a: air curing for 13 weeks after water curing, 4w13c: carbonation curing for 13 weeks after water curing)

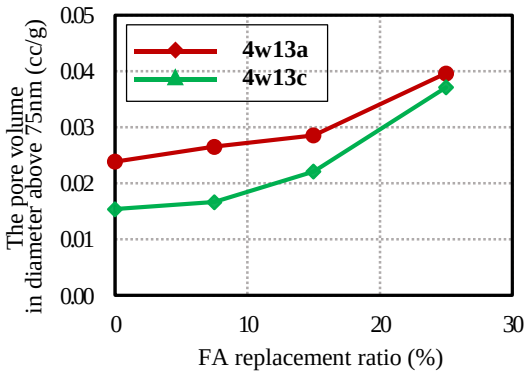

Fig. 4-26. Change in the pore volume above 75nm due to FA replacement ratio (4w13a: air curing for 13 weeks after water curing, 4w13c: carbonation curing for 13 weeks after water curing)

Fig. 4-26 shows the changes in the pore volume above 75 nm due to FA replacement ratio in the cases of 4w13a and 4w13c of Non-AE concrete. For both 4w13a and 4w13c, the pore volume increases when the FA replacement ratio increases, which is the reason that scaling mass increases with the increase FA replacement ratio (see Fig. 4-10a). Comparing the cases of 4w13a and 4w13c, the pore volume above 75 nm tends to decrease due to carbonation. With the increase FA replacement ratio, although the reduction range by carbonation of concrete tends to be small, the scaling resistance due to carbonation significantly increases (see Fig. 4-10a).

4.3.6 Contrast between the frost resistance BFS and FA concrete under the carbonation

conditions

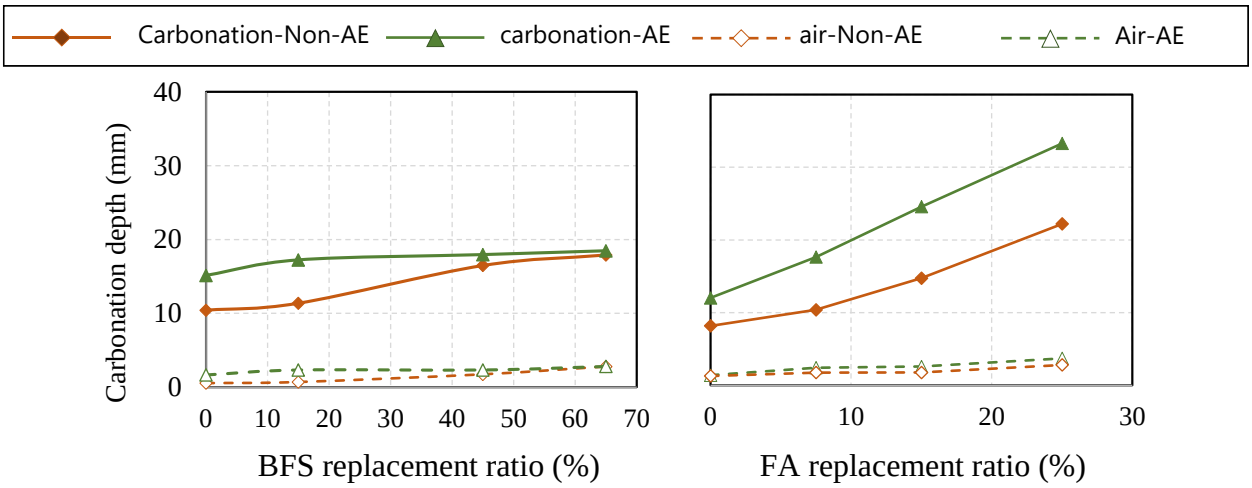

Fig.4- 27. Contrast between carbonation depth of BFS and FA concrete subjected to carbonation

Fig. 4-27 shows the contrast between carbonation depth of BFS and FA concrete in air and carbonation curing. It can be seen that: when both the BFS and FA replacement ratio increased, the carbonation depth tended to increase. For the air curing, there is little gap between the carbonation depth of BFS and FA concrete in Non-AE and AE cases. However, for the carbonation curing, although AE concrete had a low replacement ratio, the carbonation depths of FA concrete were higher than the one of BFS concrete. This is because there is CaO in the BFS component, which can provide alkalinity.

Fig. 4-28 shows the contrast between RDME of Non-AE BFS and FA concrete subjected to carbonation. For BFS concrete, when subjected to carbonation, the frost resistance tended to decrease with the use of BFS. However, the frost resistance BFS_B was the lowest, and the frost resistance of BFS_C was higher that the one of BFS_A. For the FA concrete, when subjected to carbonation, the frost resistance also tended to decrease with the use of FA. For FA_A, B, C, there was little gap during the frost resistance of them.

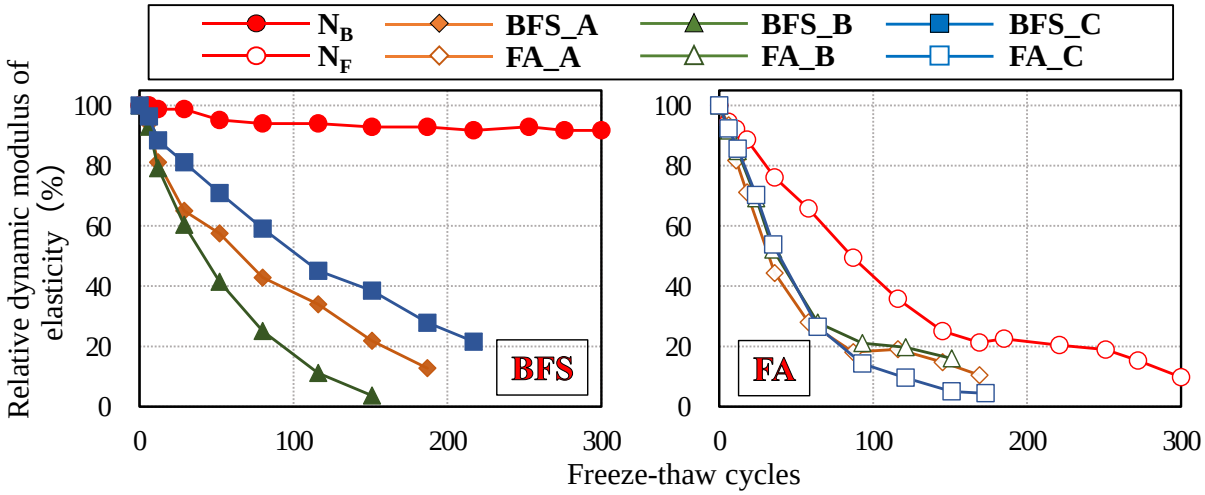

Fig. 4-28. Contrast between RDME of Non-AE BFS and FA concrete subjected to carbonation

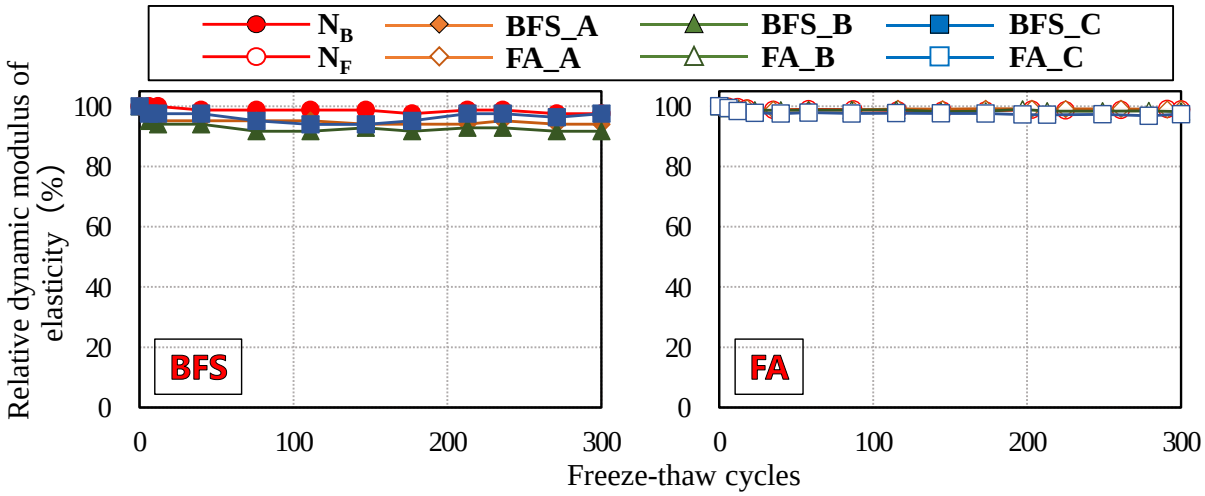

Fig. 4-29. Contrast between RDME of AE BFS and FA concrete subjected to carbonation

Fig. 4-29 shows the contrast between RDME of AE BFS and FA concrete subjected to carbonation. For both AE BFS and FA concrete, when subjected to carbonation, the frost resistance was kept at a high level, even though using BFS and FA. It can be said that for AE BFS and FA concrete, the using of BFS or FA do not reduce the resistance of concrete.

Fig. 4-30 shows the contrast between durability factor of Non-AE BFS and FA concrete. For both Non-AE BFS and FA concrete, on the whole, the durability factor tend to decrease with the increasing the BFS and FA

replacement ratio. For BFS concrete, comparing the case of air curing and carbonation curing, it can be seen that: for N_B and BFS_A, the durability factor tended to decrease due to carbonation, while for BFS_B, C, the durability factor tended to be high. In other words, for BFS concrete, carbonation changed the durability factor. However, for FA concrete, comparing the case of air curing and carbonation curing, there is little gap between them, and the durability factor is not changed by the carbonation of FA concrete.

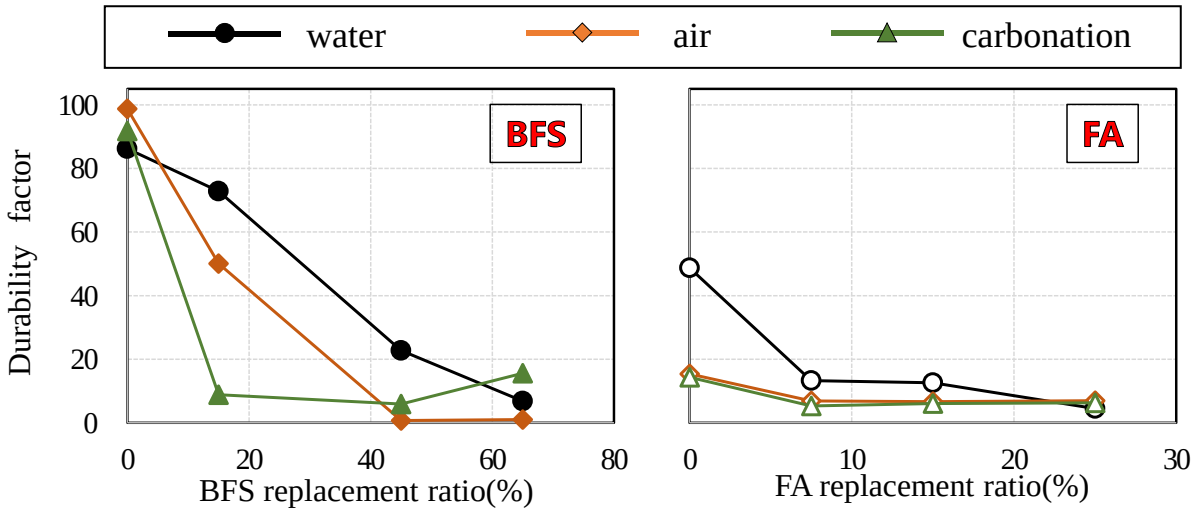

Fig. 4-30. Contrast between durability factor of Non-AE BFS and FA concrete

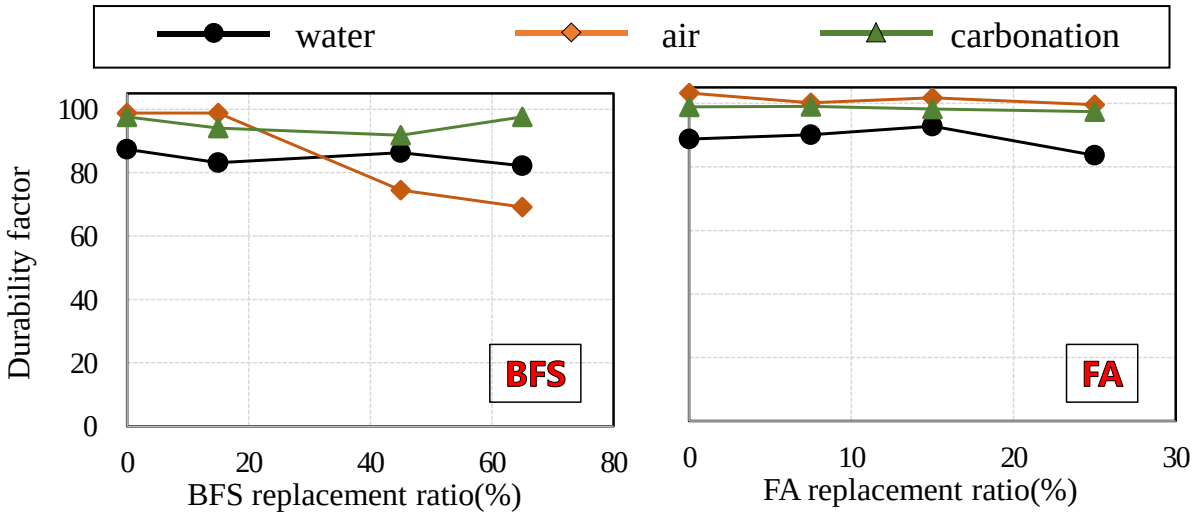

Fig. 4-31. Contrast between durability factor of AE BFS and FA concrete

Fig. 4-31 shows the contrast between durability factor of AE BFS and FA concrete. For both Non-AE BFS and FA concrete, on the whole, the durability factor was kept at a high level due to AE admixture. For BFS concrete, comparing the cases of air curing and carbonation curing, the durability factors of N and BFS_A tended to decrease slightly due to carbonation, while the durability factors of BFS_B, C were improved due to carbonation. However, for FA concrete, comparing the cases of air curing and carbonation curing, the durability factors were not changes by the carbonation of FA concrete.

The effect of carbonation depth on the durability factor would be investigated by combining the Fig. 4-27 and the Fig. 4-30, Fig. 4-31. From the Fig. 4-27a and Fig. 4-30a, it can be seen that in Non-AE concrete: for low replacement ratio or N, the carbonation depth is about 10mm, and the durability factor tend to decrease due to carbonation. While for high replacement ratio, the carbonation depth is about 18mm, and the durability factor tend to increase due to carbonation. (the reason is explained in **3 Chapter**). For AE BFS concrete, it had a same trend on the effect of carbonation depth. For both Non-AE or AE FA concrete in Fig. 4-27b and Fig. 4-30b, Fig. 4-31b, it can be seen that: the carbonation depth had not affected the durability factor for both the AE and Non-AE concrete. In this chapter, the frost resistance of FA concrete is determined by structure pore and air content, and the change due to carbonation had be explained.

4.3.7 Summary of frost damage of FA concrete exposed to carbonation condition

Based on the results and discussion in this study and previous studies, the relationships between the frost damage and the pore structure and air bubbles in concrete are summarized in Fig. 27. It can be said that the air bubbles in concrete due to AE admixture is critical to frost damage. For AE FA concrete, although carbonation can change the pore structure of concrete, carbonation cannot affect the air bubbles in concrete. Therefore, carbonation of FA concrete can be ignored for the frost damage. For Non-AE FA concrete, frost damage depends on the pore structure and water absorption, and it is obtained the results: for frost resistance, the more gel pore resulted absorbing less water when subjected to freeze-thaw, and it was confirmed that gel pore has a positive effect on frost resistance. In addition, due to capillary action, the water absorption has a close relation to the pore volume in the diameter ranges from 150 to 1000 nm. Carbonation of FA concrete does not reduce the water absorption due to capillary action, but reduces the water absorption by freeze-thaw. However, the

frost resistance is not influence by carbonation. Scaling resistance is reduced by carbonation of concrete, which may be because the water absorption is reduced when subjected to carbonation. However, when FA concrete was subjected to carbonation, with the increase FA replacement ratio, although the reduce range of water absorption due to carbonation is not changed, the improvement of scaling resistance due to carbonation tends to be higher.

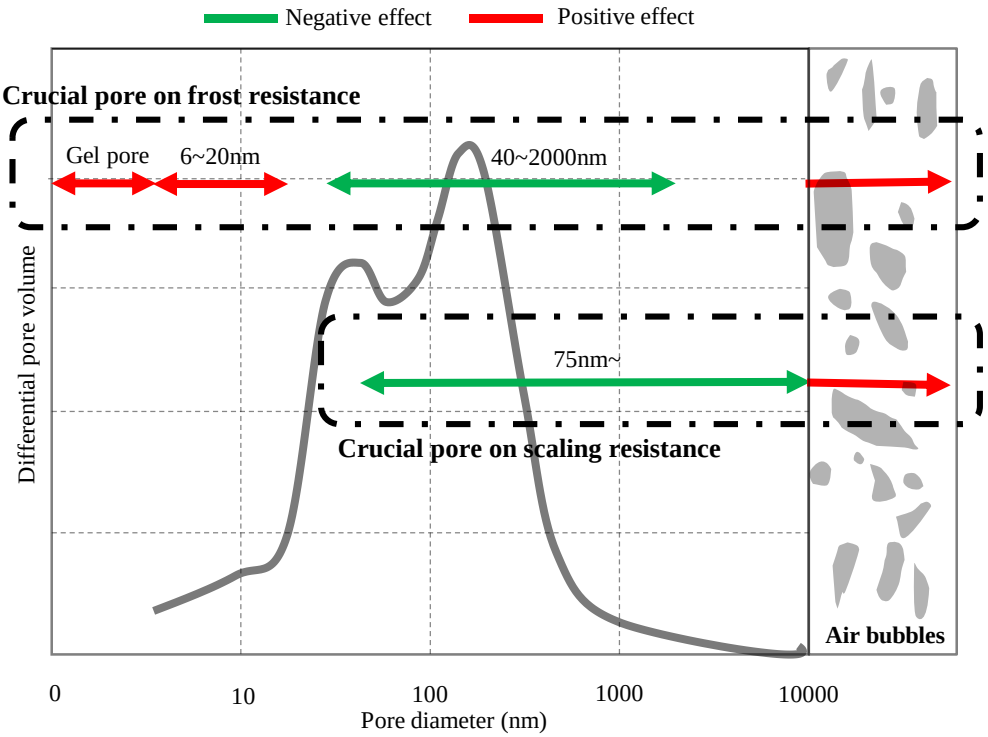

Fig. 4-32. Effect of pore structure and air bubbles in concrete on frost damage

From the view of pore structure, schematic image of pore structure changes due to carbonation of FA concrete is summarized in Fig. 28. It is clear that the addition of FA just heightened the pore size distribution peak, the trend of pore size distribution was not changed. Besides, the gel pore decreases with the addition of FA due to the decrease of hydration reaction. Therefore, with the increasing FA replacement ration, the frost resistance tends to decrease due to the decreasing gel pore, which has a positive effect, and the increasing capillary pore, which has a negative effect. Besides, it is confirmed that the pore volume in diameter above 75 nm has a negative for scaling resistance. The scaling resistance tends to decrease due to increasing pore volume in diameter above 75 nm as FA replacement increase. For carbonation of FA concrete, carbonation densifies the pore structure including gel pore, and shifts the critical pore entry diameter to a large diameter. During this

process, similar to gel pore, the pore volume in diameter from 40 to 2000 nm with a negative effect on frost resistance is also densified due to carbonation, while, the pore volume in the diameter ranges from 6 to 20 nm with a positive effect on frost resistance is not changed due to carbonation. The frost resistance of FA concrete exposed to carbonation condition is not influenced due to the balance between gel pore and the pore volume in the diameter ranges from 40 to 2000 nm. To some extent, the negative effect of capillary pore on the frost resistance is considered by the effect of the pore volume in the diameter ranges from 40 to 2000 nm. For scaling resistance, carbonation densifies the pore volume in the diameters above 75 nm, which improves the scaling resistance.

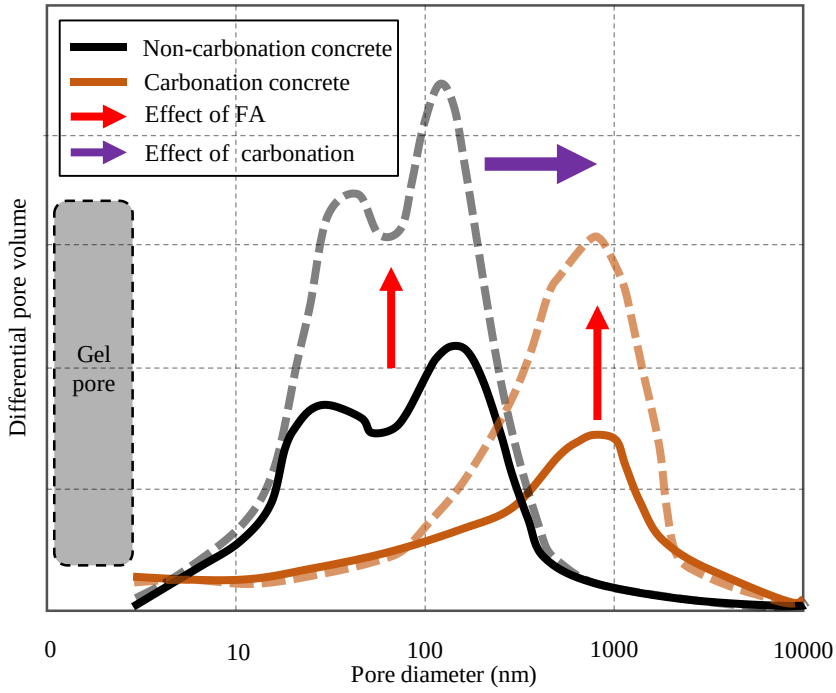

Fig. 4-33. Schematic image of pore structure changes due to carbonation of FA concrete

To sum up, the frost scaling resistance depends on the pore structure than water absorption, and it is more reliable to evaluate the frost scaling resistance by the changes in pore structure of FA concrete.

4.4 Conclusions

This study was carried out to grasp the change in frost and scaling resistance of FA concrete under the

carbonation conditions regarding the water absorption, pore structure and porosity. The relationship between the water absorption and pore structure was investigated as well. Based on the results and discussion, the following conclusions could be drawn:

1) The frost and scaling resistance of Non-AE concrete tends to decrease when the FA replacement ratio increases. For AE concrete, the frost and scaling resistance are not influenced by the added FA. For Non-AE FA concrete, the frost resistance tends to decrease by performing air and carbonation curing. For AE FA concrete, the effect of curing conditions on the frost and scaling resistance can be ignored.

2) For Non-AE FA concrete, the water absorption due to capillary action has a close relationship with the pore volume in diameter from 150 to 1000 nm, and the one due to freeze-thaw is related closely to gel porosity. The water absorption due to capillary action is not influenced by carbonation, while the one due to freeze-thaw is decreased due to carbonation.

3) The durability factor has a positive correlation with gel porosity/capillary porosity ratio (G/C) for Non-AE FA concrete. The G/C is not changed due to carbonation, which results the frost resistance is not influenced by carbonation of FA concrete.

4) The scaling resistance has a closer relationship with the pore volume above 75 nm. The scaling resistance increases due to carbonation of FA concrete, and the increase range due to carbonation tends to be great with the increase FA.

5) Comparing the water absorption and pore structure, it is more reliable to evaluate the frost scaling resistance by the changes in pore structure than water absorption.

References

[1] A. Costa, J. Appleton, Case studies of concrete deterioration in a marine environment in Portugal, Cement and Concrete Composites, 24 (2020), pp. 169-179 doi.org/10.1016/S0958-9465(01)00037-3

[2] R. Wang, Z. Yang, L. Wang, H. Zhang, Review on the deterioration and approaches to enhance the durability of concrete in the freeze–thaw environment, Construction and Building Materials, 321: 28 (2022), doi.org/10.1016/j.conbuildmat.2022.126371

[3] Z. Liu, W. Meng, Fundamental understanding of carbonation curing and durability of carbonation-cured cement-based composites: A review, Journal of CO_2 Utilization, 44 (2021), doi.org/10.1016/j.jcou.2020.101428

[4] S.H. Diab, A.M. Soliman, M.R. Nokken, Changes in mechanical properties and durability indices of concrete undergoing ASR expansion, Construction and Building Materials, 251 (2020), doi.org/10.1016/j.conbuildmat.2020.118951

[5] R. Wang, Q. Zhang, Y. Li, Deterioration of concrete under the coupling effects of freeze–thaw cycles and other actions: A review, Construction and Building Materials, 319 (2022), doi.org/10.1016/j.conbuildmat.2021.126045

[6] Proceedings of research council on combined deterioration of concrete in cold region, Hokkaido branch of Japan Concrete Institute, 2010, in Japanese

[7] C.-W. Chung, C.-S. Shon, Y.S. Kim, Chloride ion diffusivity of fly ash and silica fume concretes exposed to freeze-thaw cycles, Construction and Building Materials, 24 (2010) pp. 1739-1745, https://doi.org/10.1016/j.conbuildmat.2010.02.015.

[8] T.C. Powers, A working hypothesis for further studies of frost resistance of concrete, ACI J Proc ACI (1945), pp. 245-272

[9] S.H. Dong, D.C. Feng, S.H. Jiang, W.Z. Zhu, Effect of freezing temperature on the microstructure of negative temperature concrete, Advanced Materials Research, 663 (2013), pp. 343-348,

doi.org/10.4028/www.scientific.net/AMR.663.343

[10] C.J. Bernhardt, Damage due to freezing of fresh concrete, J. Am. Concr. Inst., 52 (1956), pp. 573-580

[11] Kamada. E, Frost damage and pore structure of concrete. Proc Jpn Concr Inst., 10 (1988), pp. 51–60, (in Japanese)

[12] N.X. Quy, J. Kim, Y. Hama, Effect of 10-year outdoor exposure and curing conditions on the pore structure characteristics of hardened cement mortar, Journal of Advanced Concrete Technology, 16 (2018), pp. 461-475, doi.org/10.3151/jact.16.461

[13] N. X. Quy, T. Noguchi, N. Seunghyun, J. Kim, Y. Hama, Distribution map of frost resistance for cement-based materials based on pore structure change, Materials, 13 (2020), doi.org/10.3390/ma13112509

[14] L. Dvorkin, Design estimation of concrete frost resistance, Construction and Building Materials, 211 (2019), pp. 779-784, doi.org/10.1016/j.conbuildmat.2019.03.108

[15] J. Wang, H. Xu, D. Xu, P. Du, Z. Zhou, L. Yuan, X. Cheng, Accelerated carbonation of hardened cement pastes: influence of porosity, Construction and Building Materials, 225 (2019), pp. 159-169, doi.org/10.1016/j.conbuildmat.2019.07.088

[16] J. Liu, S. Yao, M. Ba, Z. He, Y. Li, Effects of carbonation on micro structures of hardened cement paste, J. Wuhan Univ. Technol.-Mater. Sci. Ed., 31 (2016), pp. 146-150, doi.org/10.1007/s11595-016-1344-5

[17] M. Ferreira, H. Kuosa, M. Leivo, E. Holt, Concrete performance subject to coupled deterioration in cold environments, Nuclear Engineering and Design, 323 (2017), pp. 228-234, doi.org/10.1016/j.nucengdes.2016.10.021

[18] H. Kuosa, R.M. Ferreira, E. Holt, M. Leivo, E. Vesikari, Effect of coupled deterioration by freeze–thaw, carbonation and chlorides on concrete service life, Cement and Concrete Composites, 47 (2014), pp. 32-40, doi.org/10.1016/j.cemconcomp.2013.10.008

[19] D. Zhang, Y. Shao, Surface scaling of CO_2-cured concrete exposed to freeze-thaw cycles, Journal of CO_2

Utilization, 27 (2018), pp. 137-144, doi.org/10.1016/j.jcou.2018.07.012

[20] N. Takeda, S. Togawa, Research on the durability of concrete suffered the combined action of freeze-thaw and carbonation, Proceedings of the Japan Concrete Institute, 24 (2002), pp.735-740, (in Japanese)

[21] W. Zhang, S. Na, J. Kim, H. Choi, Y. Hama, Evaluation of the combined deterioration by freeze–thaw and carbonation of mortar incorporating BFS, limestone powder and calcium sulfate, MATERIALS AND STRUCTURES, 50 (2017), doi.org/10.1617/s11527-017-1039-1

[22] M.Á. Sanjuán, C. Andrade, P. Mora, A. Zaragoza, Carbon dioxide uptake by cement-based materials: A Spanish Case Study, Appl. Sci. 10 (2020), doi.org/10.3390/app10010339

[23] R. M. Andrew, Global CO_2 emissions from cement production, 1928–2018, Earth Syst. Sci. Data, 11(2019), pp. 1675–1710, doi.org/10.5194/essd-2019-152

[24] S.H. Na, Y. Hama, M. Taniguchi, O. Katsura, T. Sagawa, M. Zakaria, Experimental investigation on reaction rate and self-healing ability in fly ash blended cement mixtures, J Adv Concr Technol, 10 (2012), pp. 240–253, doi.org/10.3151/jact.10.240

[25] Japanese Industrial Standard Committee, Portland fly-ash cement; JIS R 5213; Japanese Standards Association, Tokyo, Japan, 2009.

[26] O. Linderoth, P. Johansson, L. Wadsö, Development of pore structure, moisture sorption and transport properties in fly ash blended cement-based materials, Construction and Building Materials, 261 (2020), doi.org/10.1016/j.conbuildmat.2020.120007

[27] P.S. L, A. G, K.R. A, S.K. K, Studies on drying shrinkage and water permeability of fine fly ash high performance concrete, Materials Today: Proceedings, 44 (2021), doi.org/10.1016/j.matpr.2021.01.069

[28] T. Matsuya, Y. Suzuki, T. Sakai, K. Fukudome, Low-carbon concrete using ground granulated blast-furnace slag and fly ash, Cement Science and Concrete Technology, 64 (2010), pp. 295-302, (in Japanese), doi.org/10.14250/cement.64.295

[29] M. Kimura, Y. Aiko, T. Ichinose, Y. Yoshida, Research on performance of concrete including fly ash,

Proceedings of the Japan Concrete Institute, 23 (2001), pp. 301-306, (in Japanese)

[30] D. Ravina, P.K. Mehta, Compressive strength of low cement/high fly ash concrete, Cement and Concrete Research, 18 (1988), pp. 571-583, doi.org/10.1016/0008-8846(88)90050-6

[31] O. Chiho, Y. Hama, Air entrainment, air void system and frost durability of fly ash concrete， J. Struct. Constr. Eng., AIJ, 67 (2002), pp.1-6, doi.org/10.3130/aijs.67.1_8, (in Japanese)

[32] J. Khunthongkeaw, S. Tangtermsirikul, T. Leelawat, A study on carbonation depth prediction for fly ash concrete, Construction and Building Materials, 20 (2006), pp. 744-753 doi.org/10.1016/j.conbuildmat.2005.01.052

[33] L. Shen, Q. Li, W. Ge, S. Xu, The mechanical property and frost resistance of roller compacted concrete by mixing silica fume and limestone powder: Experimental study, Construction and Building Materials, 239 (2020), doi.org/10.1016/j.conbuildmat.2019.117882

[34] H.A. Shah, Q. Yuan, S. Zuo, Air entrainment in fresh concrete and its effects on hardened concrete-a review, Construction and Building Materials, 274 (2021), doi.org/10.1016/j.conbuildmat.2020.121835

[35] Japanese Industrial Standard Committee, Chemical admixtures for concrete; JIS A 6204, Japanese Standards Association, Tokyo, Japan, 2011.

[36] Japanese Industrial Standard Committee, Portland cement; JIS R 5210, Japanese Standards Association, Tokyo, Japan, 2019.

[37] Japanese Industrial Standard Committee, Fly ash for use in concrete; JIS A 6201; Japanese Standards Association, Tokyo, Japan, 2015.

[38] Japanese Industrial Standard Committee, Method of accelerated carbonation test for concrete; JIS A 1153; Japanese Standards Association, Tokyo, Japan, 2012. doi.org/10.2208/jsceje.66.311

[39] Japanese Industrial Standard Committee, Test methods for pore size distribution of fine ceramic green body by mercury porosimetry, JIS R 1655, Japanese Standards Association, Tokyo, Japan, 2003

[40] Japanese Industrial Standard Committee, Method of test for compressive strength of concrete, JIS A 1108, Japanese Standards Association, Tokyo, Japan, 2018

[41] M. A. Sanjuán, C. Andrade, M. Cheyrezy, Concrete carbonation tests in natural and accelerated conditions, Advances in Cement Research, 15 (2003), pp. 171-180, doi.org/10.1680/adcr.2003.15.4.171

[42] C. Pade, M. Guimaraes, The CO_2 uptake of concrete in a 100 year perspective, Cem. Concr. Res., 37 (2007), pp. 1348-1356, doi.org/10.1016/j.cemconres.2007.06.009

[43] Japanese Industrial Standard Committee, Method of test for resistance of concrete of freezing and thawing, JIS A 1148, Japanese Standards Association, Tokyo, Japan, (2010).

[44] RILEM Recommendation TC 176-IDC, Test method of frost resistance of concrete, Materials and Structures, 34 (2001), pp. 515-531,

[45] T.L. Thomas, The effects of air content, water-cement ratio, and aggregate type on the flexural fatigue strength of plain concrete (Ph.D. thesis), Iowa State University (1979)

[46] D. Honda, N. X. Quy, J. Kim, Y. Hama, Influence of drying on frost resistance of mortar using a nitrite corrosion inhibitor and paraffin waterproofing agent, Construction and Building Materials, 283 (2021), doi.org/10.1016/j.conbuildmat.2021.122581

[47] Z. Ding, N. X. Quy, T. Noguchi, J. Kim, Y. Hama, A study on the change in frost resistance and pore structure of concrete containing blast furnace slag under the carbonation conditions, Construction and Building Materials, 331 (2022), doi.org/10.1016/j.conbuildmat.2022.127295

[48] M. Aoyama, Study on the mechanism of salt transfer in the carbonation area, Proceed. Jap. Concr. Institute 35 (1) (2013) in Japanese

[49] H. Higashi, K. Hirai, H. Mihashi, Study on the effect of mix proportions and pore structure on carbonation speed of concrete, Proceedings of the Japan Concrete Institute, 1 (1990), pp.61-73, (in Japanese)

[50] Y. Harasawa, Effects of different carbonation conditions on pore properties and carbonation products,

Proceedings of the Japan Concrete Institute, 36 (2014), pp. 808-813, (in Japanese)

[51] E. Gruyaert, P.V. Heede, N.D. Belie, Carbonation of slag concrete: Effect of the cement replacement level and curing on the carbonation coefficient - Effect of carbonation on the pore structure, Cement & Concrete Composites, 35 (2013), pp. 39-48, doi.org/10.1016/j.cemconcomp.2012.08.024

[52] T. Sagama, T. Ishida, Y. Luan, T. Nawa, Hydrate composition analysis and micro structure characteristics of Portland cement-Blast furnace slag system, Journal of Japan Society of Civil Engineers, Ser. E1 (Pavement Engineering), 66 (2010), pp. 311-324, doi.org/10.2208/jsceje.66.311

[53] L. Hanžič, R. Ilić, Relationship between liquid sorptivity and capillarity in concrete, Cem. Concr. Res., 33 (2003), pp. 1385-1388, doi.org/10.1016/S0008-8846(03)00070-X

[54] Y. Yokoyama, T. Yokoi, J. Ihara, The effects of pore size distribution and working techniques on the absorption and water content of concrete floor slab surfaces, Construction and Building Materials, 50, (2014), pp. 560-566, doi.org/10.1016/j.conbuildmat.2013.10.013

[55] M.J. Setzer, Fundamental aspects of frost damage in hardened cement paste, restoration of buildings and monuments, 19 (2013), pp.433-442, doi.org/10.1515/rbm-2013-6628

[56] S. Habara, Study on the relationship between the structure and void structure of hardened concrete and physical properties (Ph.D. thesis), Keio University (1992)

[57] G. Peiwei, Analysis on the air-void system test methods of concrete, Engineering Low Temperature Architecture Technology, 12 (2009), pp. 7-9,

[58] M. Pigeon, J. Marchand, R. Pleau, Frost resistant concrete, Constr. Build. Mater., 10 (1996), pp. 339-348, doi.org/10.1016/0950-0618(95)00067-4

[59] M. Pigeon, R. Pleau, Durability of Concrete in Cold Climates, E&FN Spon, London (1995), doi.org/10.1201/9781482271447

[60] H. Endoh, F. Taguchi, H. Shimada, Scaling behavior of concrete on long-term freeze and thaw by salt

water, Cement Science and Concrete Technology, 725 (2003), pp. 227-244, doi.org/10.2208/jscej.2003.725_227, (in Japanese)

Chapter 5

INFLUENCE OF COMBINED DETERIORATION BETWEEN FROST DAMAGE AND ALKALI-SILICA REACTION OF CONCRETE DUE TO ADDITIVE OF BLAST FURNACE SLAG AND FLY ASH

5.1 Overview

the atmospheric CO2 concentration has been increased and lead to the greenhouse effect that global temperatures increase, and a global “climate and environmental emergency” had been declared in 2019 to rise the challenge of climate change. It has become a global trend to limit and reduce carbon dioxide emissions. The study [1] shows that the CO2 emissions due to cement manufactured accounts for 8% of all in the world, approximately. Therefore, in recent years, in the trend of CO2 emission reduction, blast furnace slag (BFS) and fly ash (FA) are used more widely to reduce the cement consumption in the field of building materials, and the use of BFS and FA can result in a concrete with better durability [2] [3].

On the other hand, in cold region, the frost damage often occurs in the winter construction of concrete, which seriously threatens the performance and structural safety of concrete. The other concrete deteriorations such as salt damage, carbonation, and alkali-silica reaction (ASR) are also related closely to the durability of concrete. So far, the single deterioration mechanism is mainly studied in almost previous studies and the results have been accumulated substantially. However, for the actual concrete structures, it is not possible to suffer a single deterioration only. In general, for the cause of deterioration in a concrete structure, a deterioration phenomenon called combined deterioration is often seen, in which the deterioration characteristics generated by the interaction of different deterioration phenomenon cannot be evaluated by adding two and more single deterioration model.

In the studies of combined deterioration on the frost damage in recent years, the one between salt damage and frost damage had been studied extensively. Additionally, for the combined deterioration between carbonation and frost damage, it has been investigated in previous studied by the authors’ research group, and the influences of BFS and FA on the combined deterioration were also elaborated [4] [5]. For the combined deterioration between ASR and frost damage, Gong et al. [6] stated the preceding has little effect on the ASR expansion, and the preceding ASR can result a higher frost damage. However, the BFS and FA concrete were not used, and the influence of BFS and FA have not been investigated. Therefore, under the global trend that BFS and FA are used

wildly, it is essential to experimentally assess the combined deterioration between ASR and frost damage of BFS and FA concrete. In addition, as it is well-known, the effect of ASR is by coarse aggregate, 2 types of coarse aggregates were used to gap the effect of coarse aggregate on ASR in this study.

Therefore, the experimental program is designed to assess combined deterioration of ASR and freeze-thaw action of BFS and fly ash concrete. The influence of FA or BFS on the combined deterioration, ASR resistance and frost resistance of concrete is evaluated.

5.2 Experimental program

5.2.1 Experimental materials and mixing proportions

Table 1 shows the experiment program. The ordinary Portland cement (OPC), BFS and FA were used in this work. The cement was denoted as N with a density of 3.17 g/cm^3. BFS with a fineness of 4000cm^2/g and a density of 2.91 g/cm^3 was used to replace cement at 45% (BFS cement Type B: BB) by weight of cement, FA with a density of 2.91 g/cm^3 was used to replace cement at 15% (fly ash cement Type B: FB). The 2 types of coarse aggregates with an overall dimension of 20mm was used. For coarse aggregate A, surface-dry density was 2.68g/cm3 and water absorption was 1.78%, and the surface-dry density was 2.60g/cm3 and water absorption was 2.82% for the coarse aggregate B. The mixed coarse aggregate AB is obtained through mixing A and B in a ratio of 3:2. The surface-dry density was 2.58g/cm3 and water absorption was 2.02% for the mixed coarse aggregate AB. In addition, the surface-dry density is 2.67g/cm^3 and water absorption is 1.57% for the fine aggregate. Sodium chloride (NaCl) was added to the specimens to accelerate ASR expansion and the total alkali content in terms of Na_2Oeq was 12.0 kg/m^3. Sodium chloride (NaCl) was used for ASR acceleration. Sodium chloride was used for ASR acceleration because it is very difficult to control the air contents at the mixing stage when sodium hydroxide is added into the mixing water. It should be noted that the impacts of sodium chloride and sodium hydroxide on ASR acceleration are differentand less impact is expected with sodium chloride than sodium hydroxide because pH and the solubility of silica in pore solution are lowered by the addition of sodium chloride. Still it is evident that sodium chloride can accelerate ASR

Table 1 Experimental program

Concrete type [Replacement ratios (%)]	coarse aggregates	Curing			Testing
		Standard curing	Deterioration condition		
OPC BFS (45) FA (15)	A AB	Water curing for 4 weeks	Freeze-thaw	Accelerating ASR curing for 1 year	Compressive strength test Freezing-Thawing test Accelerating ASR test
			Accelerating ASR curing for 1 year	Freeze-thaw	

Table 2 Mixing proportions of concrete

	Symbol	w/b [%]	s/a [%]	Binder [%]			Materials contents [kg/m^3]							AE[g]	NaCl [kg/m^3]
				OPC	BFS		W	OPC	BFS	FA	S	G_A	G_{AB}		
BFS test	A-N	55	44.7	100	0	0	184	335	0	0	780	991		13	21
	A-BB			85	45	0	178	178	146	0	784	1014		148	22
	A-FB			55	0	15	181	280	0	49	788	975		13	21
	AB-N			100	0	0	184	335	0	0	783	600	400	13	21
	AB-BB			85	45	0	178	178	146	0	797	600	400	148	22
	AB-FB			55	0	15	181	280	0	49	777	600	400	13	21

expansion [26,27], so it was used in this study.

In this study, the basic mechanical properties, containing compressive strength, static modulus of elasticity, frost resistance and ASR resistance, were tested after water curing for 4 weeks. In order to investigate the effect of combined deterioration of ASR and freeze-thaw action, after the freeze-thaw and accelerating ASR curing, the accelerating ASR curing and freeze-thaw action were performed, respectively.

The compressive strength and static modulus of elasticity were tested at the material age of 4 weeks in water curing, and after accelerating ASR curing for 3 months and 1 year.

The mixing proportions of concrete and test results of fresh concrete are shown in Table 2. Concrete specimens of BFS and FA were prepared with 0.55 water-to-binder ratio (w/b) and 0.447 sand-to-aggregate ratio (s/a), in which slump was controlled at 18±2cm, and air content was controlled at 4.5±1.5% with chemical admixture (AE concrete). For OPC and BFS Concrete specimens, an AE admixture named 'MasterAir® 101' is used to increase air entrainment as a chemical admixture. While, an AE admixture agent named 'MasterAir® 785' was used in the fly ash experiment.

5.2.2 Experimental method

5.2.2.1 Compressive strength test

According to JIS A 1108 [40], the compressive strength test was conducted using three test specimens with dimension of φ100×200mm after 28 days of water curing. The maximum loads (P) until three specimens were damaged were tested and the compressive strength was calculated by the following equation:

$$f_c = \frac{P}{\pi \times \left(\frac{d}{2}\right)^2} \quad \text{Eq. (1)}$$

where, f_c is the compressive strength (N/mm^2); P is the maximum load (N); and d is the diameter of concrete specimen (mm).

The compressive strength of concrete was the average value of the three specimens.

5.2.2.2 Freeze-thaw in water test

According to JIS A 1148 A, the test specimens were subjected to freeze-thaw in water in a chamber, where the temperature was maintained the minimal temperature of -18℃ and the maximal temperature of 5℃. The resonant frequency of specimens was measured before freeze -thaw in water test, and then was measured every 30-cycle when subject to freeze-thaw until 300 cycles or it was broken. The relative dynamic modulus of elasticity was calculated using the following equation:

$$P_n = \frac{{f_n}^2}{{f_0}^2} \times 100\% \quad \text{Eq. (3)}$$

where, P_n is the dynamic modulus of elasticity after n cycles of freeze-thaw (%); f_n is the resonant frequency after n cycles of freeze-thaw (Hz); f_0 is the resonant frequency at 0 cycles of freeze-thaw (Hz);

The durability factor was obtained by the following equation:

$$DF = (P \times N)/M \quad \text{Eq. (4)}$$

where, DF is durability factor of concrete; P is the dynamic modulus of elasticity after N cycles (%); N is the small number between the number of cycles after that the relative elastic modulus becomes 60% and 300 cycles; M is 300 cycles;

5.2.2.3 Test for alkali-silica reactivity of concrete

In according to JCI-S-010-2017, alkali-silica reactivity of concrete was tested using the specimens with a dimension of 75×75×400mm.

5.3 Experiment result and discussion

5.3.1 Cracks due to ASR

Fig. 5-1 and Fig. 5-2 show the cracks progression in AB-N and N due to ASR time. From the figures, it can be seen that concrete cracked due to ASR, and the with long ASR time, cracks tended to be more. Comparing the AB-N and N, it can be seen that there is little changes between them.

Fig. 5-3 and Fig .5-4 show the cracks progression in AB-BB and BB due to ASR time. Both the AB-BB and BB, crack is not caused until 3-month, which can confirm that BFS can restrain ASR. Since 6-month although BFS is used in this study, concrete started to crack. At the 12-month, there are very few cracks.

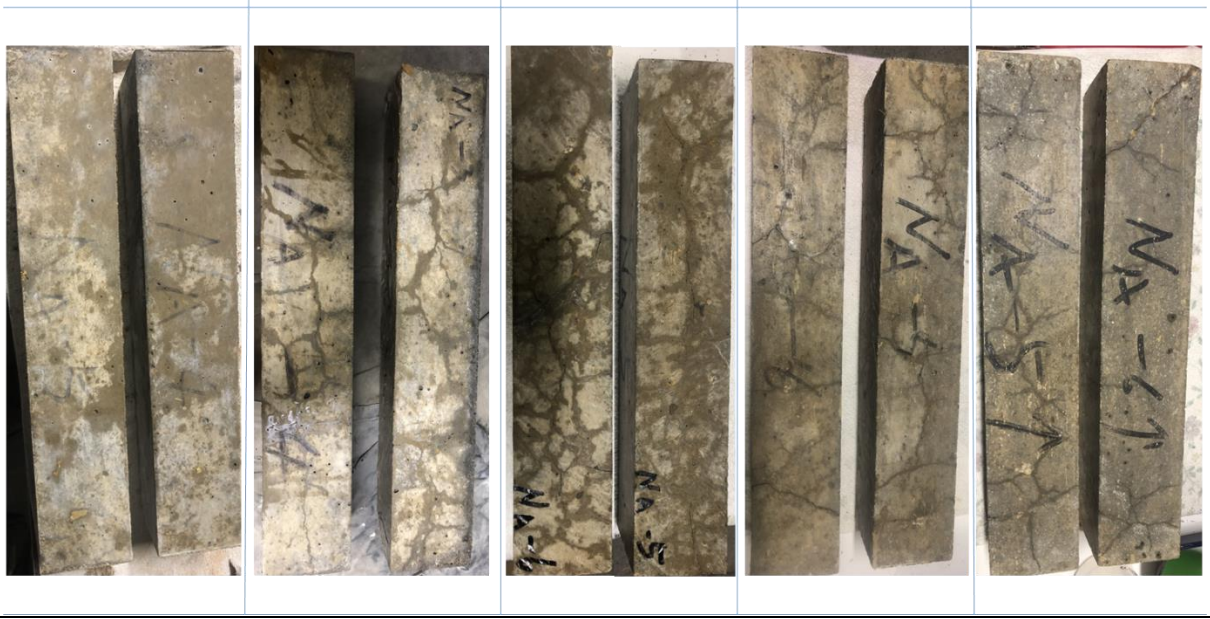

Fig. 5-1 cracks in AB-N due to ASR

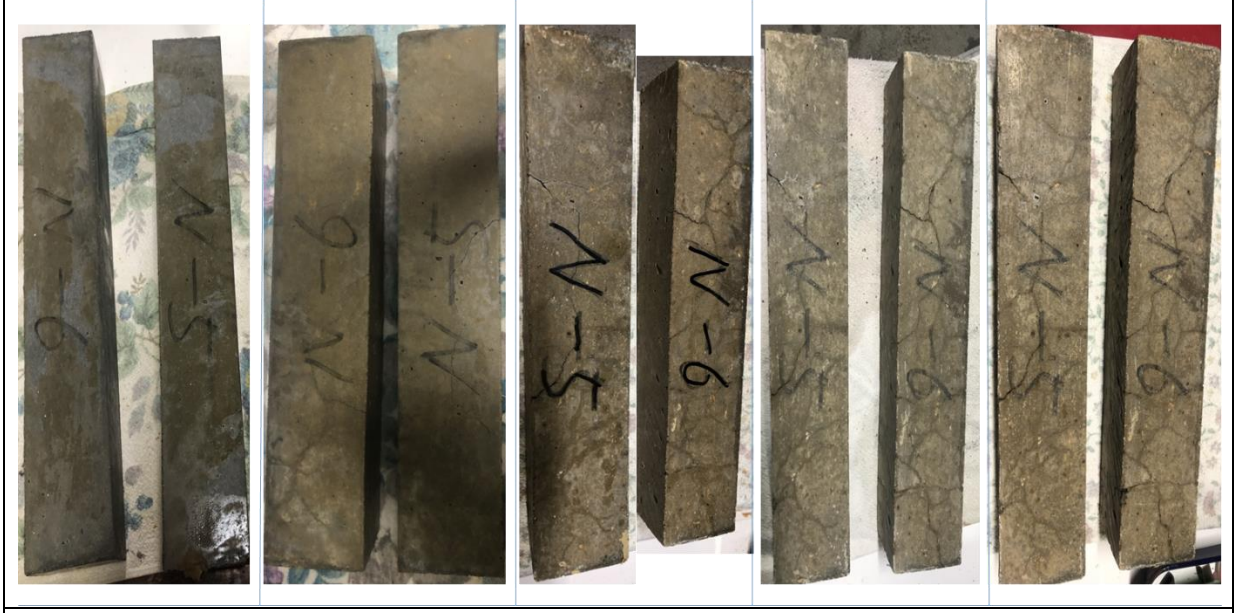

Fig. 5-2 cracks in N due to ASR

Fig. 5-3 cracks in AB-N due to ASR

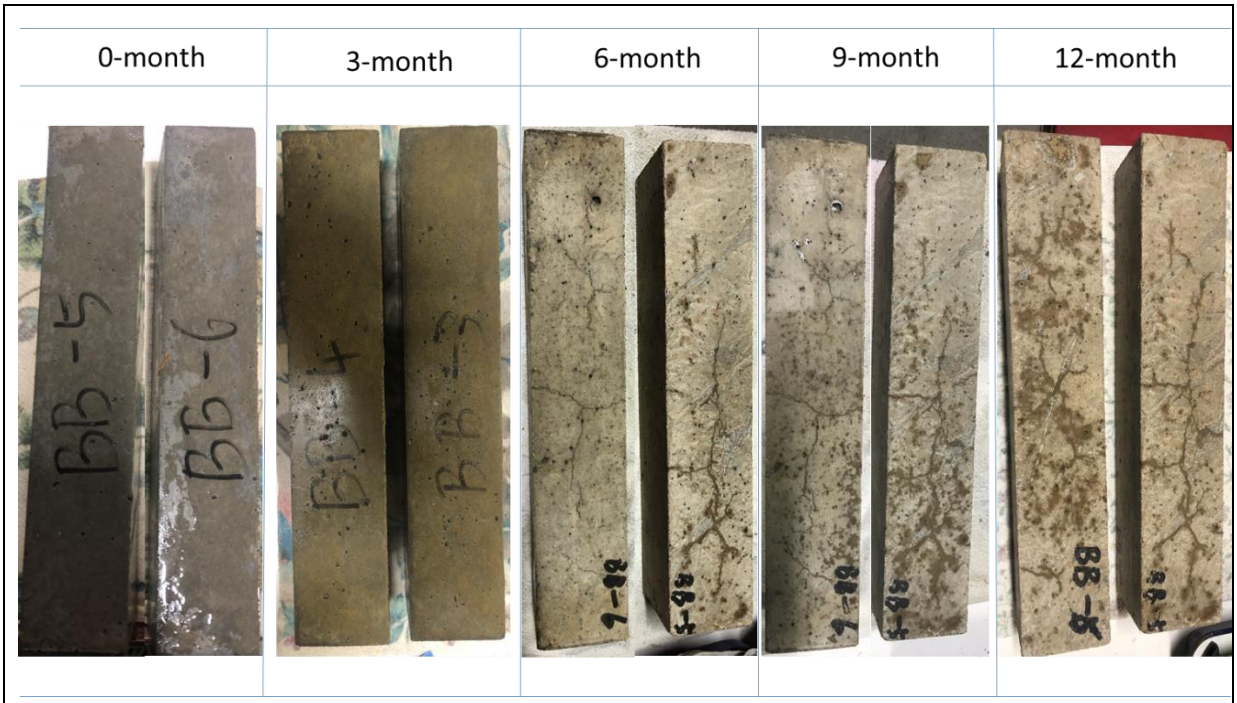

Fig. 5-4 cracks in N due to ASR

Fig. 5-5 cracks in AB-FB due to ASR

Fig. 5-6 cracks in N due to ASR

Fig. 5-5 and Fig .5-6 show the cracks progression in AB-FB and FB due to ASR time. For the AB-FB, little crack was cause in the concrete surface. While for FB, since 9-month concrete cracked. Comparing the cases between BFS and FB, FB can make concrete have a better ASR crack resistance than BFS.

5.3.2 compressive strength and modulus of static elasticity

The changes in compressive strength due to ASR are shown in Fig. 5-7. From the Fig. 5-7, it can be seen that: (1) the compressive strength tended to increase for all concrete due to 3-month ASR curing. For OPC concrete, this may be because the less ASR gel was generated by ASR action to lead to densify the pore structure. For FA and BFS concrete, the additive of FA and BFS can restrain ASR action, the increase of compressive strength may be due to the pozzolan action of FA and the hydraulicity of BFS. (2) due to 12-month ASR, for OPC and FA concrete, compressive strength tended to decrease, while, there was little change in compressive strength for BFS concrete. For OPC concrete, this is because of the crack due to ASR. For FA concrete, although the ASR action was restrained, the less ASR gel was generated to lead to cause a few cracks. For BFS concrete, the reason

may be similar to FA concrete, however, there was a balance in compressive strength due to ASR and hydraulicity.

Fig. 5-8 shows the changes in modulus of static elasticity (MSE) due to ASR. For OPC concrete, the MSE tend to decrease as ASR action is in progress. For FA and BFS concrete, although the MSE increased due to 3-month ASR, it tended to decrease due to 12-month. It can be well-known that the MSE is closely related to the cracks. The additive of FA and BFS restrained the ASR action and prevented the crack. However, in the process of ASR, the cracks were still caused due to 12-month ASR.

The relationships between MSE and compressive strength of all concrete are shown in Fig. 5-9. From the previous study [7], it is well-known that there is a close relationship between MSE and compressive strength. In Fig. 3 it can be seen that expect N after the 3-month and 12month ASR, there is a linear relation between the MSE and compressive strength. for N after 3-month and 12-month ASR, the MSE is reduced due to ASR action. Therefore, it can be said that the reduction of MSE can be used as the criterion of ASR deterioration.

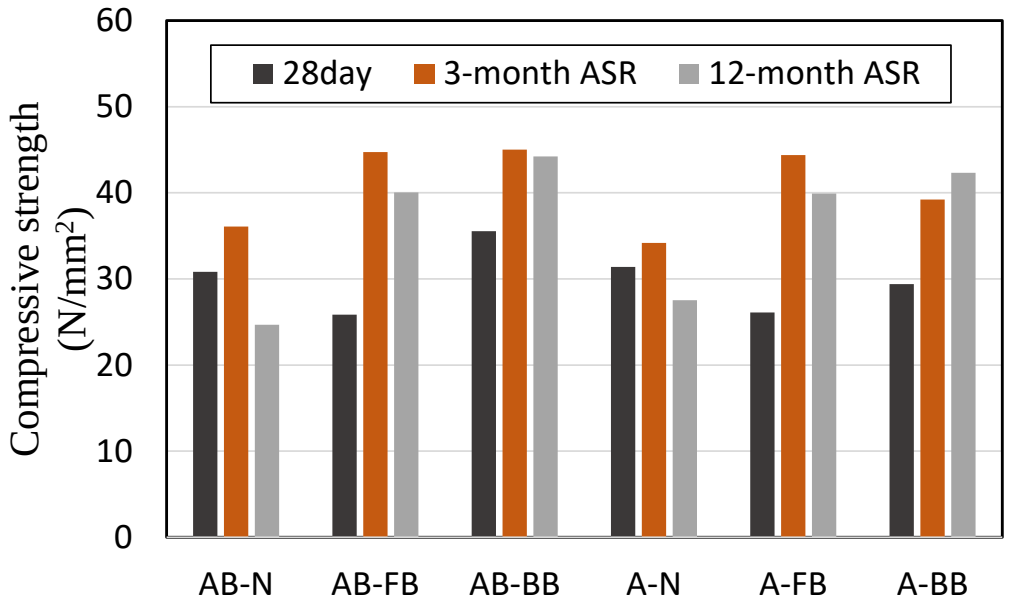

Fig. 5-7 Compressive strength due to ASR

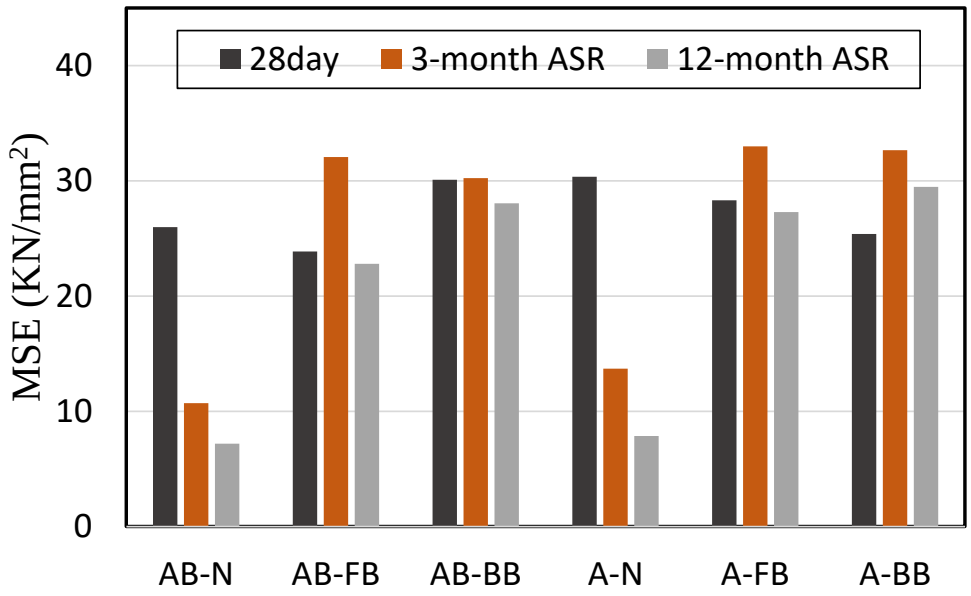

Fig. 5-8 Modulus of static elasticity due to ASR

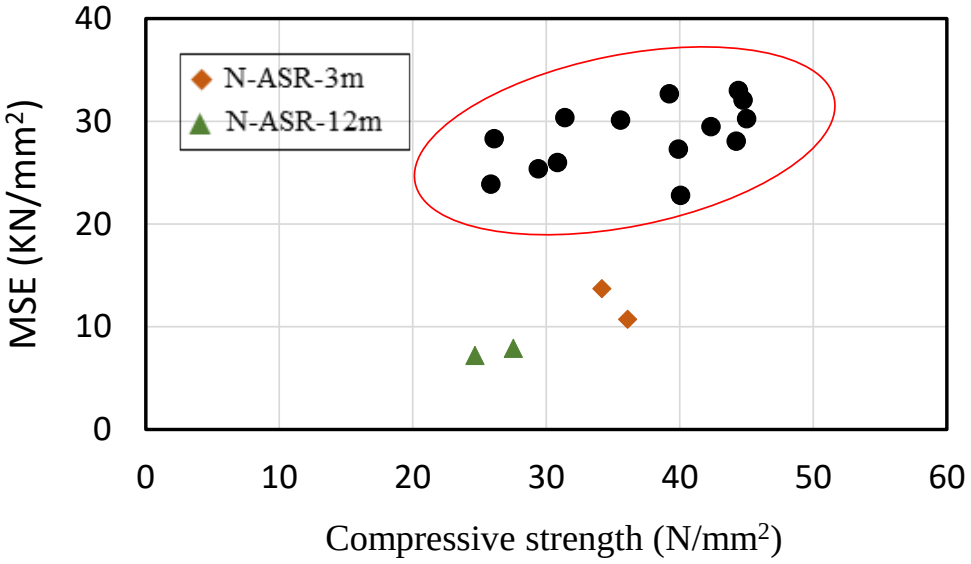

Fig. 5-9 Relationships between MSE and compressive strength

5.3.3 Combined deterioration between ASR and frost damage

Fig. 5-10a shows the change in relative dynamic modulus of elasticity (RDME) due to freeze-thaw. From the Fig. 10, it can be seen that: comparing the cases of A and AB, the coarse aggregate had little effect on the frost resistance. Based on the case of OPC, the additive of FA resulted a high frost resistance, which is different from

the previous study [5]. This may be because the salt can reduce the frost resistance, and the FA can reduce the effect caused by salt. The frost resistance was decreased due to BFS, which is same with previous study [4].

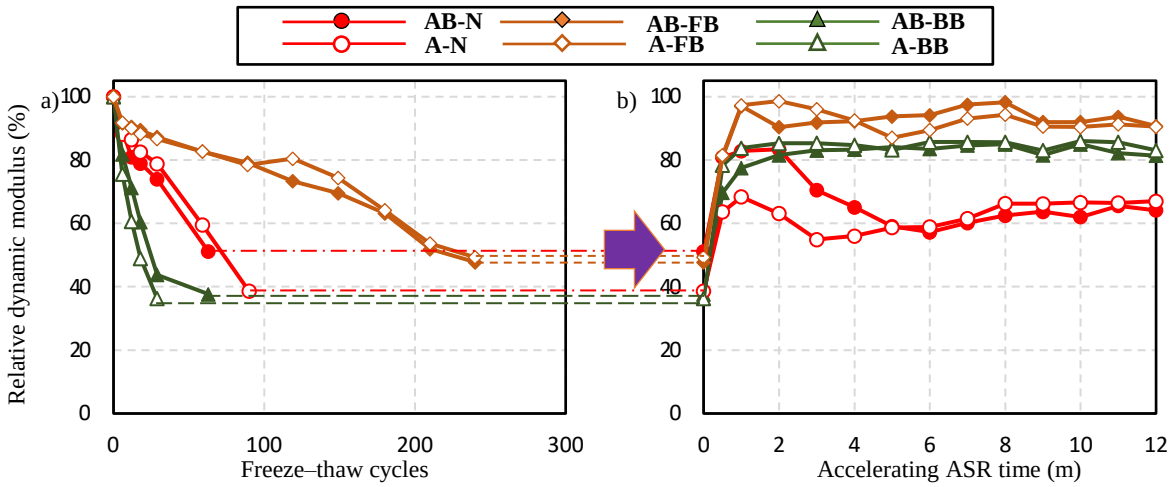

Fig. 5-10 Changes in relative dynamic elastic modulus due to freeze-thaw and the next ASR curing

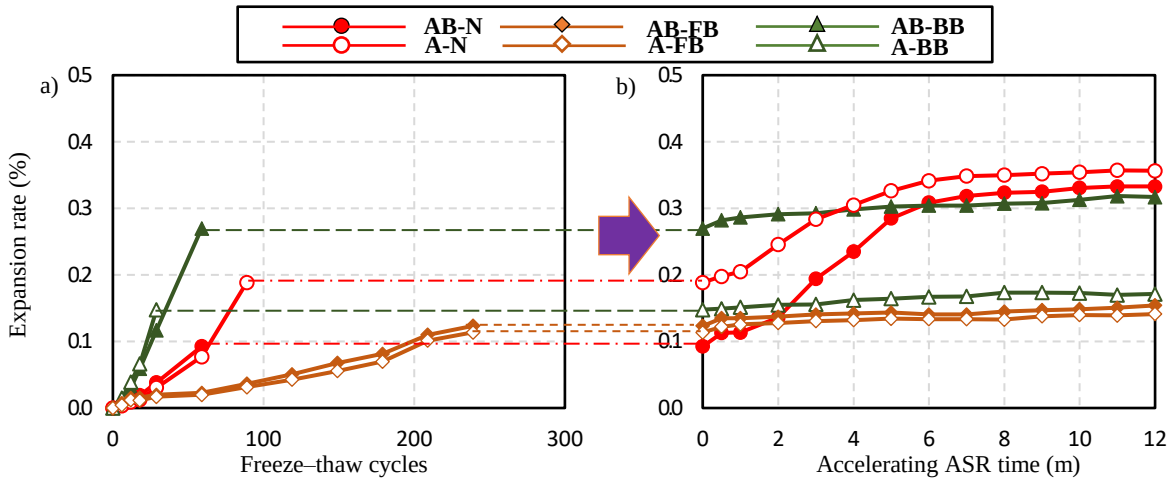

Fig. 5-11 Changes in expansion rate due to freeze-thaw and the next ASR curing

Fig. 5-10b shows the changes in RDME due to ASR action after freeze-thaw. Comparing the cases of A and AB, it also is obtained that the coarse aggregate had little effect on the RDME. In the first 2 months of ASR, the RDME tend to increase, and the physical properties of the concrete were repaired due to ASR or the pozzolan action of FA and the hydraulicity of BFS. In the next ASR curing, for OPC concrete, the RDME tended to decrease and was reduced to 60% due to ASR, and was kept around 60. For FA and BFS concrete, ASR action

was restrained due to additive of FA and BFS, which resulted the RDMEs were not reduce and were kept at a high level. Comparing the case of FA and BFS, FA can result a high RDME.

The expansion rates due to freeze-thaw are shown in Fig. 5-11a. Similar to Fig. 5-10a, the coarse aggregate had little effect on the expansion rates due to freeze-thaw, and the additive of FA could reduce the expansion rates due to freeze-thaw.

Fig. 5-11b shows the changes in the expansion rates due to ASR action after freeze-thaw. For OPC concrete, the expansion continued to increase due to ASR after freeze-thaw. The eventual expansion rates of A-N and AB-N converged. For FA and BFS concrete, regardless of A and AB, the expansion increased slowly due to ASR action. There is little change in the increase of expansion due to ASR.

Fig. 5-12a shows the change in RDME due to 3 months ASR, and Fig. 5-12b shows the change in RDME due to freeze-thaw after 12 months ASR. In Fig. 6a, for OPC concrete, since 1-month, the RDME tended to decrease due to ASR. For FA and BFS concrete, although ASR action was in progress, the RDME were kept a high level due to the additive of FA and BFS. In the next freeze-thaw after ASR in Fig. 5-12b, for OPC and BFS concrete had a rapid deterioration, the effect of coarse aggregate was tiny. For FA concrete, the use of FA resulted a high resistance. In addition, comparing the coarse aggregate A and AB, A could result a low frost resistance. This may be the preceding ASR resulted more tiny-crack for A-FB, or it is said that the ASR gel was more generated for A-FB than AB-FB.

Fig. 5-13a shows the change in expansion rate due 3 months ASR, and Fig. 5-13b shows the change in expansion rate due to freeze-thaw after 3 months ASR. In Fig. 7a, for all case, the expansion rates were kept a low level. In the next freeze-thaw in Fig. 5-13b, the expansion increased sharply due to freeze-thaw. Comparing the cases of A and AB, for OPC and BFS concrete, the coarse aggregate had little effect on the expansion. For FA concrete, the coarse aggregate A increased the expansion due to freeze-thaw than the coarse aggregate AB.

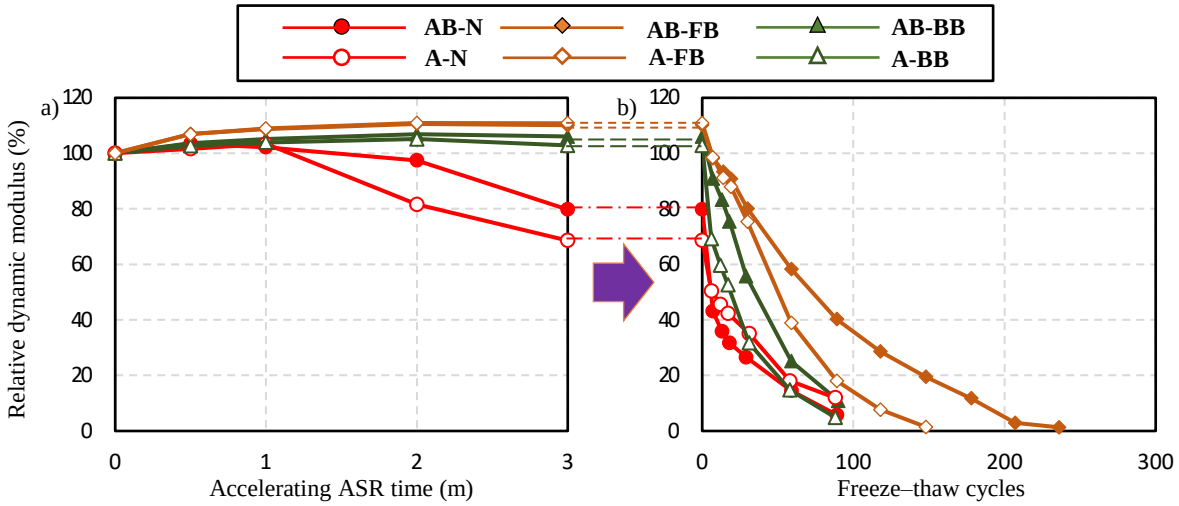

Fig. 5-12 Changes in relative dynamic elastic modulus due to freeze-thaw and the next ASR curing

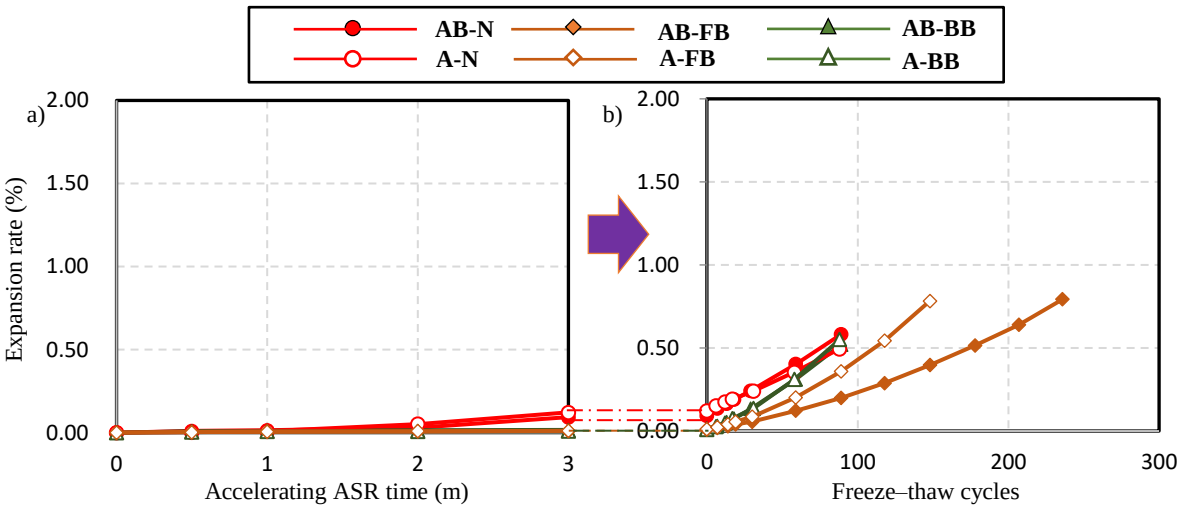

Fig. 5-13 Changes in expansion rate due to freeze-thaw and the next ASR curing

Fig. 5-14a shows the change in RDME due to 12-month ASR, and Fig. 5-14b shows the change in RDME due to freeze-thaw after 12-month ASR. In Fig. 6a, for OPC concrete, in the first 6 months of ASR, the RDME tended to decrease, and was reduced to 60%. In the next ASR curing, the RDME would be recovered a little, and were kept around 70%. For FA and BFS concrete, although ASR action was in progress, the RDME were kept a high level due to the additive of FA and BFS. In the next freeze-thaw after ASR in Fig. 5-14b, for OPC and BFS concrete had a rapid deterioration, the effect of coarse aggregate was tiny. For FA concrete, the use of FA resulted a high resistance. In addition, comparing the coarse aggregate A and AB, A could result a low frost resistance. This may be the preceding ASR resulted more tiny-crack for A-FB, or it is said that the ASR gel was more

generated for A-FB than AB-FB.

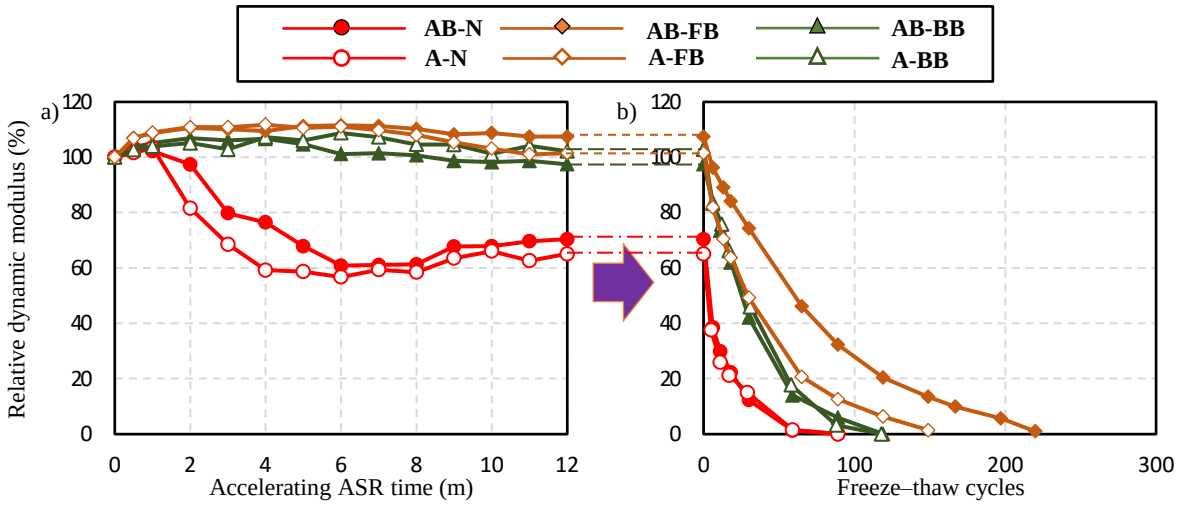

Fig. 5-14 Changes in relative dynamic elastic modulus due to freeze-thaw and the next ASR curing

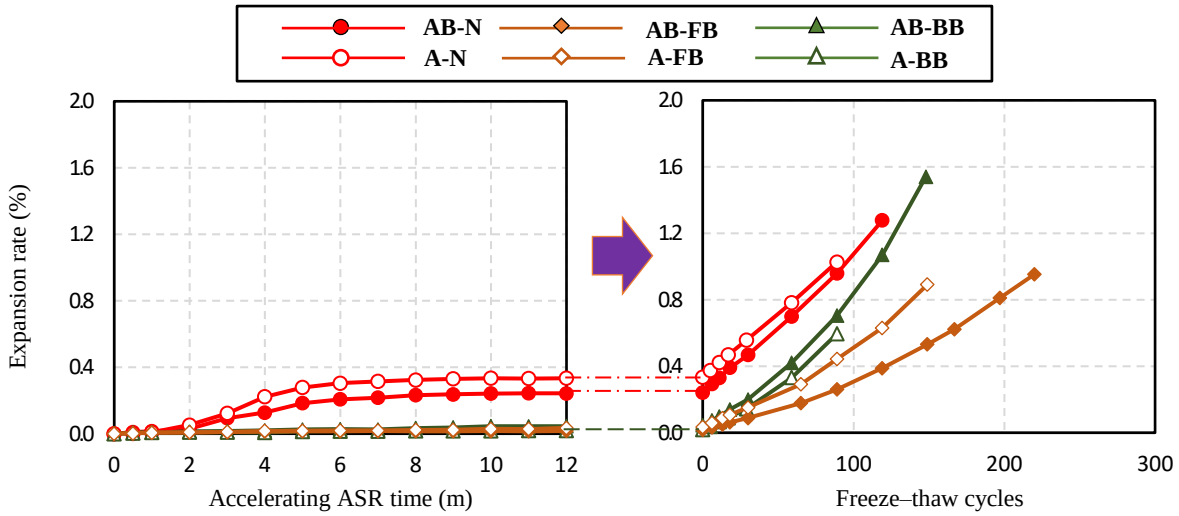

Fig. 5-15 Changes in expansion rate due to freeze-thaw and the next ASR curing

Fig. 5-15a shows the change in expansion rate due 12-month ASR, and Fig. 5-15b shows the change in expansion rate due to freeze-thaw after 12-month ASR. In Fig. 5-15a, for OPC concrete, the expansion rate tended to increase due to ASR action. comparing cases of A and AB, the coarse aggregate A had a high alkali-silica reactivity. For FA and BFS concrete, expansion rates were kept at a low level due to the inhibition of FA and BFS on ASR. In the next freeze-thaw in Fig. 5-15b, the expansion increased sharply due to freeze-thaw. Comparing the cases of A and AB, for OPC and BFS concrete, the coarse aggregate had little effect on the

expansion. For FA concrete, the coarse aggregate A increased the expansion due to freeze-thaw than the coarse aggregate AB.

5.3.4 Discuss and summary

5.3.4.1 discuss on the combined deterioration

Fig. 5-16 shows the relationship between reduction of MSE and expansion rate due to ASR. The reduction of MSE is a subtraction value which is obtained by subtracting the MSE at 28-day from the one after ASR. the R2 value is 0.9419, which indicates that there is a close relationship between reduction of MSE and expansion rate due to ASR. the expansion tended to increase due to ASR, which led to MSE tend to decrease. Therefore, the ASR deterioration can be evaluated by the reduction of MSE.

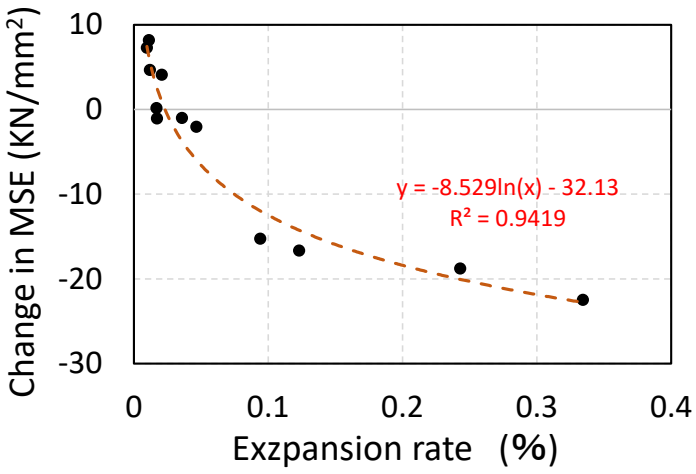

Fig. 5-16 Relationship between reduction of MSE and expansion rate due to ASR

Fig.5-17, Fig. 5-18 and Fig. 5-19 show the changes of RDME and expansion rate due to freeze-thaw at the different ASR times of all concrete, in which all the RDMEs and expansion rates at 0-cycle at the different ASR times were considered as 100% and 0. In Fig. 5-17a and Fig. 5-17b, it can be seen that: at the same ASR time, the coarse aggregate had little effect on the frost resistance. The frost resistance tended to decrease with the long ASR time. It can be said that ASR can reduce the frost resistance for OPC concrete. In Fig. 5-18a and Fig.

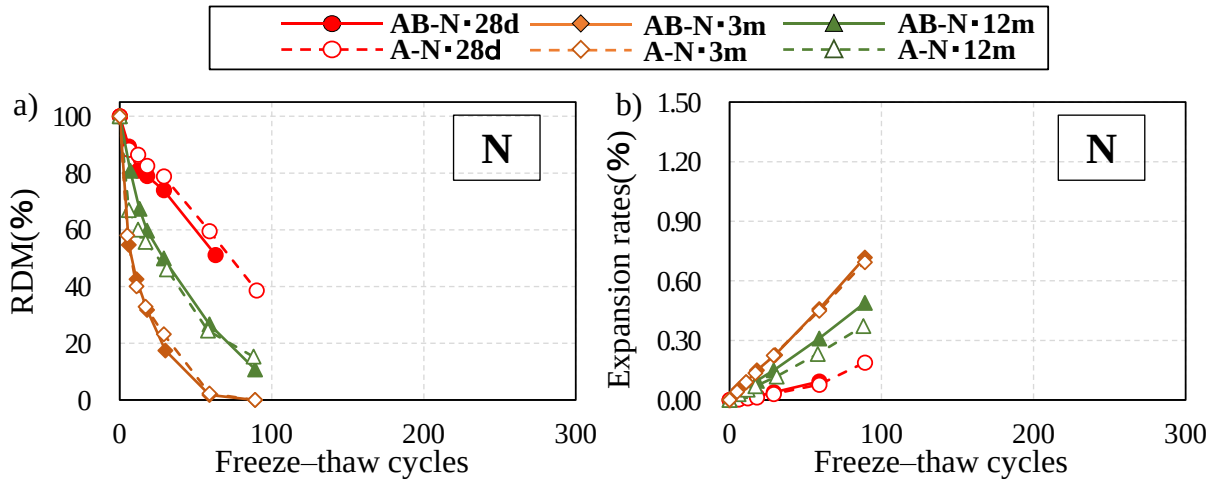

Fig. 5-17 Contrast of RDME and expansion due to freeze-thaw at different ASR time for OPC concrete

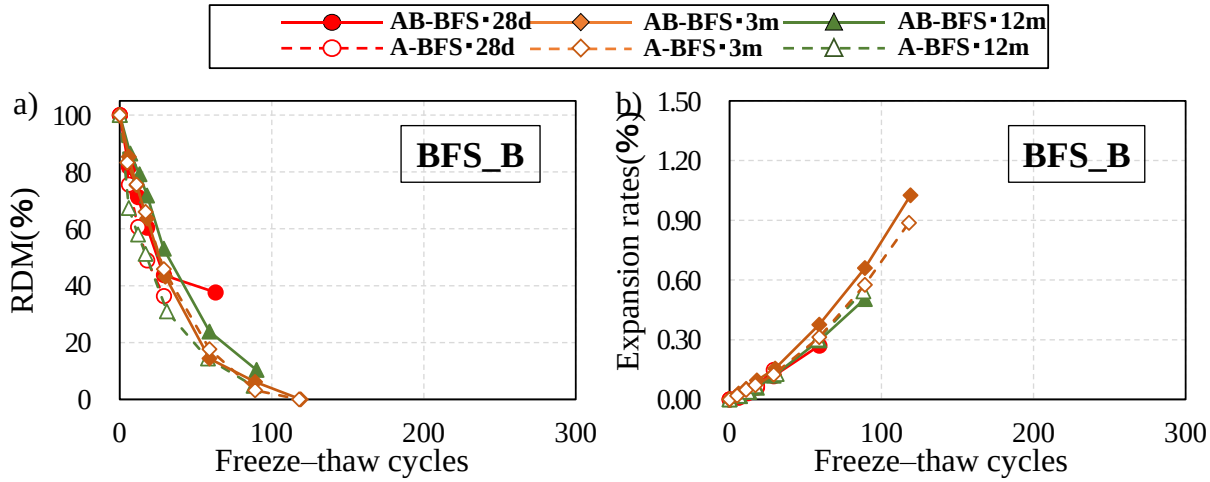

Fig. 5-18 Contrast of RDME and expansion due to freeze-thaw at different ASR time for BFS concrete

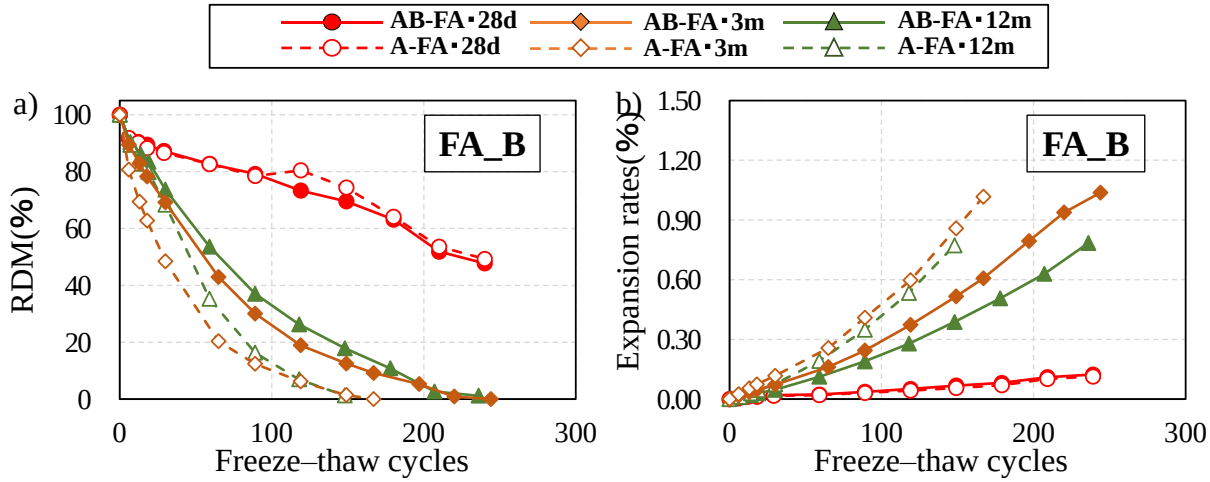

Fig. 5-19 Contrast of RDME and expansion due to freeze-thaw at different ASR time for FA concrete

5-18b, there is little change in RDME for all BFS concrete, regardless of coarse aggregate and ASR time. ASR

did not affect the frost resistance for BFS concrete.

In Fig. 5-19a and Fig. 5-19b, for the cases of 28d, the coarse aggregate had little effect on the frost resistance for FA concrete. For the cases after 3-month and 12-month ASR, it can be seen that the coarse aggregate A could reduce the frost resistance than the coarse aggregate AB. Based on the case of 28d, the frost resistance was reduced due to ASR curing. However, comparing the cases after 3-month and 12-month ASR, there is little change in RDME due to freeze-thaw. Therefore, it can be said that although ASR can reduce the frost resistance for FA concrete, the long ASR time had little effect on frost resistance.

Fig.5-20 shows the changes in durability factor due to different ASR time for all concrete. Fig. 5-20a and Fig. 5-20b show the durability factor results obtain from Fig.5-17, Fig. 5-18 and Fig. 5-19 in AB and A concrete. As seen in Fig. 5-20, for both AB and A concrete, the durability factor decreased with increasing ASR time for OPC and FA concrete. Based on the case of OPC, the durability factor of FA concrete tended to increase while, the durability factor had no change due to additive of BFS.

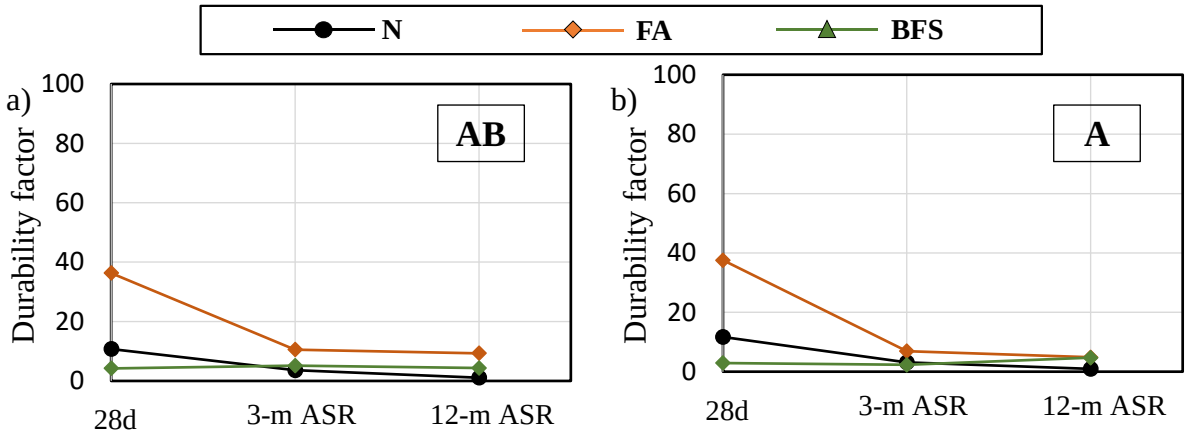

Fig. 5-20 Change in Durability factor due to different ASR time

Fig. 5-21a shows the contrast between single ASR and ASR after freeze-thaw of all concrete with the coarse aggregate AB. For OPC, FA and BFS concrete, there is little change in expansion due to single ASR and ASR after thaw. Therefore, the preceding freeze-thaw had little effect on ASR for all concrete with the coarse aggregate AB.

Fig. 5-21b shows the contrast between single ASR and ASR after freeze-thaw of all concrete with the coarse aggregate A. For OPC concrete, the preceding freeze-thaw can inhibit the next expansion due to ASR. For FA and BFS concrete, there is little change in expansion due to single ASR and ASR after thaw. It can be said that the preceding freeze-thaw had little effect on ASR for FA and BFS concrete with the coarse aggregate A.

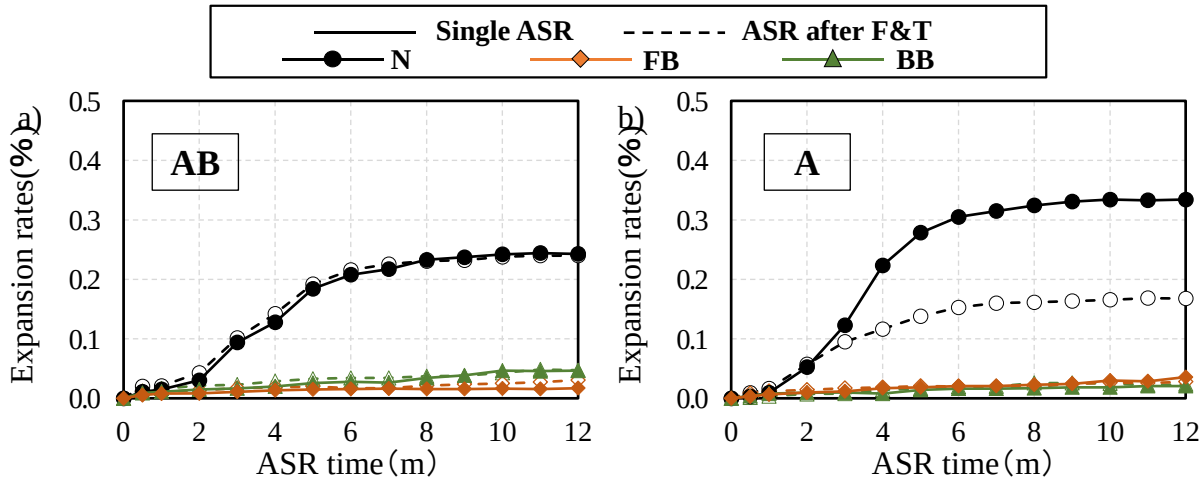

Fig. 5-21 Change in Durability factor due to different ASR time

5.3.4.2 Summary on the expansion and RDM

Fig. 5-22 shows relationship between expansion rate and RDM due to F&T at different ASR time, in which all the RDMEs and expansion rates at 0-cycle F&T of all cases at different ASR time were considered as 100% and 0. For all cases of 28d, 3-month and 12-month, there are close relation between expansion rate and RDM, regardless of cement type.

The results in Fig 5-22 are summarized and are shown in Fig. 5-23. From the Fig. 5-23, it can be seen that expansion rate of concrete is related closely to RDM, regardless of cement type and ASR time. It can said that expansion rate of concrete is determined by the degradation degree of concrete, regardless cement type. The additive of BFS and FA have no effect on the relationship between expansion rate and RDM.

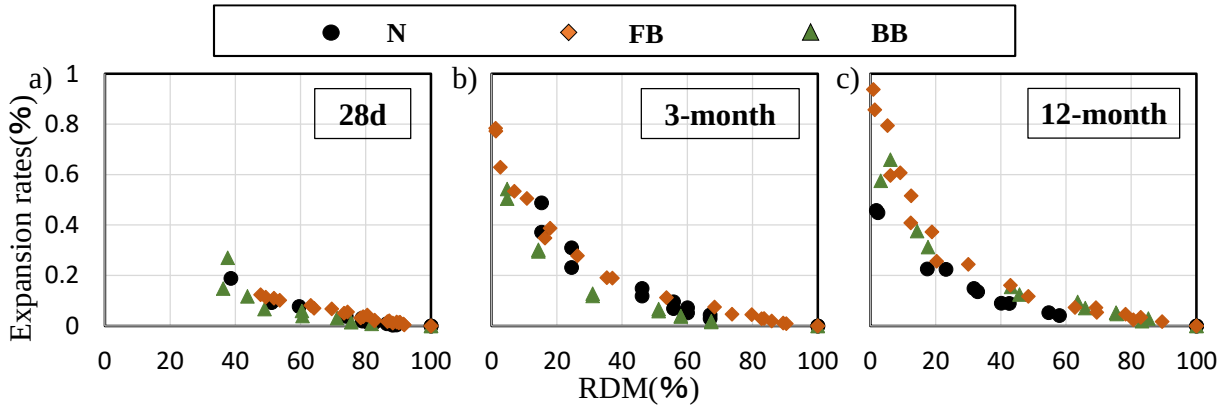

Fig. 5-22 Relationship between expansion rate and RDM due to F&T

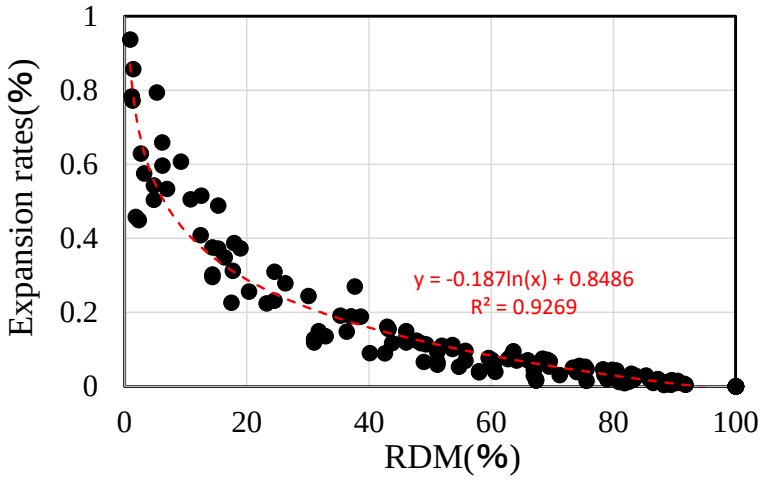

Fig. 5-23 Change in Durability factor due to different ASR time

Fig. 5-24 shows relationship between expansion rate and RDM due to F&T for N, BFS and FA concrete subjected to single F&T and the following ASR after single F&T, in which all the RDMEs and expansion rates

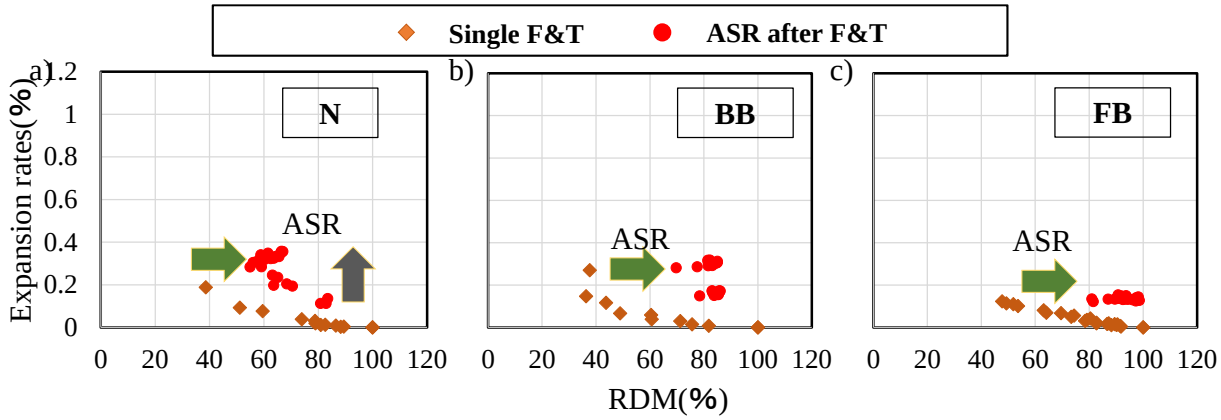

Fig. 5-24 Relationship between expansion and RDM due to F&T of concrete subjected to single F&T and the following ASR after single F&T

at 28-day of all cases were considered as 100% and 0. In Fig. 5-24a, for OPC concrete, to a certain extent, ASR can recover the RDM of concrete subjected to F&T, and increase the expansion of concrete. In Fig. 5-24b and Fig. 5-24c, For BFS and FA concrete, ASR can vastly recover the RDM of concrete subjected to F&T, and did increase the expansion of concrete.

Fig. 5-25 shows relationship between expansion rate and RDM due to F&T for N, BFS and FA concrete subjected to 3-momth single ASR and the following F&T after 3-momth single ASR, in which all the RDMEs and expansion rates at 28-day of all cases were considered as 100% and 0. In Fig. 5-24, for all cases of OPC, BFS and FA concrete, there are close relation between expansion rate and RDM.

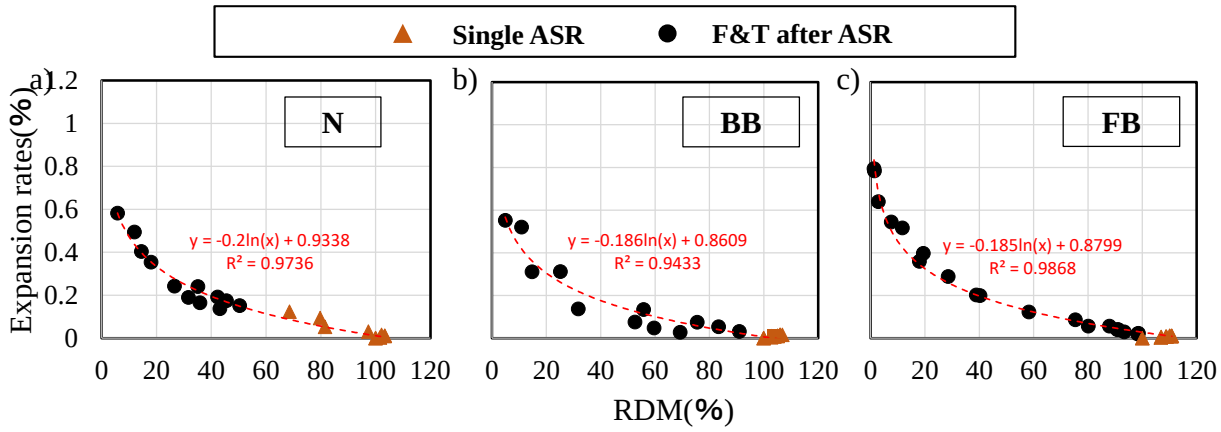

Fig. 5-25 Relationship between expansion and RDM due to F&T of concrete subjected to 3-momth single ASR and the following F&T after 3-momth single ASR

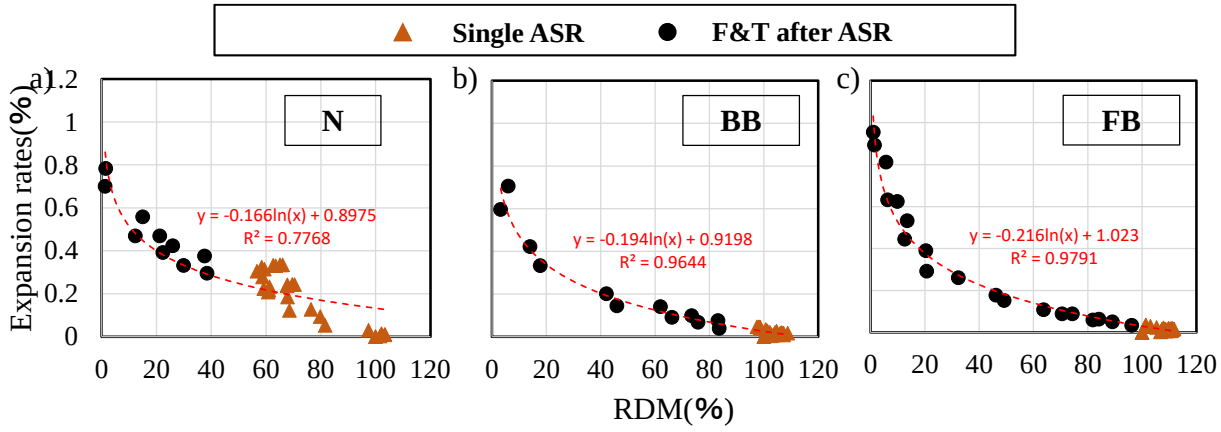

Fig. 5-26 Relationship between expansion and RDM due to F&T of concrete subjected to 12-momth single ASR and the following F&T after 12-momth single ASR

Fig. 5-26 shows relationship between expansion rate and RDM due to F&T for N, BFS and FA concrete subjected to 12-month single ASR and the following F&T after 12-month single ASR, in which all the RDMEs and expansion rates at 28-day of all cases were considered as 100% and 0. In Fig. 5-26a, although the R^2 value with 0.7768 indicates that there is a certain correlation between expansion rate and RDM, compared to Fig. 5-25a, the correlation tends to be low, which may be the long time ASR vastly increases expansion, but slightly decrease the RDM of concrete. It can be said that ASR can change relationship between expansion rate and RDM, and even change physical properties of concrete. In Fig. 5-26b and Fig 5-26c, similar to Fig. 5-25, for all cases of OPC, BFS and FA concrete, there are close relation between expansion rate and RDM. This is because the additive of BFS and FA can restrain ASR to keep the relationship between expansion rate and RDM.

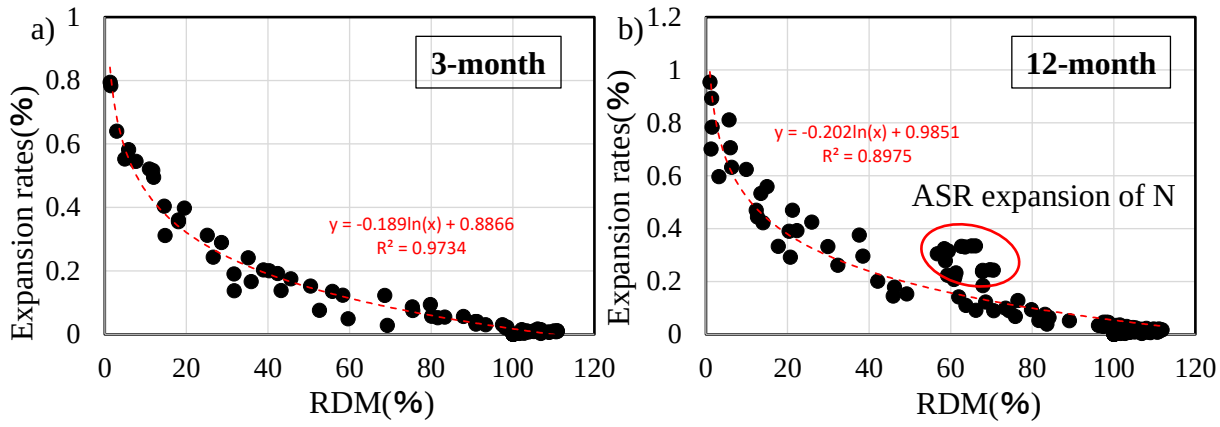

Fig. 5-27 Change in Durability factor due to different ASR time

The results in Fig. 5-25 and Fig. 5-26 are summarized and are shown in Fig. 5-27. From the Fig. 5-27a, it is well known that there is a close relationship between expansion rate and RDM, regardless of cement type. For OPC concrete, although 3-month ASR increase expansion rate, the deterioration degree is small, which little affect relationship between expansion rate and RDM. While, in Fig. 5-27b, it can be seen that some of the point don't fit the relation curve. The 12-month ASR costly change the relationship between expansion rate and RDM.

5.4 Conclusion

In this paper, the combined deterioration of ASR and frost damage of the concrete containing BFS and FA were investigated. As a result, the following conclusions were obtained:

(1) There is a close relationship between reduction of MSE and expansion rate due to ASR. the ASR deterioration can be evaluated by the reduction of MSE.

(2) ASR action after freeze-thaw can repair the concrete damage due to freeze-thaw. In addition, ASR action can reduce the RDME of OPC concrete. While for BFS and FA concrete, ASR action has little effect on the RDME.

(3) For OPC and FA concrete, the preceding ASR action can reduce the frost resistance. while, for BFS concrete, the preceding ASR has little effect on the frost resistance.

(4) Expect A-N, the preceding freeze-thaw has little effect on the next expansion due to ASR. Besides, for BFS and FA concrete, the expansion due to ASR is kept a low level regardless of freeze-thaw. For A-N, the preceding freeze-thaw can decrease the next expansion due to ASR..

(5) Although 3-month ASR increase expansion rate, the deterioration degree is small, which little affect relationship between expansion rate and RDM. While, the 12-month ASR costly change the relationship between expansion rate and RDM, which is because that the long time ASR vastly increases expansion, but slightly decrease the RDM of concrete for OPC concrete.

(6) However, for BFS and FA concrete, the additive of BFS and FA can restrain ASR, which keeps the relationship between expansion rate and RDM.

References:

1. Andrew, R. M., "Global CO2 emissions from cement production, 1928–2018", Earth Syst. Sci. Data, vol. 11, 2019, pp. 1675–1710.

2. Na, S. H., Hama, Y., Taniguchi, M., Katsura, O., Sagawa, T. and M. Zakaria, "Experimental investigation on reaction rate and self-healing ability in fly ash blended cement mixtures", J Adv Concr Technol, vol. 10, 2012, pp. 240–253.

3. Zhang, W., Hama, Y. and Na, S. H, "Drying shrinkage and microstructure characteristics of mortar incorporating ground granulated blast furnace slag and shrinkage reducing admixture", Constr. Build. Mater, vol. 93, 2015, pp.267–277.

4. Ding, Z., Quy, N. X., Noguchi, T., Kim, J. and Hama, Y., A study on the change in frost resistance and pore structure of concrete containing blast furnace slag under the carbonation conditions", Constr. Build. Mater, vol. 331, 2022,

5. Ding, Z., Quy, N. X., Kim, J. and Hama, Y., Evaluations of frost and scaling resistance of fly ash concrete in terms of changes in water absorption and pore structure under the accelerated carbonation conditions", Constr. Build. Mater, vol. 345, 2022,

6. Gong, F., Takahashi. Y., Segawa, I. and Maekawa, K., "Mechanical properties of concrete with smeared cracking by alkali-silica reaction and freeze-thaw cycles", Cement and Concrete Composites, vol. 11, 2020,

7. Nakata, Y., Sawamoto, T., Otsuka, S. and Haruyama, N., "Effect of strength development of high-strength concrete using different sorts of cement on elastic modulus of elasticity", J. Struct. Constr. Eng. AIJ, No. 622, 17−23, 2007.

Chapter 6

Conclusions

6.1 Conclusions

1 Introduction

The present research investigated the combined deterioration of frost damage of concrete containing BFS and FA. Since the combined deterioration between salt damage and frost damage has been expansively studied, this study mainly investigated the the combined deterioration between carbonation and frost damage, ASR and frost damage.

2 Effect of C-S-H type accelerator on the compressive strength at early curing age as blended BFS (Chapter 2)

This chapter presents previous studies on frost damage to clarify the position of this study.

For concrete structures in cold regions, concrete is subject to frost damage in winter, the effect of frost damage of concrete suffered the other three types of deterioration, which progress throughout the year, has been focused on. The combined deterioration between frost damage and salt damage has been expensively sturdily in the world. However, for most of concrete structures, carbonation is in presses to reduce the pH of concrete with intrusion of CO_2 into concrete due to a long-term exposure to air. Besides, ASR expansion is caused due to ASR aggregate to serious endanger the safety of concrete, which has been attracting new wild attention. The study on the combined deterioration between carbonation and frost damage, and ASR and frost damage. In addition, the additive of BFS and FA can decrease the carbonation resistance and restrain the ASR, which lead to change the mechanisms of combined deterioration. There is little study on this in the world.

Therefore, this study will investigate the combined deterioration between carbonation and frost damage, and ASR and frost damage of concrete containing BFS and FA, the effect on the combined deterioration would be also made clear.

3 Effect of limestone powder and gypsum on the compressive strength mixture design of

blended BFS (Chapter 3)

In this chapter, the change in frost resistance and pore structure of concrete containing blast furnace slag with various replacement ratio due to carbonation were investigated. As a result, there is a close relationship between the carbonation speed and 28-day compressive strength in blast furnace slag concrete. The frost resistance, carbonation resistance and scaling resistance of blast furnace slag cement concrete decrease as blast furnace slag replacement ratio increases. Furthermore, due to carbonation, the frost durability of ordinary Portland cement concrete and the concrete with a low replacement ratio of blast furnace slag tends to decrease. However, the concrete with a high replacement ratio of blast furnace slag tends to increase. Under the carbonation conditions, the pore volume decreases due to carbonation of calcium hydroxide, and the pore structure will be coarsened due to carbonation of C-S-H. In addition, it is expected that permeability of concrete is raised and scaling is inhibited due to carbonation, and the surface area with a certain thickness in the carbonated concrete will be scaled due to freeze-thaw.

4 Evaluation of the combined deterioration by freeze-thaw and carbonation of mortar incorporating BFS (Chapter 4)

In this chapter, the frost and scaling resistance of concrete with various fly ash (FA) replacement ratios exposure to air and accelerated carbonation conditions were investigated. The changes in water absorption were measured by RILEM / CIF test and in pore structure were measured by the Archimedes method and the mercury intrusion porosimetry method due to carbonation.

Results show that the influence of FA and carbonation on the frost and scaling resistance of concrete can be ignored due to air bubbles by air entraining (AE) admixture in case of AE FA concrete. For Non-AE FA concrete, carbonation of FA concrete does not change the gel porosity/capillary porosity ratio, which is the reason for the frost resistance is not influenced by carbonation of FA concrete. Additionally, it is noteworthy to note that the scaling resistance is strongly connected to the pore volume above 75 nm, and that when exposed to carbonation,

the scaling resistance tends to rise as a result of the increase in pore volume above 75 nm that occurs as a result of carbonation. Because of the addition of FA and carbonation, the frost and scaling resistance are far more reliant on the changes in pore structure than they are on the water absorption.

5 Curing age and carbonation characteristics incorporating BFS (Chapter 5)

A deterioration phenomenon called combined deterioration due to the interaction of different deterioration phenomenon have been in focus for the durability of concrete. In order to evaluate the durability of concrete containing BFS and FA, it is necessary to grasp the effect of BFS and FA on the combined deterioration. ASR expansion is caused due to ASR aggregate to serious endanger the safety of concrete, which has been attracting new wild attention. In clod region, concrete is always subject to frost damage in winter. In this chapter, the combined deterioration between frost damage and alkali-silica reaction was investigated.

As a result, for OPC concrete, the expansion due to alkali-silica reaction could be restrained when subjected to freeze-thaw. While, for BFS and FA concrete, it is kept a low level whether subject to freeze-thaw or not. For OPC and FA concrete, the frost resistance can be reduced when subjected to alkali-silica reaction, and for BFS concrete, there is little change in frost resistance whether subjected to alkali-silica reaction or not. There is a close relationship between reduction of MSE and expansion rate due to ASR. the ASR deterioration can be evaluated by the reduction of MSE. Although 3-month ASR increase expansion rate, the deterioration degree is small, which little affect relationship between expansion rate and RDM. While, the 12-month ASR costly change the relationship between expansion rate and RDM, which is because that the long time ASR vastly increases expansion, but slightly decrease the RDM of concrete for OPC concrete. However, for BFS and FA concrete, the additive of BFS and FA can restrain ASR, which keeps the relationship between expansion rate and RDM.

6.2 Summary

This thesis investigated the combined deterioration of frost damage of concrete containing BFS and FA, and

the effects of BFS and FA on the combined deterioration were also made clear.

The atmospheric CO_2 concentration has been increased and lead to the greenhouse effect that global temperatures increase, and a global “climate and environmental emergency” had been declared in 2019 to rise the challenge of climate change. It has become a global trend to limit and reduce carbon dioxide emissions. some studies show that the CO_2 emissions due to cement manufactured accounts for 8% of all in the world, approximately. Therefore, in recent years, in the trend of CO_2 emission reduction, BFS and FA are used more widely to reduce the cement consumption in the field of building materials, and the use of BFS and FA can result in a concrete with better durability.

From chapter 2, it can be well known that, for AE concrete, the use BFS and FA don’t reduce the frost resistance of concrete subjected to salt damage. And for Non-AE concrete, the use of BFS and FA can result in a better frost resistance due to long-term age.

From chapter 3 and chapter 4, it can be well known that, for AE concrete, the frost resistance of concrete subjected to carbonation is kept at a high level when using BFS and FA. While, for Non-AE concrete, the frost and scaling resistance subjected to carbonation tends to decrease with the additive of BFS and FA.

From chapter 5, it can be well known that, for AE concrete, the use of BFS and FA can restrain the cracks due to ASR, which can improve the frost resistance of concrete subject to ASR.

In real environment, AE concrete is used wildly for concrete construction. In various specification, AE admixture is required to add, which can ensure the good frost resistance of concrete. Therefore, in the study, it can be obtained that the use of BFS and FA don’t reduce of frost resistance of concrete subjected to salt damage and carbonation, and increase the frost resistance of concrete subjected to ASR. overall evaluation, the use of BFS and FA are beneficial to the safety of concrete.

LIST OF PAPERS

Publications:

Zhenzhao Ding, Nguyen Xuan Quy, Jihoon Kim, Yukio Hama，Evaluations of frost and scaling resistance of fly ash concrete in terms of changes in water absorption and pore structure under the accelerated carbonation conditions，Construction and Building Materials（7.693，Q1）.Vol. 345, 22 August 2022, 128273，doi.org/10.1016/j.conbuildmat.2022.128273

Zhenzhao Ding, Nguyen Xuan Quy, Takumi Noguchi, Jihoon Kim, Yukio Hama, A study on the change in frost resistance and pore structure of concrete containing blast furnace slag under the carbonation conditions，Construction and Building Materials（7.693，Q1）.Vol. 331, 9 May 2022, 127295，doi.org/10.1016/j.conbuildmat.2022.127295

Presentations:

INFLUENCE OF CARBONATION ON FROST RESISTANCE OF CONCRETE WITH DIFFERENT FLY ASH AND BLAST FURNACE SLAG REPLACEMENT RATIOS，Proceedings of 14th International Symposium Between Japan, China and Korea Performance Improvement of Concrete for Long Life Span Structure，2021.08

Influence of Combined Deterioration between Frost Damage and Alkali-Silica Reaction of Concrete due to Additive of Blast Furnace Slag or Fly Ash，Proceedings of 15th International Symposium Between Japan, China and Korea Performance Improvement of Concrete for Long Life Span Structure，2022.08